

2004

Faculteit Wetenschappen

Synthesis and Characterisation of Polar PPV Derivatives through the Sulfinyl Precursor Route

Proefschrift voorgelegd tot het behalen van de graad van
Doctor in de Wetenschappen, richting Scheikunde,
te verdedigen door

Filip MOTMANS

Promotor : Prof. dr. D. Vanderzande



INSTITUUT VOOR MATERIAALONDERZOEK



PARTNER IN DE UNIVERSITEIT LIMBURG

Dankwoord

Het voorbije jaar had heel veel weg van een waar annus horribilis en dat had zeker niet (alleen) met het schrijven van deze thesis te maken. Toch hou ik er aan om enkele mensen van harte te bedanken voor hun medewerking en steun bij het tot stand komen van dit werkje. Aangezien dit deeltje het meest -en door velen liefst- gelezen onderdeel van de thesis is, lijkt me dit dan ook de aangewezen plaats daarvoor.

Prof. Dirk Vanderzande dank ik voor de mogelijkheid die hij mij gegeven heeft om een doctoraat aan het LUC aan te vatten. Zijn "wild" en soms "challenging" ideas waren steeds een bron om nieuwe dingen te proberen om zo een gepaste oplossing voor één van de talrijke problemen gedurende vier jaar doctoreren te vinden. Hoewel ik na tweede kan gezworen had om nooit organische scheikunde te gaan doen ben ik toch gaan inzien dat het eigenlijk enkel draait om negatieve ladingen die op de positieve aanvallen. Buiten het puur wetenschappelijke aspect van het doctoreren ben ik erg dankbaar voor de kans die ik kreeg om te proeven van de didactische taken in onze onderzoeksgroep. Ik ben dan ook zeer blij dat ik je in die examencontext heb kunnen uitleggen dat Octaaf de Bolle enkel bij Gert en Samson voorkomt en dat Kathy en Annie Jonisch fictieve tweelingszussen zijn.

Prof. Jan Gelan, co-promotor van dit werkje, bedank ik voor zijn interesse in ons doctoraatsonderzoek en in onze persoonlijke leventjes, vaak ging het dan over de nieuwe aanwinsten in onze respectievelijke families.

Prof. Peter Adriaensens, bedankt voor de soms ingewikkelde NMR-toestanden, jij hebt herhaaldelijk laten zien dat er met NMR-spectroscopie veel meer mogelijk is dan wat er tijdens de licentiaatsopleiding getoond wordt.

Dr. Laurence Lutsen, voor één keer probeer ik het in het Frans: Je vous remercie pour votre attribution à cette thèse. A plusieurs reprises votre contribution scientifique a été d'une grande importance. Apart de ce part scientifique, les mémorables «lab cleanings» ont pris une place persistante dans mes mémoires. Merci pour tout.

De mensen van FTO o.l.v. Prof. Robert Carleer ben ik zeer dankbaar voor de vele tijd die ze gestoken hebben in de opnames en de bespreking van diverse analyses. Bedankt Jan voor de talrijke massa's, Guy voor de thermische analyses, Yvo (enkel voor de besprekingen) en de overige leden van die afdeling.

De anorganici bedank ik voor hun bijdrage aan de flauwe zever in de koffiekamer en voor het op poten zetten van een uitwisselingsproject tussen hun en onze onderzoeksgroep.

En dan komen we bij de zware gevallen waar weinig tot geen hulp meer kan baten. In min of meer chronologische volgorde: Lieve, jouw initiële experimenten met Miranda hebben mij goed op weg geholpen in dit deel van de geconjugeerde polymeren. Anne, bedankt voor de opgeloste oefeningen en de interessante gesprekken over uitbreidingen en dergelijke. Liesbet, altijd bereid om te luisteren en te vertellen en niet te beroerd om geregeld te vallen. Bart, die korte tijd was toch lang genoeg om telkens weer te lachen, vooral uw imitatie van Joël en Michel van de minuut was hilarisch. Robby, ik wens u veel succes met het vaderschap, maar dat zal wel loslopen zeker. Stijn, lange, die tijd met u in het labo was soms memorabel en de plaats hier is te beperkt en totaal ongeschikt voor verdere uitwijdingen omdat we toch snel zouden hervallen in Oud-Georgische spreekwoorden. Els, dankzij het car-poolen hebben we toch serieus wat uitgespaard. Anja, we hebben ondanks alle miserie toch nog al wat afgelachen hé. En Hilde, woorden schieten schromelijk tekort: enkele gedenkwaardige citaten: "Oh nee, ze gaan me toch niet aanhouden hé!?" "Bah, wat ne microbennest." Raoul Gonzalez de Galdeano Adamski, ik ben blij dat ik door u wat uit te dagen iets uit u gekregen heb, hopelijk worden zowel Geel als FC 't Anker dit jaar kampioen. Jos 'dzjoakien', gij hebt herhaaldelijk gedemonstreerd dat een mens geen bed hoeft om te slapen en Veerle, gij hebt afrit 9 niet nodig om te weten dat ge sterk bezig zijt, doe zo verder. Colladetti, hoewel gij tot een ander team behoort viel ge goed mee, vooral uw imitaties van leden van het professorenkorps waren schitterend, natuurlijk ben ik u zeer erkentelijk voor 'dachetzijt, zechet' en voor uw verbeterbijdrage aan dit werkje. Ine, op 1 april lost magnesiumsulfaat niet op in dichloormethaan, ook spijtig dat we juist gene foto hadden van uw sierlijke trapafdeling, van andere dingen hadden we die wel. En dan Sofie, ge hebt het soms hard te verduren gekregen maar ge hebt ons (uzelf trouwens ook) talrijke keren doen wenen van het lachen. Met groot respect denk ik terug aan de gebeurtenissen rond de shit zoe, stop met wenen pafpafpaf, en de magnetische gasfles, ze moesten het weten. Iriske, juffrouw Duyssens, gij hebt ons steeds weer verwonderd met uw jonge snaken waar ge steun bij kon vinden als het in het labo soms echt te gortig werd. Ook Huguette verdient hier een woordje van dank voor de talloze UV-Vis eliminaties en voor de culinaire uitwisselingsprojecten. Zarina, Fateme en Raoul wens ik een behouden vaart doorheen vier of meer jaren doctoraatsonderzoek.

Breboh (Lien) tevens lid van het andere team verdient hier een speciale vermelding, ze weet zelf wel waarom.

Ook mijn thesisstudent Tim verdient een woord van dank niet in het minst omdat zijn nieuwe dansspasjes een echte rage geworden zijn.

De mensen die instonden voor de logistiek verdienen natuurlijk ook een woordje van dank. Christel Rappoort voor de bestellingen en de snoepjes, Jos voor de werktuigen, Koen voor de NMR opnames en Sali (voor ..., ja voor wat eigenlijk?;-)) meneer Gène voor de babbels en de medewerkers en Steven van het SBG-secretariaat die ervoor zorgden dat alles in goede banen geleid werd/wordt.

Het LUC ben ik dankbaar voor de financiële steun gedurende vier jaar doctoreren.

Ma en pa (moeke en Boppi) jullie hebben eigenlijk nog het meest geïnvesteerd in dit werkje. Zonder jullie niet-aflatende steun gedurende 28 jaar zou ik waarschijnlijk heel ergens anders (daarom niet slechter hé) terechtgekomen zijn. Hopelijk vinden jullie het geen verspilde energie. Peter en Wouter jullie weten nog altijd niet wat ik eigenlijk doe maar dat is ook van geen belang, ik heb me goed geamuseerd.

En dan bijna last but not least, Inge, jij was er gedurende de laatste jaren altijd voor mij en ik ben blij dat alles uiteindelijk nog goed afgedraaid is, voor hetzelfde geld of een pak minder zag alles er heel anders uit. Merci voor alles, zonder jouw steun, motivatie en doorzettingsvermogen hebben we zowel dit werkje als al onze gezinsperikelen (voor de buitenstaanders hiermee worden geen relatieproblemen bedoeld hé) tot een goed einde weten te brengen. En dan Thijs, gij veel te vroege vogel, ge zijt nog iets te jong om het te beseffen maar ook uw bijdrage was van groot belang. Gij hebt mooi aangetoond dat er ook andere mooiere dingen dan scheikunde bestaan. Als ge later scheikunde wilt gaan studeren zal ik u eerst eens goed tegen de kop kloppen en u dan naar het labo voor organische en polymeerchemie sturen, daar is het fijn toeven.

Bedankt

Table of contents

Chapter 1- Introduction

1. Introduction	1
2. Conjugated polymers: Organic Semiconductors	4
3. Synthesis	4
3.1. The sulfonium precursor route.....	6
3.2. The dehalogenation route.....	8
3.3. The xanthate route	9
3.4. The sulfinyl precursor route	10
3.4.1. Monomer synthesis	12
3.4.2. Polymerisation.....	14
3.4.3. Conversion to the conjugated structure	14
4. Applications	15
4.1. Light Emitting Diodes (LED)	15
4.2. Photovoltaic devices ('solar cells').....	17
4.3. Polymer based sensors	18
4.4. Light emitting electrochemical cells (LEC).....	19
5. Aim and outline of the thesis.....	21
6. References	23

Chapter 2 - Synthesis of polar PPV precursor polymers

1. Introduction	27
1.1. Monomer synthesis through the sulfinyl route	27
1.2. Synthesis of polar and functional monomers.....	29
2. Synthesis and polymerisation of functional PPV monomers	32
2.1. Synthesis of a triethylene glycol derived sulfinyl polymer.....	32
2.1.1. Monomer synthesis	32
2.1.2. p-Quinodimethane formation.....	34
2.1.3. Polymerisation of monomer 14	36
2.1.4. Conversion of the precursor polymer into the conjugated material.....	37

2.2. Synthesis of an alcohol derived polymer	40
2.2.1. Monomer synthesis	40
2.2.2. p-Quinodimethane formation	40
2.2.3. Polymerisation of the monomer	41
2.2.4. Conversion of polymer into the conjugated structure	43
2.2.5. Protection of the alcohol function	45
2.2.6. Copolymerisation reactions	46
2.3. Synthesis of an ester derived polymer	47
2.3.1. Monomer synthesis	47
2.3.2. p-Quinodimethane formation	48
2.3.3. Polymerisation of monomer 26	49
2.4. Synthesis of a sulfonate derived polymer	53
2.4.1. Monomer synthesis	53
2.4.2. p-Quinodimethane formation	54
2.4.3. Polymerisation of monomer 30	55
2.4.4. Conversion of the polymer into the conjugated polymer	55
3. Applications of elimination behaviour – elimination induced by infrared absorption	56
4. Conclusions	59
5. Experimental Section	60
6. References	69

Chapter 3 - Synthesis of polar PPV derivatives

1. Introduction	73
2.1. Synthesis of triethylene glycol derived polymers 1 and 2	74
2.1.1. Monomer synthesis	74
2.1.2. Characterisation of the monomers	77
2.1.2.1. Nuclear Overhauser Enhancement (NOE)	77
2.1.2.2. Direct coupling HETCOR experiment	79
2.1.2.3. Long range HETCOR (J=8Hz)	80
2.1.3. p-Quinodimethane formation	83
2.1.4. Polymerisation of monomer 8	83
2.1.5. Polymerisation of monomer 14 (mixture of 14a and 14b)	85
2.1.6. Thermal conversion of precursor polymer 15 to the conjugated structure	86
2.1.7. Thermal conversion of precursor polymer 16 into the conjugated structure	89

2.1.8. Elimination of the precursor polymers in solution	91
2.2. Synthesis of an alcohol derived polymer	91
2.2.1. Monomer synthesis	92
2.2.2. Polymerisation of monomer 22	93
2.2.3. Conversion of precursor polymer 23 to the conjugated structure	93
2.2.4. Elimination in solution	95
2.2.5. Copolymerisation reactions	95
2.2.6. Elimination behaviour of the copolymers 25-26	96
2.3. Synthesis of an ester derived polymer	98
2.3.1. Monomer synthesis	100
2.3.2. Polymerisation of the ester monomer	101
2.3.3. Conversion of precursor polymer 35 to the conjugated structure	102
2.3.4. Hydrolysis of the ester function	103
2.3.5. Functionalisation of the carboxylic acid	104
2.4. Synthesis of a sulfonate derived polymer	105
3. Thermochromic effect – Thermal stability of the polymers 1, 2, 24 and 36.	108
3.1. Heating-cooling experiments	109
4. Electrochemical characterisation of the conjugated polymers	111
4.1. Determination of the optical band gap and comparison with electrochemical results	113
5. Conclusion	114
6. Experimental Section	115
7. References	137

Chapter 4 - A kinetic study on p-quinodimethane formation

1. Introduction	139
1.2. A kinetic refreshment	140
1.2.1. Kinetics of a first and second order reaction	140
1.2.2. Pseudo first order reaction kinetics	141
1.2.3. Consecutive first order reaction kinetics	142
2. Different types of elimination reaction	144
3. Previous work and literature data on p-quinodimethane formation	146
3.1. Wessling route	146
3.2. The Gilch precursor route (dehydrohalogenation)	148
3.3. The Sulfinyl precursor route	149

4. Study of the p-quinodimethane formation in 2-butanol	150
4.1. Experimental set-up.....	150
4.2. Experimental procedure	151
4.3. Qualitative study on p-quinodimethane formation	153
4.4. Quantitative study on p-quinodimethane formation	155
4.4.1. Synthesis of the required monomers	156
4.4.2. Treatment of experimental data	157
The Guggenheim method ¹¹	157
Non-linear least-squares method ¹³	158
5. Copolymerisations of different p-quinodimethane systems	162
5.1. Copolymerisation of OC ₁ C ₁₀ -sulfon with PPV sulfoxide	163
5.2. Elimination behaviour of the copolymers.....	166
6. Conclusions	168
7. Experimental part.....	168
8. References	173
Summary	175
Samenvatting.....	179

Chapter 1

Introduction

1. Introduction

The word polymer originates from the Greek “poly meros” which literally means “many units”. Polymers can thus be seen as a string consisting of numerous building blocks called monomers. Nowadays imagination of our daily lives without any polymer seems impossible. Think of plastic bags, bottles, bakelite, plastic toys etcetera. These polymers thank their important place in our live to their specific properties such as low weight, mechanical strength and ease of processibility. Also, polymers (or plastics) are known to be good electrical insulators preventing for instance shortcuts in an electrical switch.

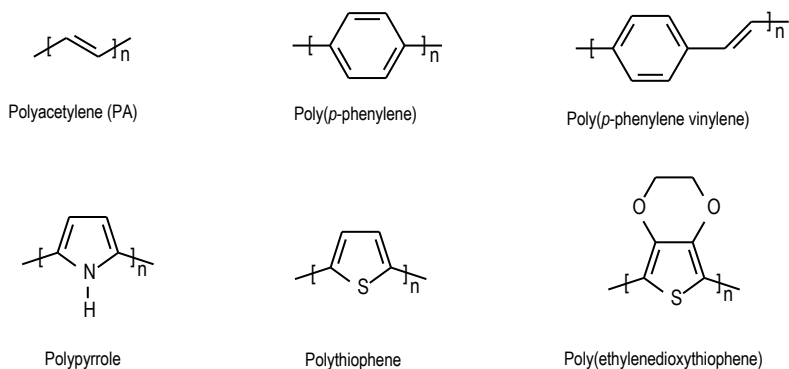
In contrast to the common idea that polymers are good insulators, nowadays a lot of attention is given to so called conjugated polymers. These conjugated polymers are a relatively new class of organic materials, which are of major interest both from industrial and academic point of view. In 1977 a major breakthrough in the field of conjugated polymers was achieved when high conductivities were observed by doping polyacetylene with oxidising agents¹. For their contribution to the research in this domain Heeger, MacDiarmid and Shirakawa (Figure 1) were rewarded the Nobel Prize 2000 in chemistry.



Figure 1. Picture of the three Nobel Prize winners in the field of the conjugated polymers (left to right: Shirakawa, Heeger, MacDiarmid)

Chapter 1

The special properties of conjugated polymers originate from the alternating single and double bonds along the polymer backbone. Some of the most common conjugated polymers are depicted in scheme 1.



Scheme 1. Overview of some basic conjugated polymers

It has been shown already for a long time that conjugated double bonds strongly absorb in the visible part of the spectrum. Some very well known natural species contain conjugated segments for example chlorophyll a, a porphyrine derivative, that plays an important role in green plants photosynthesis (Figure 2). Due to this conjugated double bonds these conjugated polymers have their specific optical properties.

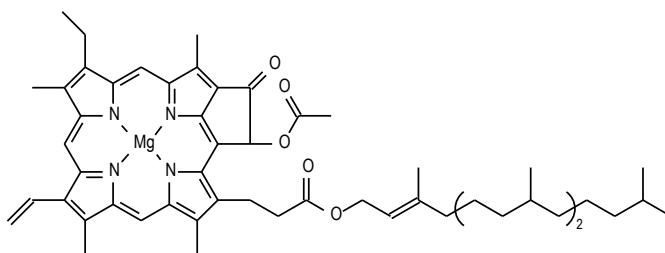


Figure 2. Chemical structure of Chlorophyll a

The essential structural characteristic of all conjugated polymers is their quasi-infinite π -system extending over a large number of repeating monomer units. This feature results in materials with directional conductivity, strongest along the axis of the chain. The simplest

possible form is of course the archetype polyacetylene shown in scheme 1. While polyacetylene itself is too unstable to be of any practical use, its structure shows the fundamental bonding pattern present in all conjugated polymers. Owing to its structural and electronic simplicity, polyacetylene is well suited to ab initio and semi-empirical calculations and has therefore played a critical role in the elucidation of the theoretical aspects of conducting polymers². Electronically conducting polymers are extensively conjugated molecules, and it is believed that they possess a spatially delocalised band-like electronic structure. These bands stem from the splitting of interacting molecular orbitals of the constituent monomer units in a manner reminiscent of the band structure of solid-state semiconductors (Figure 3).

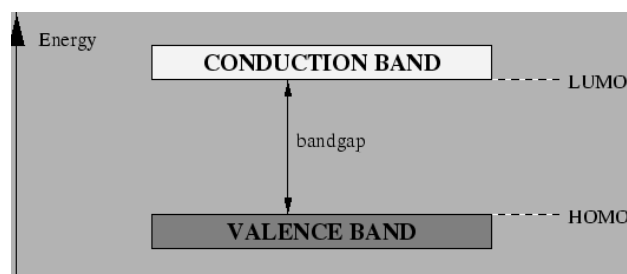


Figure 3. Band structure in an electronically conducting polymer

It is generally agreed upon that the mechanism of conductivity in these polymers is based on the motion of charged defects within the conjugated framework. The charge carriers, either positive p-type or negative n-type, are the result of an oxidising or reducing process in the polymer respectively. The highest occupied band (which originates from the HOMO of the repeating unit) is called the valence band (VB) and the lowest unoccupied band (which originates from the LUMO of the repeating unit) is called the conduction band (CB). The difference between these energy levels is called the band gap and is determined by the nature of the polymer structure (figure 3). For comparison, in metals this band gap is zero where it varies between approximately 1 and 4 eV for conjugated polymers.

2. Conjugated polymers: Organic Semiconductors

The most important aspect of conjugated polymers from an application perspective is their ability to act as electronic conductors. Not surprisingly π -electron polymers have been the focus of extensive research, ranging from applications of “conventional” polymers (e.g., polythiophene, polyaniline, polypyrrole) in charge storage devices such as batteries and supercapacitors, to new polymers with specialised conductivity properties such as low band-gap and intrinsically conducting polymers. Indeed, many successful commercial applications of these polymers have been available for more than fifteen years, including electrolytic capacitors, batteries, magnetic storage media, electrostatic loudspeakers and anti-static bags. It has been estimated that the annual global sales of conducting polymers in the year 2000 would have surpassed one billion US dollars. Clearly these materials have considerable commercial potential both from the continued development of well-established technologies and from the generation of new concepts such as those to be presented in this thesis.

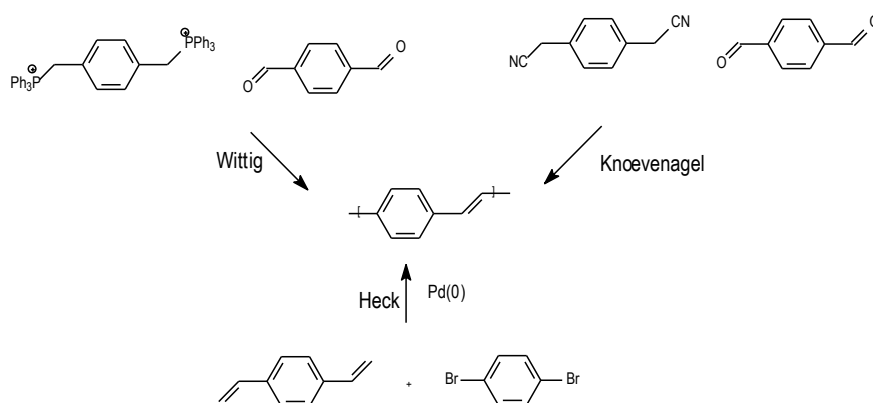
3. Synthesis

Within the broad range of possible conjugated polymers we will only focus on the conjugated polymer poly-(*p*-phenylene vinylene), PPV and some of its derivatives.

In 1991 Burroughes *et al.* reported on the electro-luminescence of PPV³. Since then a lot of research was spent on this family of conjugated polymers. PPV exhibits the single-double bond alternation throughout the polymer backbone consisting of consecutive phenylene and vinylene units. The pristine PPV is an insoluble and unmelttable material and hence it is very difficult to process. However the solubility of PPV can be enhanced by attaching long and flexible chains on the polymer backbone^{4,5,6}. In this way a soluble conjugated material can be obtained. In our laboratory such a soluble PPV derivative acts as the working horse for several experiments.

From synthetic point of view, two different approaches for obtaining PPV derivatives are known. A first approach is the direct synthesis of PPV where the double bond is generated in situ (scheme 2). Known examples of such routes are the Wittig⁷ and Knoevenagel^{8,9} polycondensation reactions. Also palladium catalysed reactions were applied in PPV synthesis e.g. in the Heck¹⁰ coupling reaction between ethylene and aromatic dibromides. However these routes to PPV have the disadvantage of giving insoluble, unworkable

products. To overcome this problem various side groups (usually alkyl, alkoxy, or phenyl) are built in and the conjugated polymer becomes soluble in organic solvents such as chloroform and toluene, but these side groups can change the optical and electronic properties of the polymer. Also these reactions yield polymers with only low or moderate molecular weight, which can jeopardise their film forming properties.

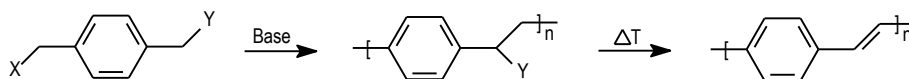


Scheme 2. An overview of some direct routes towards PPV

Another possible strategy is the use of a soluble precursor polymer that can be appropriately processed into film and fibers prior to being thermally converted to insoluble PPV under expulsion of a small molecule per monomer unit.

Up till now four different precursor routes towards PPV have been discussed in literature. The general principle of such precursor route is depicted in scheme 3. Treatment of a p-xylene derivative with a strong base yields a soluble precursor polymer. Thermal treatment of this precursor polymer affords the fully conjugated material. The routes differ in the substituents on the p-xylene derivative and will be discussed separately further on.

Chapter 1



Wessling X = Y = $R_2S^+Cl^-$

Gilch X = Y = Cl or Br

Xanthate X = Y = S-C(S)-OEt

Sulfinyl X = halogen atom Y = S(O)alkyl

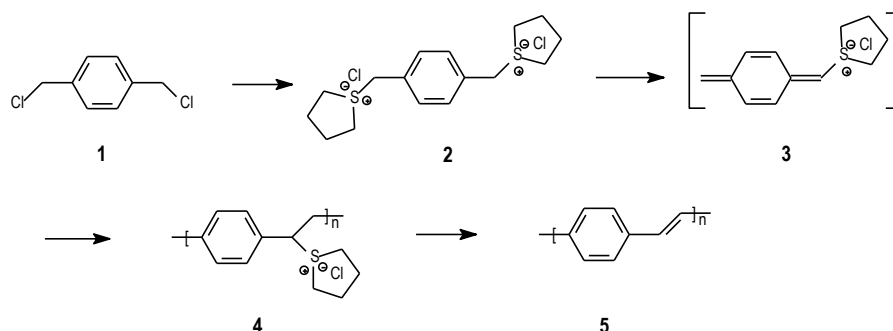
Scheme 3. General reaction scheme of the four precursor routes towards PPV

3.1. The sulfonium precursor route

The first precursor route described is the bissulfonium precursor route. In 1968 Wessling and Zimmerman discovered this route towards PPV^{11,12}. In literature this route is also often referred to as the Wessling route. For more than twenty-five years it is the most widely studied precursor route (scheme 4).

Monomer synthesis is very easy to perform and can be achieved by reacting α,α' -dichloro-p-xylene **1** with an excess of dialkyl sulfide. Both linear and cyclic thioethers can be used for this reaction but the latter are preferred due to fewer unwanted side reactions¹³.

Polymerisation of the bissulfonium salt **2** is achieved by basic treatment of the salt in water or methanol, which gives a p-quinodimethane system **3** that acts as the real monomer in the polymerisation. This p-quinodimethane system readily polymerises to the precursor polymer **4**. Different groups worldwide studied the mechanism of polymerisation. First a proton is abstracted to give an anion that undergoes elimination of a sulfonium group. The mechanism was proposed by Cho and coworkers and is an E_{1cb} reversible elimination mechanism where the rate-determining step is the expulsion of the leaving group¹⁴. The next step is the actual polymerisation of the quinoid system through a radical chain reaction probably initiated by dimerisation of two p-quinodimethane systems. The formation of the quinoidal p-xylylene intermediate can be monitored by the appearance of a peak in the UV-Vis spectrum around 310 nm.



Scheme 4. General scheme for the Wessling precursor route

Low temperatures ($T < 0^\circ\text{C}$), dilute monomer concentrations (0.05 - 0.2 mM) and equimolar or slightly less than one equivalent of base do afford high molecular weight polymers in an excellent yield¹⁵ (up to 90%).

Since an ionic precursor polymer is obtained, GPC measurements are rather difficult and unreliable. Therefore substitution of the remaining sulfonium group is performed with phenyl thiolate¹⁶ or methoxide¹⁷ anions to give a precursor both soluble in chloroform and THF.

The sulfonium group in the precursor polymer **4** is a good leaving group and hence the precursor shows reduced stability and undergoes all kind of side reactions such as substitution and preliminary elimination to create a partial conjugated structure eventually leading to an insoluble product. These possible defect structures¹⁸ are shown in figure 4.

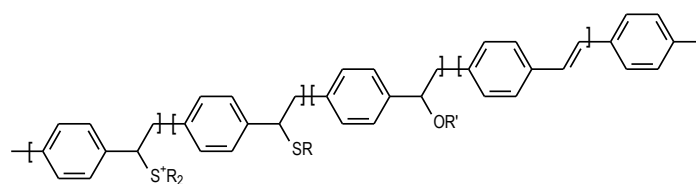


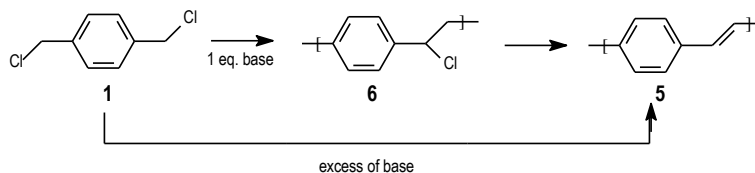
Figure 4. Possible defect structures in a Wessling precursor polymer

The precursor polymers **4** are converted into the conjugated analogues **5** by thermal treatment in a range of 160-300°C during 2 to 20 hours¹⁹. However the optimal elimination conditions described by different groups differ to a large extent concerning the applied procedure. During elimination a thioether and a hydrogen halide are set free. This hydrogen

halide has to be removed from the polymer matrix since it has a bad influence on eventual device behaviour. Nevertheless the Wessling route is a very versatile route that allows polymerisation of many PPV derivatives²⁰. A large variety of substituents can be tolerated on the aromatic ring, including aromatic, alkoxy, alkyl, silyl, halogen, sulfur, and amino groups. However, electron poor aromatic systems (e.g. nitro- or cyano- substituents) polymerise with extreme difficulty²¹.

3.2. The dehalogenation route

The second precursor route, the dehalogenation route, was first reported by Gilch and Wheelwright²² and is often referred to as the “Gilch route”. It involves basic treatment of a α,α' -dihalogen (mainly chlorine) p-xylene derivative with an excess of base (potassium t-butoxide) in organic solvents to afford an insoluble plain PPV. To obtain a more soluble precursor polymer **6** through this route one equivalent of base has to be used instead of tenfold excess²³. This precursor can be converted to the conjugated structure by thermal treatment (300°C, 1 hour) or basic elimination in case of a completely soluble PPV derivative.



Scheme 5. General scheme for the Gilch precursor route

At present the Gilch route is the most widely used route for the synthesis of soluble conjugated PPV derivatives such as MEH-PPV and OC₁C₁₀-PPV (figure 5).

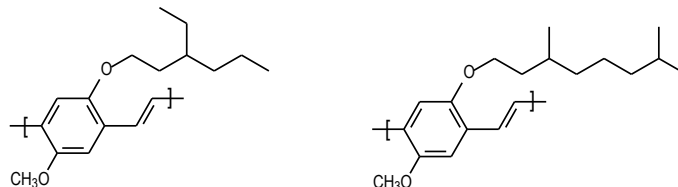


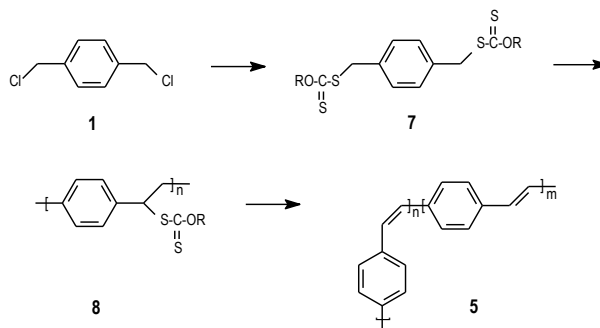
Figure 5. Chemical structures of two soluble PPV derivatives MEH-PPV (left) and OC₁C₁₀-PPV (right)

A few years ago there was an ongoing discussion in literature concerning the exact mechanism of polymerisation. Both an anionic²⁴ and a radical mechanism were proposed. In our group evidence was found for a radical process with little occurrence of anionic processes involving nucleophilic attack on the p-quinodimethane system²⁵.

Note that also in this route hydrogen chloride or bromide is set free during elimination that has to be removed in order to avoid poor device performance.

3.3. The xanthate route

A quite recently described precursor route is the xanthate precursor route that was developed by Son and coworkers²⁶. The monomer **7** in this route is readily obtained by reacting a α,α' -dihalogen p-xylene **1** with the commercially available potassium xanthic acid. Basic treatment with potassium t-butoxide in THF at 0°C yields a precursor polymer **8** that is soluble in common organic solvents. Although nowhere any evidence is given for p-quinodimethane formation neither in our laboratory nor in other research groups, it is believed that this reactive species also in this route acts as the real monomer. Moderate yields of a high molecular weight polymer can be obtained when the polymerisation temperature is sufficiently low.



Scheme 6. General scheme for the xanthate precursor route

Elimination of a xanthate group from the precursor polymer **8** is best performed between 160 and 250 °C indicating that the precursor is stable at room temperature. The advantage of this route would be the higher electroluminescence of the material. This higher electroluminescence efficiency for a single layer LED device, ITO / PPV / Al, (0.22% compared to the earlier value of 0.01%) was first attributed to the presence of cis-vinylene

linkages which reduces the effective conjugation length as observed from IR-signals at 860 cm^{-1} . However Burns proved that the higher efficiency originates from the absence of hydrogen chloride during elimination²⁷.

Compared to the Wessling route, the xanthate precursor route offers certain advantages among which the enhanced stability of the precursor.

3.4. The sulfinyl precursor route

The precursor route used in this work is the sulfinyl precursor route²⁸. The three routes described above all have in common that they use a symmetrically substituted p-xylene derivative as the monomer where the same functional group both acts as leaving group to yield a p-quinodimethane system and also as a polariser that is expelled during thermal treatment resulting in the conjugated structure. This symmetry can cause unwanted side reactions such as substitution or preliminary elimination and hence will have a negative influence on device preparation and performance.

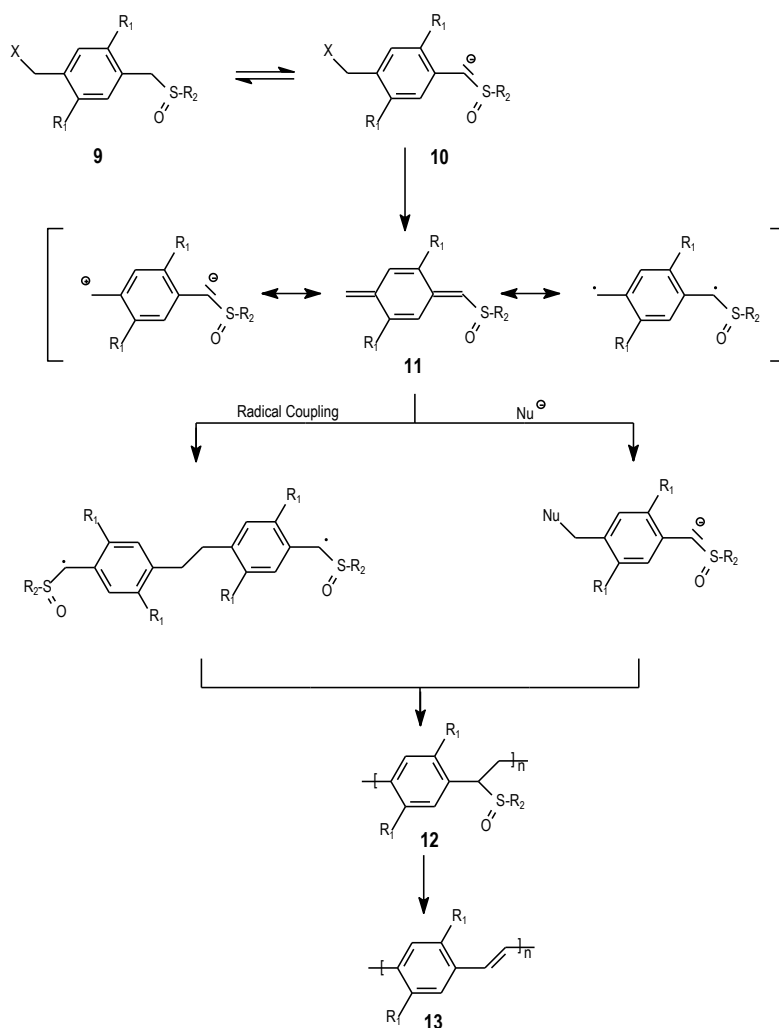
To overcome these problems a non-symmetrically substituted p-xylene derivative **9** was synthesised. This monomer does possess a sulfinyl S=O group acting as a polariser. The polariser has to fulfil three important functions. It allows proton abstraction easily at the benzylic position next to the S=O group guaranteeing a good p-quinodimethane formation. A second function is that it allows a good solubility for the eventual precursor polymer, which makes processibility from solution possible. A third key feature of this group is that it is stable at lower temperatures and that it is easily expelled at elevated temperatures to realise complete elimination to yield the fully conjugated structure. Interesting is that during the elimination process of the sulfinyl group no harmful hydrogen halides are produced unlike the Wessling and Gilch precursor routes. Due to a combination of steric and electronic effects the sulfinyl p-quinodimethane systems also guarantee a good head to tail addition resulting in fewer sp and sp^3 defect structures compared to the other routes. For a detailed study on defect structures we refer to the work of Hilde Roex²⁹.

A general scheme for the sulfinyl precursor route is depicted in scheme 7. The sulfinyl compound **9** is treated with a base solution resulting in the formation of a benzylic anion **10** that can undergo a 1,6-elimination to afford a p-quinodimethane system **11**, the real monomer in this kind of polymerisations. The p-quinodimethane system can be drawn both under its diamagnetic and paramagnetic resonance form. Different p-quinodimethane

systems polymerise to a high molecular weight precursor polymer **12** through a radical chain mechanism although in some cases an anionic pathway is proposed. It is believed that this anionic polymerisation mechanism rather results in low molecular weight materials.

The precursor polymer can be obtained or purified by precipitation in a non-solvent and collected through filtration. The precursor is stable at room temperature and conversion to the conjugated structure **13** is achieved by applying a thermal treatment of about 100°C. The p-quinodimethane formation was confirmed by UV-Vis measurements because this species has a specific absorption at about 315 nm, which is comparable with Wessling quinoid systems. The sulfinyl route has proven to be a versatile route allowing the polymerisation of different PPV derived monomers either with electron withdrawing or donating substituents to yield high molecular weight polymers. This is in contrast to the Wessling route where polymerisation of electron poor monomers failed.

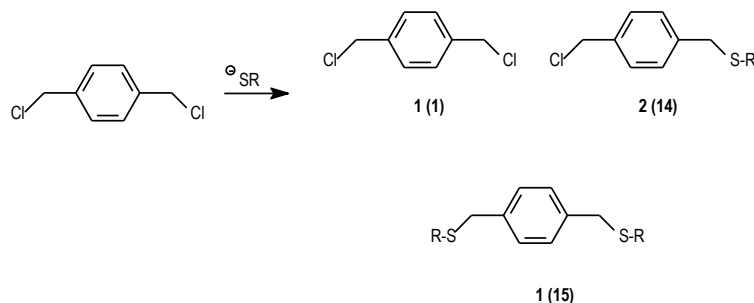
Chapter 1



Scheme 7. General scheme for the sulfinyl precursor route

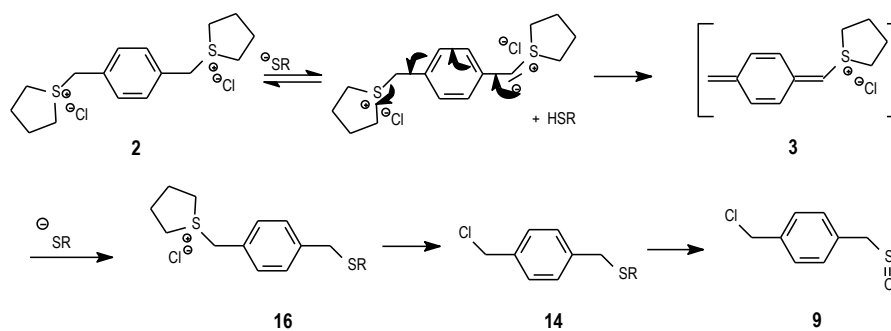
3.4.1. Monomer synthesis

At first sight the synthesis of a sulfinyl monomer seems quite easy but actually it is the most inventive and challenging step in the whole sulfinyl precursor route. Simple nucleophilic substitution of an α,α' -dichloro-*p*-xylene derivative with a thiolate anion yields a statistical 2/1/1 mixture of mono-thioether **14**, di-thioether **15** and the starting product **1**.



Scheme 8. Product distribution for thioether synthesis starting from α,α' -dichloro-*p*-xylene

To obtain the monosubstituted thioether our research group has come up with a very smooth synthetic procedure to obtain selectively this compound in a high yield^{30a}. Therefore an α,α' -bissulfonium-*p*-xylene **2**, i.e. the monomer in the Wessling precursor route is reacted with an equimolar amount of a thiolate anion. This anion acts as a base with abstraction of a benzylic proton. Subsequent 1,6-elimination of a THT group affords a *p*-quinodimethane system **3** that undergoes thiolate attack and an α -sulfonium- α' -thioether *p*-xylene **16** is obtained. Azeotropic removal of the THT results in the corresponding chloro-compound **14** in a high yield.



Scheme 9. Monomer synthesis according to the sulfinyl precursor route

The thioether **14** can be oxidised to the sulfoxide analogue **9** by using a tellurium dioxide catalysed oxidation with H_2O_2 as the oxidant^{30b}.

3.4.2. Polymerisation

The sulfinyl monomers are normally polymerised according to a standard procedure developed in our group. In a set-up depicted in figure 6 are brought the monomer and the base solution. The concentration of the monomer is 0.1M when the total amount of solvent is taken into account. Both base and monomer solutions are purged with a flow of nitrogen and the reaction temperature is maintained at 30°C. After addition of the base solution to the monomer the reaction is stirred for one hour. Subsequently the mixture is poured into water and extracted with dichloromethane or chloroform. After evaporation of the organic layer the precursor polymer is precipitated in a non-solvent, collected and dried in vacuo.

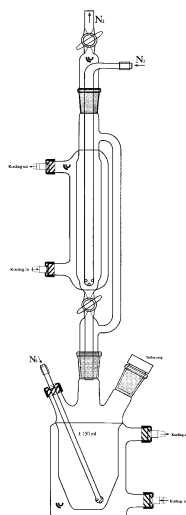
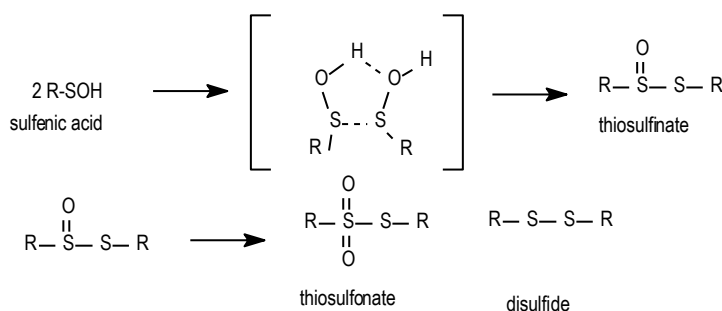
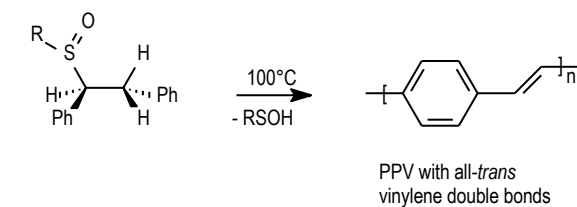


Figure 6. Polymerisation set-up used in the sulfinyl precursor route

3.4.3. Conversion to the conjugated structure

The final step in PPV synthesis according to the sulfinyl precursor route is the thermal elimination of the sulfinyl group to convert the precursor in its conjugated analogue. The elimination process is well documented in literature and proceeds through a syn-elimination in which the intermediate is believed to have a planar structure. Due to steric hindrance in the transition state only the trans-vinylene bonds are obtained. The expelled sulfenic acids will dimerise with formation of a thiosulfinate³¹. Eventually a disulfide and a thiosulfonate can be obtained from a disproportionation reaction involving two molecules of thiosulfinate.



Scheme 10. Possible reactions of the eliminated sulfenic acids

4. Applications

Conjugated polymers are a versatile class of organic materials that promise utility in a variety of applications ranging from antistatic coatings, electrodes, and transistors, to light-emitting diodes, light-emitting electrochemical cells, large area displays, photovoltaic cells, sensors and lasers. Some of the most important applications will be discussed next.

4.1. Light Emitting Diodes (LED)

A quite recent development for the application of conjugated polymers, which is attracting much attention, both in academic and industrial research groups, is the use of conjugated polymers as the active layer in light-emitting diodes (LED)³². Commercial light-emitting diodes are based on inorganic materials such as GaAs, GaP, SiC etc., which have a p-n junction. The quantum efficiency, which is defined as the rate of emission of photons divided by the rate of supply of electrons, of commercial inorganic materials varies from 0.1 to 1%. The emission wavelength of these materials varies from 400 to 1200 nm. Materials emitting in the blue region are particularly problematic. Because of the large energy gap they tend to have high resistivities resulting in low brightness. Furthermore these inorganic crystals often

have high melting points and low structural stability. Apart from the problems with blue LED's mentioned, the technology of inorganic crystals is complicated and the construction of large areas is difficult to realize.

Light-emitting diodes (LEDs) made with conjugated polymers became an active area of research in 1990 when electroluminescence from poly-(p-phenylene vinylene) was demonstrated by Burroughes and coworkers. Polymer-based LEDs are envisioned for applications such as screen displays because of their flexibility, high-energy efficiency, potential for large surfaces and ability to emit throughout the visible spectrum. Most importantly, LED devices made with organic materials are easy to manufacture and to design. These organic LED devices operate by injecting electrons and holes into thin polymer films. The electrons and holes travel through the polymer and combine to form an exciton, or bound electron-hole pair, which then emits visible light. Figure 7 is a depiction of such an organic LED made with PPV sandwiched between two electrode layers.

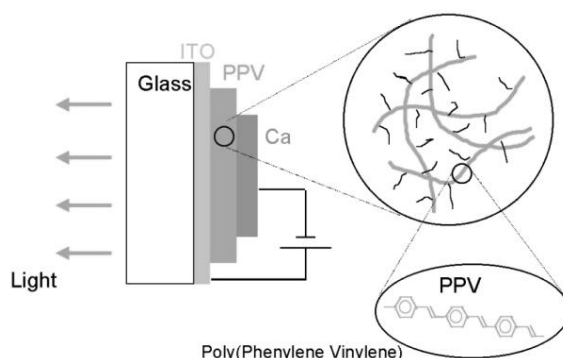


Figure 7. Schematic representation of a LED

The hole-injecting electrode layer is typically made of a material with a high work function, such as the transparent indium tin oxide (ITO), and the electron-injecting electrode layer is one with a low work function, such as calcium, aluminum, or magnesium. For optimal efficiency, the amount of electrons and holes injected into the polymer needs to be balanced, since excessive amounts of one of the charge carriers prohibit efficient exciton formation. Organic materials tend to preferentially transport holes (called p-type semiconductors) because of their low electron affinities, so an electron transport layer is

also typically placed into the device to improve device performance. LED device performance is dependent upon the luminescence efficiency of the polymer material. The luminescence of these polymers tends to be lower in the solid state than for isolated chain molecules because the excitons can migrate to quenching sites, such as aggregates or chemical defects³³. Inter-chain interactions can be reduced by attaching bulky side groups to the conjugated polymer backbone, such as alkyl groups. These side groups serve to dilute the polymer backbones, which minimizes the effects of aggregation, but they can also inhibit the transport of charges through the polymer film.

4.2. Photovoltaic devices ('solar cells')

Both from an economical and ecological point of view people are constantly looking for renewable energy sources. The use of free energy of the sun that can be converted into electrical energy seems very appealing for this purpose. Inorganic solar cells have been around for a long time but only recently it was discovered that conjugated polymers could also be used in these device structures³⁴. A polymeric solar cell will combine the optoelectronic properties of conventional semiconductors with the excellent mechanical and processing properties of polymers. Devices can be processed relatively easy from solution onto e.g. flexible substrates using simple and therefore cheaper deposition methods like spin coating and film casting. The working principle of an organic photovoltaic device is opposite to the LED, however the same basic device construction is used. A conjugated polymer in most cases blended with an electron accepting species such as fullerene (C_{60}) is sandwiched between two electrodes. Another approach uses a double layer construction instead of a blend. Incident sunlight can give rise to the formation of an exciton (photo-induced charge generation) and this exciton can break up when an electron is transferred to the energetic more favoured electron accepting species. Due to a driving force the charges can be pushed through an external circuit. The splitting of an exciton into a positive and negative charge (hole and electron) can only occur if the accepting species is spatially close enough to the excited polymer in a way that relaxation of the exciton to its ground state is prevented.

Nowadays the highest efficiencies (3%) reached in PPV based photovoltaic devices use OC_1C_{10} as a donor material blended with PCBM, a fullerene derivative, as an acceptor in a

1:3 ratio³⁵. This efficiency is still far from the 25-30% efficiencies reached by crystalline inorganic solar cells but the polymeric solar cells are constantly improving.

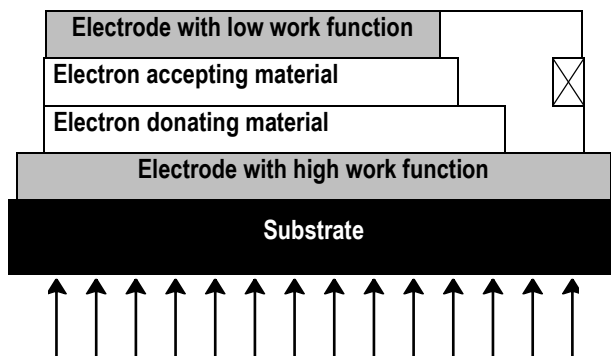


Figure 8. Schematic representation of a photovoltaic cell.

4.3. Polymer based sensors

The electrical, optical, and electrochemical properties of conjugated polymers can be modified by chemical synthesis and are strongly affected by relatively small perturbations, including changes in temperature, solvent or chemical environment. As a result of this sensitivity, conjugated polymers are promising materials to act as sensory materials³⁶. Sensing may be accomplished by transducing or amplifying physical or chemical changes into electrical, optical, or electrochemical signals. Conjugated polymers have been used to detect chemical species (chemo-sensors), such as ions, gases such as trinitrotoluene, and other chemicals, or biomolecular such as proteins, antibodies and DNA, using electrical, chromic, electrochemical, photo luminescent, chemo luminescent, or gravimetric responses. Contemporary biosensor and bioassay developments have focused on mimicking natural host-receptor interactions. “Lock-and-key” molecular recognition can occur between enzyme and substrate, ligand and receptor, antibody and antigen, or between two strands of nucleic acids with complementary sequences.

Biosensors based on conjugated polymers as sensory materials exhibit real-time response (electrochemical or optical) to the ligand-receptor recognition event. The coupling of a recognition event to photo induced electron transfer or a change in the electronic structure of the conjugated polymer produces changes in the luminescence, UV-Visible absorption, or

redox potential of the polymer. Extensive research has been carried out by using conjugated polymers as chromic or electrochemical biosensors. However, the relatively low sensitivity of UV-Visible absorption measurements, the complex electrochemical instrumentation required, and the nonspecific interactions between biomolecules and conjugated polymers have prevented practical and general use.

Water-soluble conjugated polymers (conjugated poly-electrolytes) show potential for use as a new class of high-sensitivity rapid-response chemical and biological sensors. The fluorescence of these polymers can be quenched by very small amounts of charged molecules (quenchers) that quench the excited state by energy transfer or electron transfer. This quenching can be adapted to biosensing by coupling a quencher to a biological ligand. In aqueous solution, the photoluminescence (PL) from the polymer is quenched when the quencher–ligand conjugate associates with the poly-electrolyte to form a relatively weak conjugate–polymer complex, as a consequence of electrostatic and hydrophobic interactions. Exposure of the conjugate–polymer complex to a biological receptor results in formation of a biospecific receptor–conjugate complex and release of the polymer with concomitant unquenching of the polymer fluorescence.

4.4. Light emitting electrochemical cells (LEC)

Polymer light emitting electrochemical cells provide an alternative way for achieving light emission from electroluminescent polymers³⁷. LECs were first reported in 1995 using the blends of PPV and poly ethylene oxide (PEO) complexed with lithium trifluoromethane sulfonate as the active materials sandwiched between ITO and a metal electrode. PPV acts as the luminescent polymer and PEO complexed with a lithium salt is a polymer electrolyte with relatively high conductivity. The use of a polymer blend however in these devices can result in phase separation between the emissive layer and the polymer electrolyte, which, in turn, can be detrimental to device performance. To overcome this problem, new polymers were designed with covalent linkages between oligo ethylene oxide side chains and the conjugated backbone. Another way to circumvent this phase separation was described by Sun et al. They created a series of block-copolymers in order to improve the compatibility of the two components of the polymer blend. Segments containing three phenylene vinylene units covalently linked with PEO segments were designed.

Chapter 1

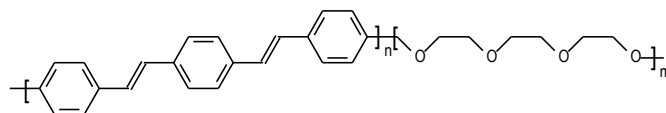


Figure 9. PPV-PEO block copolymer preventing phase separation

LECs are believed to offer a number of potential advantages over LEDs including low operating voltage, high efficiency and insensitivity to the electrode materials.

In the solid state LECs the conjugated polymer is p-doped at the anode and n-doped at the cathode of the device and a light emissive p-n junction is created between the p- and n-doped area. Due to an applied voltage the charges (holes and electrons) migrate through the device and recombination of opposite charges creates an exciton that can undergo a radiative decay and emit light.

Nowadays also colour-variable LECs have been demonstrated consisting of a polymer bilayer structure, BTEO-PPV and a copolymer of BTEO-PPV with normal PPV.

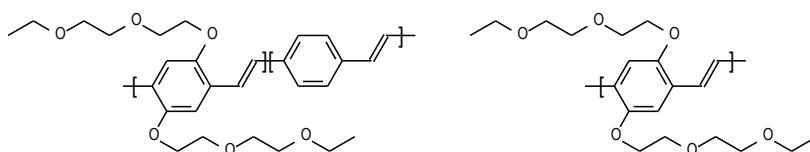


Figure 10. Components of the colour-variable LEC. BTEO-PPV and a copolymer of BTEO-PPV with normal PPV

Due to the asymmetry of electron and hole injection and transport the p-n junction is closer to one of the electrodes. Wiring the electrode closest to the homopolymer as negative results in an orange-red light emission. On the other hand wiring the electrode close to the copolymer layer as negative results in a yellow-green emission.

5. Aim and outline of the thesis

The aim of the research presented in this work is the synthesis and characterisation of some polar and functionalised PPV derivatives through the sulfinyl precursor route. These polar and functional conjugated polymers have become a new and very interesting topic in the field of the conjugated polymers over the last few years³⁸. The functional polymers exhibit unique properties often due to the fact that the functional groups are mostly different from the polymer backbone. Because of the functional groups the polymer becomes a subject for performing post-polymerisation functionalisation reactions where new or other functional groups are covalently linked to the backbone. Another new field in the conjugated polymer section is the synthesis of water-soluble polymers with ionic side groups that can find their possible applications in the (biosensor) field.

In literature only very little functional or water-soluble PPV derivatives have been discussed. Such functionalised PPV derivatives may be very useful in several applications. So the need of creating these functional PPV derivatives becomes clear, not only from a fundamental scientific point of view but also to mimic or even improve other systems that have already proven to be useful in a device structure.

In this work the route used towards the synthesis of these functional polymers is the sulfinyl precursor route that has already proven its versatility for several different monomer systems and which enables the researcher to make small adaptations to different experimental parameters without a decrease in the yield or molecular weight.

Due to specific synthetic problems at some points, small adaptations were made to the sulfinyl precursor route in order to polymerise certain monomers. This work will show repeatedly that the sulfinyl route is the most versatile precursor route towards PPV and its derivatives.

In chapter 2 some PPV derivatives containing polar or functionalised sulfinyl side chains will be presented. Both synthesis and characterisation will be addressed. The synthesis of these monomers stems more for a proof of principle since the functional groups are eliminated upon conversion of the precursor polymer to the conjugated structure. However the knowledge we get from these rather easy obtainable systems will be used to set up other more complex synthetic experiments as will be shown during this work.

Chapter 3 deals with the synthesis and characterisation of PPV derivatives bearing the same polar groups or functionalities described in chapter 2 on their phenyl core. In contrast

Chapter 1

to the polymers that are discussed in the previous chapter, here the polar groups remain in the conjugated structure.

Finally in chapter 4 a mechanistic study for the p-quinodimethane formation of sulfinyl monomers is described. This work was given some practical feedback by performing some copolymerisation reactions involving different p-quinodimethane systems.

Note that in the remainder of this thesis, the nomenclature of chemical compounds, schemes, figures and tables starts all over in each chapter.

6. References

- ¹ Shirakawa, H.; Louis, E. J.; MacDiarmid, A. G.; Chiang, C. K.; Heeger, A. H. *J. Chem. Soc. Chem. Comm.* **1977**, 578.
- ² Brédas, J.-L.; Street, G. B. *Acc. Chem. Rev.* **18**, **1985**, 309.
- ³ Burroughes, J. H.; Bradley, D. D. C.; Brown, A. R.; Marks, R. N.; Mackay, K.; Friend, R. H.; Burns, P. L.; Holmes, A. B. *Nature* **347**, **1990**, 539.
- ⁴ Braun, D.; Heeger, A. J. *Appl. Phys. Lett.* **58**, **1991**, 1982.
- ⁵ Wudl, F.; Sardarov, G. *US Patent* **5**, 189, 136, **1993**.
- ⁶ Becker, H.; Spreitzer, H.; Kreuder, W.; Kluge, E.; Schenk, H.; Parker, I.; Cao Y. *Adv. Mater.* **12**(1), **2000**, 42.
- ⁷ Hörhold, H.-H.; Opfermann, J. *Makromol. Chem.* **131**, **1970**, 105.
- ⁸ Lenz, R. W.; Handlovits, C. E. *J. Org. Chem.* **25**, **1960**, 813.
- ⁹ Greenham, N. C.; Moratti, S. C.; Bradley, D. D. C.; Friend, R. H.; Holmes, A. B. *Nature* **365**, **1993**, 628.
- ¹⁰ Heck, R. F. *Accounts Chem. Res.* **12**, **1979**, 146.
- ¹¹ Wessling, R. A.; Zimmerman, R. G. *US Patent* **1969**, 3401152.
- ¹² Wessling, R. A. *J. Polym. Sci., Polym. Symp.* **72**, **1985**, 55.
- ¹³ Lenz, R. W.; Han, C.-C.; Stenger-Smith, J.; Karasz, F. E. *J. Polym. Sci. Polym. Chem.* **26**, **1988**, 3241.
- ¹⁴ a) Denton, F. R. III; Lahti, P. M.; Karasz, F. E. *J. Polym. Sci. Part A: Polym. Chem.* **30**, **1992**, 2223.
b) Cho, B. R.; Kim, Y. K.; Han, M. S. *Macromolecules* **31**, **1998**, 2098.
- ¹⁵ Garay, R.; Lenz, R. W. *Makromol. Chem. Suppl.* **15**, **1989**, 1.
- ¹⁶ Machado, J.M.; Denton, F.R.; Schlenoff, J.B.; Karasz, F.C.; Lathi, P.M.; *J. Polym. Sci. Part B: Polym. Phys.*, **27**, **1989**, 199.
- ¹⁷ Cherry, M.J.; Moratti, S.C.; Holmes, A.B.; Taylor, P.L.; Grüner, J.; Friend, R.H., *Synth. Met.*, **69**, **1995**, 493.
- ¹⁸ a) Gmeiner, J.; Karg, S.; Meier, M.; Riess, W.; Strhriegl, P.; Schwöerer, M. *Acta Polym.* **44**, **1993**, 201. b) Hsieh, B. R.; Antoniadis, H.; Abkowitz, M. A.; Stolka, H. *Polym. Prep.* **33**, **1992**, 414.
- ¹⁹ a) Garay, R. O.; Baier, U.; Bubeck, C.; Mullen, K. *Adv. Mater.* **5**, **1993**, 561. b) Zhang, C.; Braun, D.; Heeger, A. J. *J. Appl. Phys.* **76**, **1993**, 5177.
- ²⁰ Garay, R.; Karasz, F. E.; Lenz, R. W. *J. Macromol. Sci.-Pure Appl. Chem. A* **32**, **1995**, 905.
McCoy, R. K.; Karasz, F. E. *Chem. Mater.* **3**, **1991**, 941.

Chapter 1

- ²¹ Denton, F.R.; Sarker, A.; Lahti, P. M.; Garay, R. O.; Karasz, F. E. *J. Polym. Sci. Part A: Polym. Chem.* 30, **1992**, 2233. Sarker, A.; Lahti, P. M. *Polym. Prep.* 35(1), **1994**, 790.
- ²² Gilch, H. G.; Wheelwright, W. L. *J. Polym. Sci.* 4, **1966**, 1337.
- ²³ Swatos, W. J.; Gordon, B. *Polym. Prep.* 31(1), **1990**, 505.
- ²⁴ Hsieh, B.R.; Yu, Y.; Van Laeken, A.C.; *Macromol.*, 30, **1997**, 8094. Yu, Y.; Van Laeken, A.C.; Lee, H.; Hsieh, B.R.; *Polym. Prepr.*, 39, **1998**, 161. Hsieh, B.R.; Yu, Y.; Forsythe, E.W.; Schaaf, G.M.; Feld, W.A.; *J. Am. Chem. Soc.*, 120, **1998**, 231. Neef, C.J.; Ferraris, J.P.; *Macromol.*, 33, **2000**, 2311.
- ²⁵ Lieve Hontis, *PhD Dissertation*, Limburgs Universitair Centrum, Diepenbeek, **2002**.
- ²⁶ Son S.; Dodabalapur A.; Lovinger A. J.; Galvin M. E. *Science* 269, **1995**, 376. Lo S-C.; Sheridan, A. K.; Samuel I. D. W.; Burn P. L. *J. Mat. Chem.* 10, **2000**, 275. Lo S-C.; Sheridan, A. K.; Samuel I. D. W.; Burn P. L. *J. Mat. Chem.* 9, **1999**, 2165.
- ²⁸ a) Louwet, F.; Vanderzande, D.; Gelan, J.; *Synth. Met.* 52, **1992**, 125. b) Louwet, F.; Vanderzande, D.; Gelan, J.; Mullens, J. *Macromolecules* 28, **1995**, 1330. c) Vanderzande, D.; Issaris, A.; Van Der Borght, M.; van Breemen, A.; de Kok, M.; Gelan, J. *Macromol. Symp.* 125, **1997**, 189.
- ²⁹ Roex Hilde, *PhD Dissertation*, Limburgs Universitair Centrum, Diepenbeek, **2003**.
- ³⁰ a) van Breemen, A.; Vanderzande, D.; Adriaensens, P.; Gelan, J. *J. Org. Chem.* 64, **1999**, 3106. van Breemen, A. *Ph.D. Dissertation*, **1999**, Limburgs Universitair Centrum, Diepenbeek, Belgium. b) Kim, K. S.; Hwang, H. J.; Cheong, C. S.; Hahn, C. S. *Tetrahedron Lett.* 31, **1990**, 2893.
- ³¹ Kesters E.; Lutsen L.; Vanderzande D.; Gelan J.; Nguyen T. P.; Molinié P. *Thin Solid Films* 403-404, **2002**, 120. Els Kesters, *PhD Dissertation*, Limburgs Universitair Centrum, Diepenbeek, **2002**. Durst, T. *Comprehensive Organic Chemistry volume 3* Jones, D. N., Oxford Pergamon **1979**, 121. Trost, B. M.; Salzmann, T. N.; Hiroi, K. J. *J. Am. Chem. Soc.* 98, **1976**, 4887. Trost, B. M. *Acc. Chem. Res.* 11, 1978, 453. Paptai, S. *The chemistry of Sulphones and Sulphoxides*, John Wiley & Sons Ltd., Chichester, UK, **1988**.
- ³² a) Bradley, D. D. C. *Synth. Met.* 54, **1993**, 401. b) Friend, R. H.; Gymer, R. W.; Holmes, A. B.; Burroughes, J. H.; Marks, R. N.; Taliani, C.; Bradley, D. D. C.; Dos Santos, D. A.; Brédas, J. L.; Lögdlund, M.; Salaneck, W. R. *Nature* 397, **1999**, 121.
- ³³ Rothberg, L. J.; Yan, M.; Papadimitrakopoulos, F.; Galvin, M. E.; Kwock, E. W.; Miller, T. M. *Synth. Met.* 80, **1996**, 41.
- ³⁴ a) Brabec, C. J.; Sariciftci, N. S.; Hummelen, J. C. *Adv. Funct. Mater.* 11, **2001**, 15. b) Brabec, C. J.; Sariciftci, N. S. *Monatshefte für Chemie* 132, **2001**, 421. c) Yu, G.; Gao, J.; Hummelen, J. C.;

Wudl, F.; Heeger, A. J. *Science* 270, **1995**, 1789. d) Halls, J. J. M.; Walsh, C. A.; Greenham, N. C.; Marseglia, E. A.; Friend, R. H.; Moratti, S. C.; Holmes, A. B. *Nature* 376, **1995**, 498.

³⁵ Munters T.; Martens T.; Goris L.; Vrindts V.; Manca J.; Lutsen L.; De Ceuninck P.; Vanderzande D.; De Schepper L.; Gelan J.; Sariciftci S.; Brabec C. *Thin Solid Films* 403-404, **2002**, 247.

³⁶ Akcelrud, L. *Prog. Polym. Sci.*, 28, **2003**, 875. Pron, A. *Prog. Polym. Sci.*, 27, **2002**, 135. Shi, S.; Wudl, F. *Macromolecules*, 23, **1990**, 2119. Wang, J.; Wang, D.; Miller, E.K.; Moses, D.; Bazan, G.C.; Heeger, A.J. *Macromolecules*, 33, **2000**, 5153. Fan, C.; Plaxco, K.W.; Heeger, A.J. *J. Am. Chem. Soc.*, 124, **2002**, 5642. Gaylord, B.S.; Wang, S.; Heeger, A.J.; Bazan, G.C. *J. Am. Chem. Soc.*, **2001**, 18. Hong, J.W.; Gaylord, B.S.; Bazan, G.C. *J. Am. Chem. Soc.*, 124, **2002**, 11868. Wallace, G.G.; Kane-Maguire, L.A.P. *Adv. Mater.*, 14, **2002**, 13. Li, Y.; Yang, M.J., *Sensors and actuators*, 85, **2002**, 73.

³⁷ Huang, C.; Huang, W.; Guo, J.; Yang, C.Z.; Kang, E.T. *Polymer*, 42, **2001**, 3929. Li, F.; Coa, Y.; Gao, J.; Wang, D.; Yu, G.; Heeger, J.A. *Synth. Met.*, 99, **1999**, 243. He, G.; Yang, C.; Wang, R.; Li, Y. *Displays*, 21, **2000**, 69. Garay, R.O.; Mayer, B.; Karasz, F.E.; Lenz, R.W. *Journal of the polymer Science*, 33, **1995**, 525. Morgado, J.; Cacialli, F.; Friend, R.H.; Chuah, B.S.; Rost, H.; Holmes, A.B. *Macromolecules*, 34, **2001**, 3094. Yang, C.; He, G.; Sun, Q.; Li, Y. *Synth. Met.*, 124, **2001**, 449. Tasch, S.; Holzer, L.; Wenzl, F.P.; Gao, J.; Winkler, B.; Dai, L.; Mau, A.W.H.; Sotgiu, R.; Sampietro, M.; Scherf, U.; Müllun, K.; Heeger, A.J.; Leising, G. *Synth. Met.*, 102, **1999**, 1046. Holzer, L.; Winkler, B.; Wenzl, F.P.; Tasch, S.; Dai, L.; Mau, A.W.H.; Leising, G. *Synth. Met.*, 100, **1999**, 71. Morgado, J.; Friend, R.H.; Cacialli, F.; Chuah, B.S.; Rost, H.; Moratti, S.C.; Holmes, A.B. *Synth. Met.*, 122, **2001**, 111. Sun, Q.J.; Wang, H.Q.; Yang, X.G.; Wang, C.H.; Liu, D.S.; Li, Y.F. *Thin Solid Films*, 417, **2002**, 14. Huang, C.; Huang, G.; Guo, J.; Huang, W.; Kang, E.T.; Yang, C.Z. *Polymer preprints*, 43, **2002**, 574.

³⁸ Pinto, M.R.; Schanze, K.S., *Synthesis*, 9, **2002**, 1293.

Chapter 2

Synthesis and Characterisation of Functional Sulfinyl PPV Precursor Polymers

1. Introduction

1.1. Monomer synthesis through the sulfinyl route

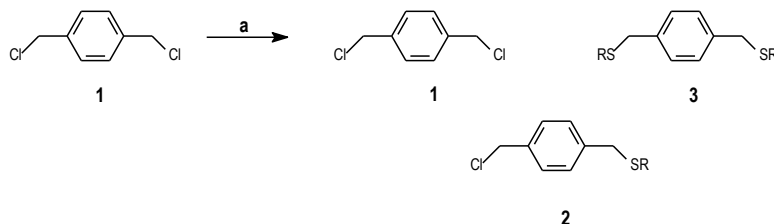
As mentioned in chapter 1, the sulfinyl precursor route commands the use of a non-symmetrical substituted *p*-xylene derivative. This compound is equipped with a halogen atom, commonly chlorine, in the α -position of the *p*-xylene. This halogen atom acts as the leaving group to afford a *p*-quinodimethane system. On the α' -position the *p*-xylene derivative bears a sulfinyl group. This group is used because it can readily stabilize the benzylic anion, which is formed by basic proton abstraction next to the sulfinyl group of the compound. Also the sulfinyl group is a stable group at room temperature but is a very good eliminable group at elevated temperatures.

The sulfinyl monomer in this precursor route can easily be obtained through mild oxidation of a sulfanyl compound¹. Mild oxidative conditions prevent over-oxidation to the sulfonyl stage. This sulfonyl functionality is less desired since it requires higher elimination temperatures to convert the precursor polymer into the conjugated material². Where the conversion of the sulfanyl compound into the sulfinyl is an easy and straightforward step, the synthesis of the thioether is somewhat more difficult.

We will give a short overview of the synthesis of such non-symmetrically substituted sulfanyl compounds. Apparently the easiest method for synthesis of the desired thioether is treatment of α, α' -dichloro-*p*-xylene **1** with a thiolate anion in a 1/1 ratio^{3a}. However only moderate yields can be obtained since a mixture of three products in a statistical distribution will be obtained. The α, α' -dichloro-*p*-xylene **1**, the α -chloro- α' -alkylsulfanyl-*p*-xylene **2** and

Chapter 2

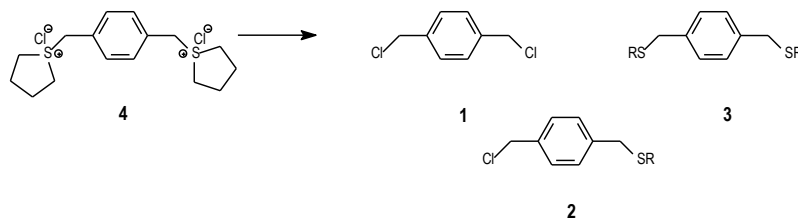
the α,α' -dialkylsulfanyl-*p*-xylene **3** are obtained in a typical 1 / 2 / 1 ratio. Although such yield of fifty percent is not unsatisfactory, purification of the mixture using simple column chromatography will be complicated as these three compounds differ little in R_f-value as observed on TLC.



Scheme 1. Thioether synthesis starting from α,α' -dichloro-*p*-xylene yielding a statistical 1/2/1 mixture.
a : MeOH, R-S, room temperature

Another way for introducing a higher selectivity towards synthesis of the non-symmetrical substituted *p*-xylene derivative is the use of a phase transfer catalyst^{3b} (Aliquat 336). There the α,α' -dichloro-*p*-xylene is dissolved in the organic phase (toluene) and the thiolate anion is dissolved in the aqueous phase. To avoid the formation of the unwanted dialkyl sulfanyl derivative an excess of the α,α' -dichloro-*p*-xylene (2.2 equivalents) is used. However again a mixture of three compounds **1**, **2** and **3** is formed with still the same purification problems. The third and most inventive route towards the synthesis of the thioether is the use of a bissulfonium salt **4** as a starting product (Scheme 2). This method was developed within our research group by Albert Van Breemen⁴. Treatment of the α,α' -bissulfonium-*p*-xylene **4** with a strong base yields a *p*-quinodimethane system. In chapter one we mentioned the Wessling precursor route where the same *p*-quinodimethane system readily polymerises to yield a precursor polymer **5**. However in the presence of a nucleophile an addition reaction on the *p*-quinodimethane system can occur by varying the concentration of the reaction mixture. In these conditions very high yields of the mono-thioether can be obtained. Thanks to this high selectivity this route is used further on. Strict conditions have to be applied to obtain the highest selectivity and a 1/1/1 ratio of base, thiol and bissulfonium salt is recommended.

Synthesis of functional PPV precursor polymers



Scheme 2. Thioether synthesis starting from a α, α' -bissulfonium-xylene yielding the three compounds **1**, **2** and **3** in a 5/90/5 ratio

The bissulfonium salt solution (0.1 M) is stirred at room temperature. Another solution containing the thiol (1 equivalent) and the base (1 equivalent) is prepared and added to the bissulfonium salt solution. The resulting mixture is stirred for one more hour and then the solvent (methanol) is evaporated. Azeotropic distillation of the THT with *n*-octane or high boiling petroleum ether yields the thioether **2** in a high yield. Mostly the thioether yet contaminated with small amounts of dichloride **1** and dithioether **3** is oxidized without any purification.

1.2. Synthesis of polar and functional monomers

Nowadays in literature a lot of attention has been paid to polar, functional and water-soluble conjugated polymers⁶. These polymers may have promising properties for applications such as (bio)-sensor devices⁷ and light emitting electrochemical cells⁸ or they can act as a substrate for post-polymerisation functionalisation reactions.

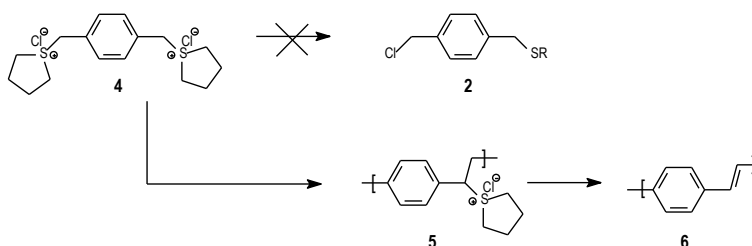
Inspired by this quest in literature the idea for the synthesis of polar and/or water-soluble poly-electrolytes grew within our research group. The use of water or alcohols as a probable solvent for the polymerisation reaction and processing has major advantages concerning ecological and economical perspectives. Also the presence of an extra functionality in the polymer offers a broad range of possible applications.

In a first step, the synthetic introduction of different functionalities on the backbone of the PPV precursor polymer was achieved by functional alkylthiols. This procedure has the advantage that in only a few synthetic steps the functional polymer can be obtained. This method thus acts more like a proof of principle since the functional groups will be eliminated when converting the precursor polymer in its conjugated counterpart. However interesting

information can be obtained from such experiments concerning compatibility of the different functional groups with the chemistry of the sulfinyl precursor route.

Possible applications for such precursor polymers with an eliminable functional sulfinyl chain seem not manifold. However as a proof of principle some preliminary experiments were performed on laser assisted elimination of the sulfinyl group. Here the precursor polymer is cast from a common solvent. After laser conversion of some parts of the precursor film into the conjugated structure the remaining precursor polymer can be removed by washing the sample. The conjugated part remains on the substrate.

At first sight the synthesis of PPV precursor polymers with a polar sulfinyl side chain looks rather easy but it turned out to be quite challenging. Applying the reaction conditions proposed by Albert Van Breemen did not yield the thioether **2** in high yield. In contrast the solution of the bissulfonium salt **4** turned dark yellow upon addition of the thiolate solution. It turned out that a Wessling precursor polymer **5** was formed and this polymer probably underwent already some basic elimination of the sulfonium groups resulting in a partially conjugated polymer with a yellow colour (Scheme 3).



Scheme 3. Formation of a Wessling precursor polymer inhibiting the formation of the desired thioether when the bissulfonium salt concentration is too high

Several attempts were made to inhibit this unwanted side reaction. Since the Wessling route is proposed to proceed through a radical chain mechanism⁹ the addition of radical inhibitors seemed a possible solution to circumvent the problem of unwanted polymerisation. Upon adding TEMPO (tetramethylpiperidinyloxide), an example of a radical inhibitor¹⁰, to the bissulfonium salt solution the desired compound could be obtained but only in very low yield (2-3%). (Figure 1)

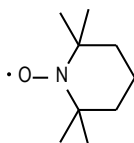
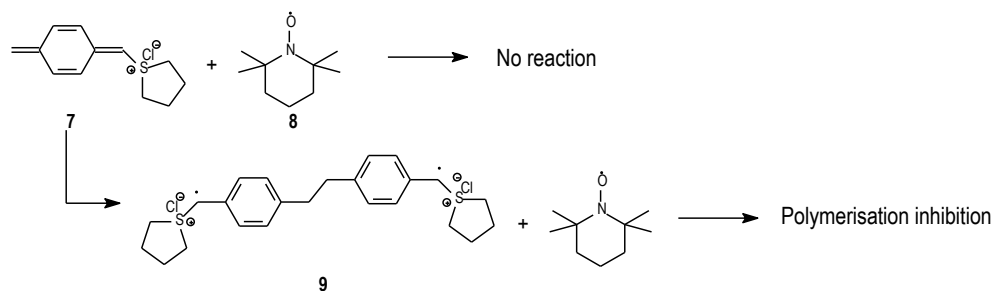


Figure 1. Chemical structure of TEMPO

This can be explained as TEMPO **8** can only interact with radical species and the radicals in the solution are only formed after initiation of the polymerisation, since initiation is believed to occur through dimerisation¹¹ of two *p*-quinodimethane systems **7**. Hence only the polymerisation reaction initiated by the initiating dimers will be inhibited resulting in only low thioether amounts.



Scheme 4. Possible reactions upon addition of TEMPO to the bisulfonium salt solution

Another and eventually a better attempt to solve this problem of unwanted Wessling polymerisation was to adjust for the concentration of the solutions in which the thioether has to be synthesised. As mentioned earlier it is understood that initiation of the Wessling polymerisation only takes place when the combination of two *p*-quinodimethane systems yields a biradical that acts as the radical initiator in polymerisation. The rate equation for the dimerisation reaction is thus proportional to the second power of the *p*-quinodimethane concentration [QM].

$$v_i \approx k_i [QM]^2$$

Where v_i is the rate of the initiation and k_i is the rate constant for this particular reaction. So normally by diluting the solutions, the rate of radical initiation can be reduced and nucleophile attack will be preferred to initiation since the rate of nucleophilic addition to the

Chapter 2

p-quinodimethane system is only proportional to the concentration of the *p*-quinodimethane system in first order.

$$V_{nucl} \approx k_{nucl} [Nu][QM]$$

So when diluting the solutions seven times to obtain a 0.014 molar bissulfonium salt solution indeed a large increase of the thioether yield was observed. Yields up to 76 % were obtained for the monomers discussed further on. For the diluted solutions the reaction time was also prolonged from one hour to four hours or more. Diluting the solutions not only had a positive effect on the yield of the reaction, moreover another interesting advantage was observed. Normally in the thioether synthesis of aliphatic derivatives also a small amount of the dithioether compound (5%) can be detected which complicates purification even more. For the polar derivatives no dithioether was formed and the α,α' -dichloro-*p*-xylene and the thioether had R_f values that differ enough one from another to allow a very simple and effective column purification.

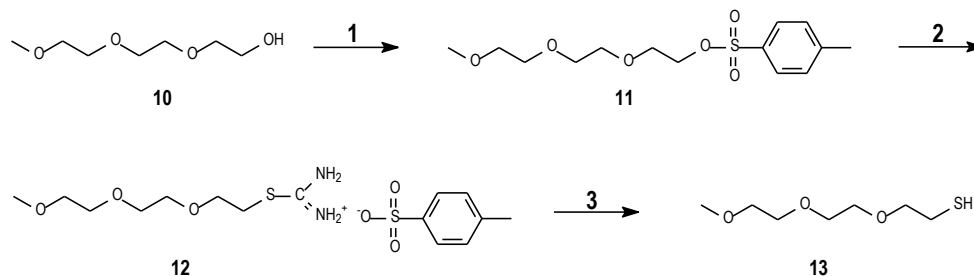
2. Synthesis and polymerisation of functional PPV monomers

In this chapter the synthesis of four monomers is described all with different functionalities on their sulfinyl side chain. The functionalities are an alcohol, an ester, a sulfonate salt and a triethylene glycol derived group. The exact synthetic conditions and polymerisation results are resumed further on for each monomer separately.

2.1. Synthesis of a triethylene glycol derived sulfinyl polymer

2.1.1. Monomer synthesis

The first monomer discussed is the one with an oligo ethylene oxide sulfinyl chain. This tail was chosen because of its polar and water-soluble properties. Such chains are also known for their cation binding properties, which makes them interesting species for cation recognition in solution. The required thiol **13**, 2-(2-(2-methoxy-ethoxy)ethoxy)ethanethiol, had to be synthesised since it is not commercially available. Starting from the corresponding alcohol **10** the tosylate ester **11** can be obtained in very good yield¹². After purification this tosylate ester can be converted to the thiol using thio urea and subsequent hydrolysis of the thio urea salt¹³ (scheme 5).



Scheme 5. Synthesis of 2-(2-(2-methoxy-ethoxy)ethoxy)ethanethiol 1 : NEt_3 , $TosCl$, $CHCl_3$, room temperature, 2 : thiourea, acetone, reflux, 3 : $NaHCO_3/H_2O$, HCl

Two procedures for the thiol synthesis were tested. The first literature procedure was performed in ethanol where the thiolate anion is formed in situ¹⁴. This approach only gave low yield of the desired thiol (Table 1). The second attempt where the thio urea salt **12** is formed in acetone and subsequently hydrolysed using K_2CO_3/H_2O gave better yields. A reason for this difference was not found.

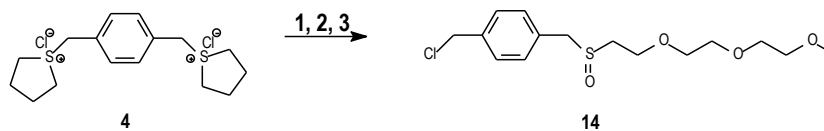
Solvent	Yield (%)	Conditions
Ethanol	21	One pot
Acetone	78	Two step

Table 1. Overview of reaction conditions of thiol synthesis

Commonly in literature alkyl bromides are used for thiol synthesis involving thio urea. The reason for the use of the uncommon tosylate ester is that the reaction can be monitored using simple TLC.

The thioether was synthesised as described before. A methanol solution of the thiol **13** and sodium t-butoxide as the base is added dropwise to a solution of α, α' -bissulfonium-*p*-xylene **4** and the mixture is stirred for four hours at room temperature. After removal of the methanol, n-octane is added to remove the THT. This step is repeated three times. Then the solution is extracted with dichloromethane/ water and the organic phase is dried. A column chromatographic purification on SiO_2 and ether as the eluent yields the desired product.

Oxidation of the thioether with H_2O_2 using methanol as the solvent and TeO_2/HCl as the catalyst system gives us the desired sulfinyl compound (Scheme 6).



Scheme 6. Synthesis of monomer **14** 1 : 2-(2-(2-methoxy-ethoxy)ethoxy)ethanethiol, Na-tBuO, 2 : n-octane, ΔT , 3 : TeO₂/H₂O₂, MeOH, HCl_{cat}

2.1.2. p-Quinodimethane formation

The key step in the polymerisation of sulfinyl monomers is the formation of a reactive *p*-quinodimethane system that acts as the real monomer in the polymerisation reaction¹⁵. The absence of this *p*-quinodimethane system rules out the possibility of a radical chain polymerisation since no initiation by coupling of two quinoid structures can occur. On the other hand, the presence of a *p*-quinodimethane system neither does imply that there will be formation of the precursor polymer. In literature several examples of stable *p*-quinodimethane system have been described that do not polymerise without an external initiator. The most cited among these stable *p*-quinodimethane system is the tetra-cyano derivative¹⁶ (Figure 2). This electron accepting *p*-quinodimethane system has extensively been studied in connection with its charge-transfer complexes showing high electric conductivities, often referred to as organic metal.

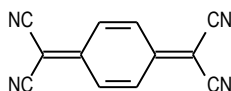


Figure 2. Structure of 7,7,8,8-tetracyanoquinodimethane, a stable quinoid system

As mentioned in chapter one the formation of a *p*-quinodimethane system can be clearly monitored by means of UV-Vis spectroscopy. *p*-Quinodimethane systems have a typical absorption band around 313 nm. The solvent was 2-butanol and a 10⁻⁴ molar solution of the monomer in a quartz cuvet was treated with an excess of base. In such a UV-Vis experiment the spectrum is scanned periodically and three trends become clear. At lower wavelength the signal of the monomer decreases constantly in time. At 313 nm a new absorption band appears, indicating the formation of the *p*-quinodimethane system (Figure

3). After a quick increase of this signal a decrease is observed due to solvent substitution. After a while a third band appears as a result of this solvent substitution (Figure 4).

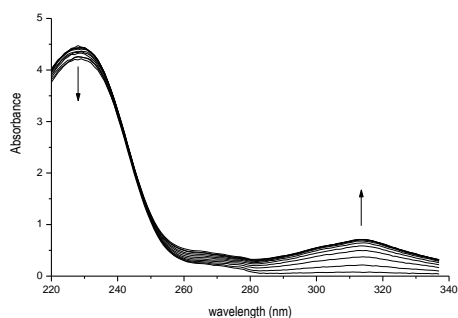


Figure 3. Formation of the *p*-quinodimethane system and decrease of the monomer

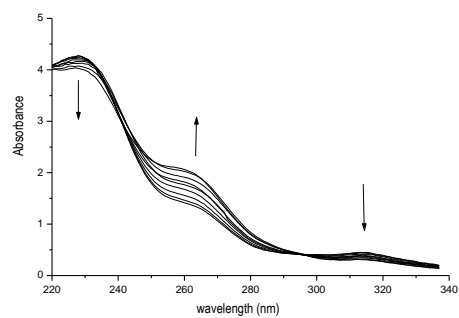


Figure 4. Decrease of the *p*-quinodimethane and formation of the solvent substituted product.

The three signals of interest can be plotted as a function of time as depicted in figure 5.

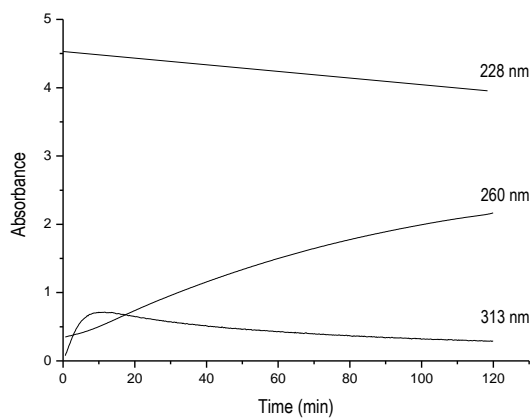
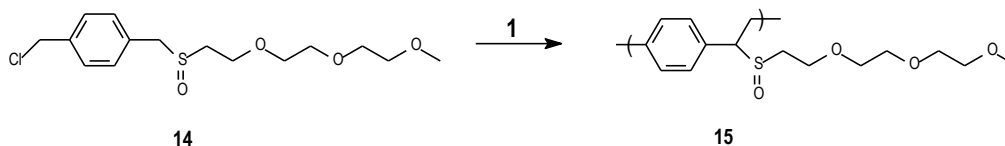


Figure 5. Plot of the signals at 220, 315 and 250 nm versus time

2.1.3. Polymerisation of monomer **14**Scheme 7. Polymerisation of monomer **14**. 1 : 2-BuOH, Na-tBuO (1.3 equivalents), 30°C, N₂

The polymerisation reactions of the obtained monomers are performed using the standard conditions developed by A. Van Breemen *et al.*. A solution of the monomer (2 mmol) in 14 ml of solvent (2-butanol unless stated otherwise) is stirred at 30 °C while passing through a continuous stream of nitrogen. A base solution (sodium t-butoxide, 2.6 mmol) in 6 ml of the same solvent is added in one portion and the resulting mixture is stirred for one hour while still passing nitrogen through the solution (Scheme 7). The mixture is poured into an amount of water and extracted with chloroform or dichloromethane. After evaporation of the organic solvent, the precursor polymer **15** is precipitated in a non-solvent, collected through filtration and dried in vacuo. High molecular weight polymers can be obtained using this route as determined using SEC measurements versus polystyrene standards in DMF. Also the influence of the concentration on the yield and molecular weight were investigated. When the monomer concentration is increased the molecular weight of the precursor polymer becomes higher while there is no significant change in the yield and the polydispersity (Table 2). From figure 6 it can be seen that there is almost a linear correlation between the concentration of the monomer and the molecular weight. This observation is consistent with a rate of polymerisation much faster than the rate of the initiation reaction and thus a high *p*-quinodimethane concentration does not result in more polymer chains but in an increase of the molecular weight of the polymers.

Concentration mM	Yield (%)	Mw ($\times 10^3$)
1.03	68	499
1.24	65	570
1.57	72	714
1.87	67	817

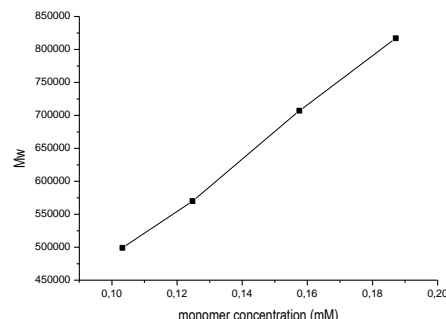
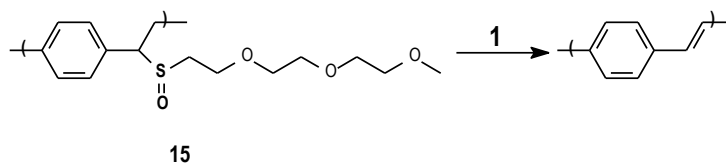


Table 2. Influence of the monomer concentration on molecular weight

Figure 6. Plot of the molecular weight of precursor polymer **15** as a function of the monomer concentration in the polymerisation reaction

2.1.4. Conversion of the precursor polymer into the conjugated material



Scheme 8. Formation of the fully conjugated PPV. 1: ΔT

The final step in the sulfinyl precursor route is the formation of a fully conjugated polymer by applying a thermal treatment to the precursor polymer **15** resulting in the expulsion of a sulfenic acid (scheme 8). This conversion step of the precursor polymer into the conjugated form was analysed with different in situ analytical techniques like UV-Vis spectroscopy, FT-IR spectroscopy and DIP-MS.

The in situ UV-Vis measurements were carried out on a polymer film that is spincoated on a quartz disc. This quartz disc is placed in a specially designed oven allowing a dynamic heating program of 2 degrees per minute up to 300°C or more under a continuous flow of nitrogen. The oven is placed in the beam of the spectrometer and the monitoring of the elimination process is readily started. Initially the precursor polymer has a strong absorption at circa 230 nm. Upon heating the polymer sample new absorption bands appear that

gradually redshift with increasing temperature. A maximum wavelength of 415 nm for the conjugated system is observed (figure 7). Figure 8 shows the absorption at 415 nm versus the temperature of the oven. From this plot it is clear that the elimination process is started at circa 56 °C. The polymer shows thermal stability up to 250°C.

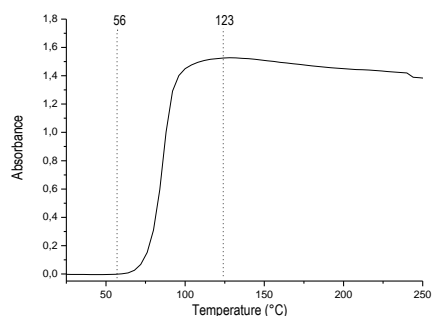
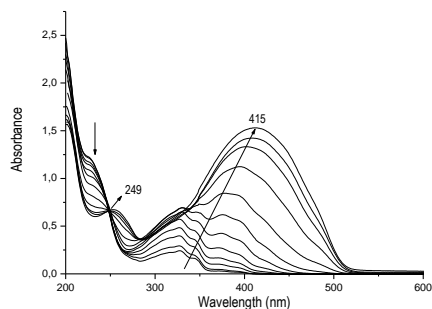


Figure 7. Gradual formation of the conjugated structure for polymer **15** Figure 8. Plot of the absorbance at 415 nm versus temperature.

The thermal elimination process was also studied with in situ FT-IR spectroscopy. An identical set-up was used as described for the in situ UV-Vis measurements except that the quartz disc is replaced with a KBr pellet. FT-IR spectroscopy allows the monitoring of specific functional groups in the molecule. The signal at 1040 cm^{-1} arises from the S=O stretching and the signal around 960 cm^{-1} is assigned to the vinylene group. As the heating program is applied the S=O signal decreases with increasing temperature while the vinylene signal becomes stronger indicating expulsion of the sulfenic acid and formation of the double bond (figure 9). Plotting of the S=O and vinylene signal versus temperature yields a figure as depicted in figure 10. The formation of the double bonds starts at 53 °C. The S=O signal shows the opposite trend resulting in a decrease of the signal at 1040 cm^{-1} .

The data obtained both from the UV-Vis and FT-IR measurements are in good accordance with each other.

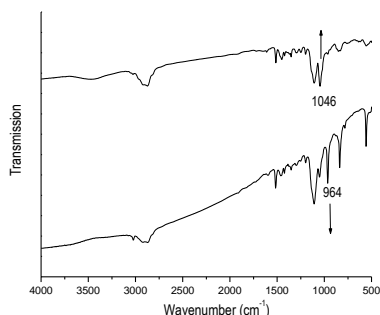


Figure 9. FT-IR spectrum of polymer **15** before (below) and after (upper) thermal conversion

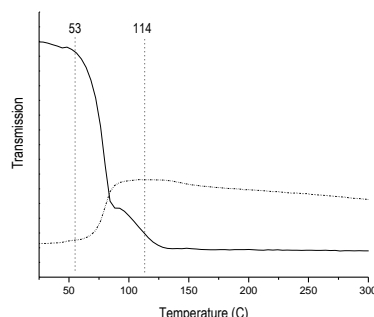


Figure 10. Plot of signals at 960 and 1040 cm^{-1} versus temperature

A third technique used to monitor the elimination process is direct insert probe mass spectroscopy. With this technique information about the different elimination products is obtained. The precursor polymer is placed on the probe and a heating program of 10 degrees per minute is applied under vacuum conditions. With this technique normally a plot of the total ion current versus the temperature is obtained where two distinct signals can be observed. The first signal at 112°C arises from the elimination and evaporation of the sulfenic acid and its derived products. The second signal at 500°C is assigned to the total degradation and evaporation of the degradation products. In table 3 the observed mass fragments are presented.

Signal at 112°C	
<i>m/z</i>	<i>fragment</i>
358	$\text{CH}_3(\text{OC}_2\text{H}_4)_3\text{SS}(\text{C}_2\text{H}_4\text{O})\text{CH}_3$
228	$\text{CH}_3(\text{OC}_2\text{H}_4)_3\text{S}(\text{O})\text{S}$
212	$\text{CH}_3(\text{OC}_2\text{H}_4)_3\text{SS}$
179	$\text{CH}_3(\text{OC}_2\text{H}_4)_3\text{S}$
147	$\text{CH}_3(\text{OC}_2\text{H}_4)_3$
103	$\text{C}_5\text{H}_{11}\text{O}_2$

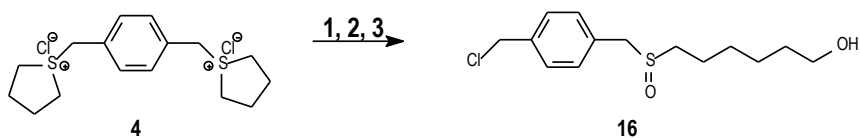
Table 3. Overview of DIP-MS fragments at 112°C

2.2. Synthesis of an alcohol derived polymer

A second monomer now with an alcohol functionality on the sulfinyl chain is presented here. For the synthesis of the monomer the same diluted reaction conditions were used as described for monomer 1. In contrast with the ethylene glycol derived thiol, the alcohol functionalised thiol is commercially available. The presence of an alcohol function can be a very grateful feature since hydroxy groups can easily be converted into other functional groups using quite simple chemistry. The articles about alcohol conversions are unlimited. Some very well known examples are the conversion into alkyl halides, esters, oxidation to aldehydes and carboxylic acids.

2.2.1. Monomer synthesis

The thiol used in this case was 6-mercapto-1-hexanol since it was the longest chain available. The choice for a longer aliphatic chain relates to an improved solubility since the longer the chain the better the solubility will be. Again a methanol solution of thiol and the base is added to a stirred solution of the bisulfonium salt **4** and the mixture is stirred for four hours. Evaporation of the methanol followed by azeotropic removal of the THT with *n*-octane yields the thioether in high yield. Oxidation yields the sulfinyl compound **16** as a yellow oil. Note that a free alcohol function does not interfere during reaction due to a higher acidity and nucleophilicity of a sulfur anion compared to an alkoxide.



Scheme 9. Synthesis of monomer **16**. 1 : 6-mercapto-1-hexanol, Na-*t*BuO, 2 : *n*-octane, ΔT , 3 : TeO₂/H₂O₂, MeOH, HCl_{cat}

2.2.2. *p*-Quinodimethane formation

The possibility of polymerisation of the alcohol monomer in the presence of a base was first tested on the formation of the necessary *p*-quinodimethane system using UV-Vis spectroscopy. Again the solvent was 2-butanol and a 10⁻⁴ molar solution of the monomer in a quartz cuvet was treated with an excess of base. Again the three signals described in the

experiments above become visible. There is the decrease of the monomer signal, the in growth and decrease of the *p*-quinodimethane system at 313 nm and the formation of the solvent substituted product (figure 11, 12). Since we obtain a substantial *p*-quinodimethane system signal at 313 nm conditions are likely to favour polymerisation.

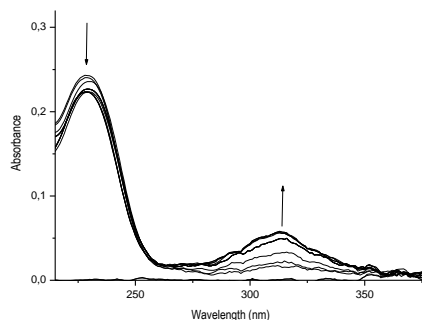


Figure 11. Formation of the quinodimethane system and decrease of the monomer

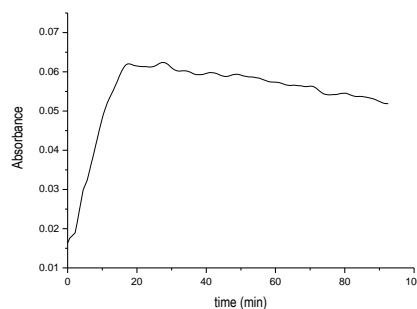
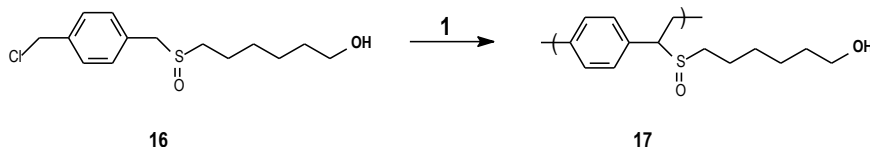


Figure 12. Plot of absorption at 313 nm versus time

2.2.3. Polymerisation of the monomer



Scheme 10. Polymerisation of monomer **16**. 1 : 2-BuOH, Na-tBuO (1.3 equivalents), 30°C, N₂

The alcohol monomer was polymerised using standard polymerisation conditions. The solution of the monomer is treated with 1.3 equivalents of base and the resulting mixture was stirred for one hour under an inert atmosphere at 30°C (scheme 10). The reaction is then poured into an amount of ice water whereupon the precursor polymer precipitated. However unlike previous reactions this polymer could not be dissolved in common organic solvents like chloroform or dichloromethane. Only upon addition of 2-butanol to the mixture the polymer was dissolved and extraction of the mixture could be performed. The organic layers were combined and the solvent was removed as much as possible under reduced

pressure. The polymer was precipitated in a non-solvent and dried in vacuo to yield a white solid. This dried material turned out to be again insoluble, even in alcohols, making characterisation impossible since simple NMR-spectroscopy or GPC measurements require completely dissolved polymer samples. This insolubility is most likely caused by inter-chain hydrogen bonding resulting in a physically, non-covalently linked resin.

This kind of interaction in PPV derivatives was also described by Ajayaghosh and co-workers¹⁶ who synthesised an alcohol functionalised PPV trimer which assembled through these hydrogen bridges and π -stacking resulting in self-assembled organogel nanostructures (figure 13). However the gelling efficiency of this compound was strongly reduced by the addition of small amounts of hydrogen bonding solvents such as methanol resulting in the solving of the compound. The difference of this compound and our precursor polymer is the much higher molecular weight of the latter which corresponds to more interaction sites per chain.

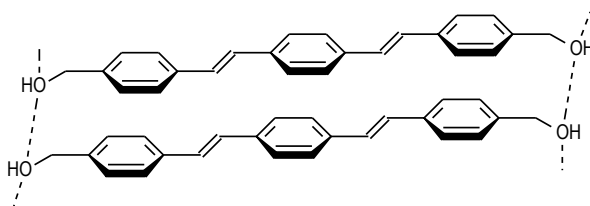
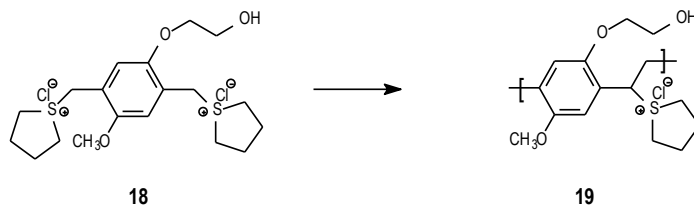


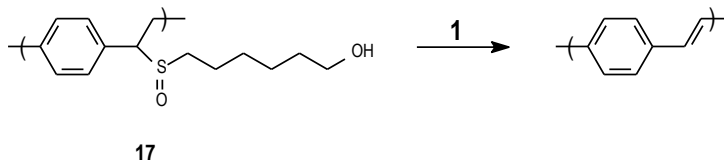
Figure 13. Formation of organogel nanostructure due to hydrogen bonding of an alcohol functionalised PPV oligomer

The insolubility problem of alcohol functionalised PPV derivatives was also observed by Benjamin and coworkers¹⁷ who studied the Wessling polymerisation of compound **18**. Homo-polymerisation of this monomer resulted in an insoluble precursor polymer **19** due to aggregation.



Scheme 11. Wessling polymerisation of an alcohol functionalised monomer yielding an insoluble precursor polymer

2.2.4. Conversion of polymer into the conjugated structure



Scheme 12. Formation of the fully conjugated PPV. 1: ΔT

Although polymerisation of the alcohol monomer resulted in an insoluble precursor polymer allowing almost no characterisation, the conversion of this precursor (scheme 12) into the conjugated material can be monitored by in situ UV-Vis and FT-IR spectroscopy and DIP-MS.

For the UV-Vis experiment a piece of precursor polymer was added to 2 ml methanol. As mentioned before the polymer did not dissolve but an enormous swelling of the sample could be observed. The swollen precursor polymer was wiped on a quartz disc and then the solvent was evaporated by flushing air over the sample. This was repeated three times to ensure an acceptable thickness of the polymer film. The quartz disc is placed in an oven in the spectrometer and a heating program of 2°C per minute up to 350°C is applied. Again new absorption bands appear as the sample is heated red shifting to a maximum absorption at 422 nm (figure 14). A plot of the absorption at 422 nm as a function of temperature is depicted in figure 15. According to this plot elimination starts at 67 °C. The polymer seems stable up to at least 350°C.

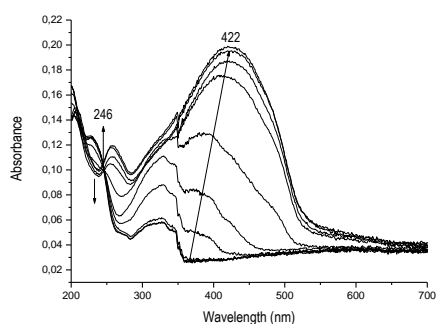


Figure 14. Gradual formation of the conjugated structure

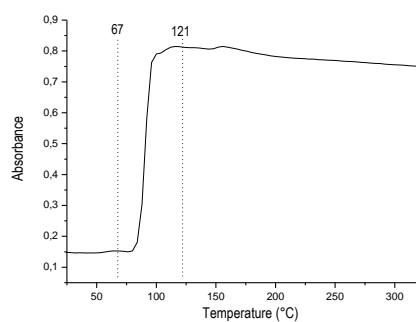


Figure 15. Plot of absorption at 422 nm versus temperature

Chapter 2

For the in situ FT-IR measurements the methanolic precursor polymer was wiped over the KBr pellet and the pellet was placed in the oven. The same dynamic heating program as used for the UV-Vis measurements was used and the signals of interest are plotted as a function of time (figure 17). Formation of the double bond starts at 66°C. Again the S=O signal at 1022 cm⁻¹ shows the opposite trend. Note also that the signal at 3400 cm⁻¹, arising from the OH groups decreases with increasing temperature indicating that the alcohol groups are also expelled from the polymer matrix (figure 16).

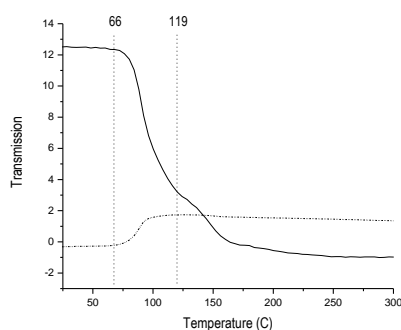
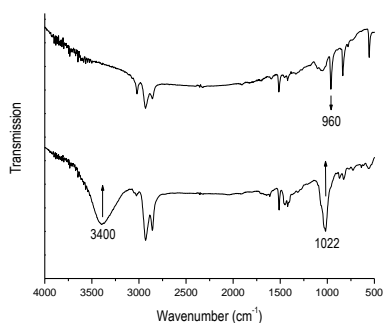


Figure 16. FT-IR spectrum of polymer **17** before (below) and after (upper) thermal conversion

Figure 17. Plot of signals at 960 and 1022 cm⁻¹ versus temperature

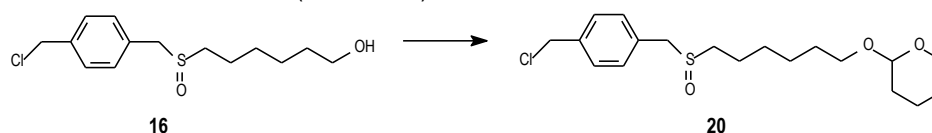
The third technique applied to characterise the alcohol precursor polymer is DIP-MS. Again the solid sample is placed on the probe and a heating program of 10°C per minute is applied. Here a spectrum shape is observed identical to the spectrum of all other sulfinyl precursor polymers. Clearly two signals can be detected. The first, at 128 °C is attributed to the elimination of the sulfinyl chain resulting in a range of elimination products (table 4). The second peak at 531°C is due to evaporation of the degradation products of the conjugated polymer.

Signal at 128°C	
<i>m/z</i>	<i>fragments</i>
298	$\text{HOC}_6\text{H}_{12}\text{S}(\text{O})_2\text{SC}_6\text{H}_{12}\text{OH}$
266	$\text{HOC}_6\text{H}_{12}\text{SSC}_6\text{H}_{12}\text{OH}$
132	$\text{HOC}_6\text{H}_{12}\text{S}$
101	$\text{C}_6\text{H}_{12}\text{OH}$

Table 4. Overview of DIP-MS fragments at 128°C

2.2.5. Protection of the alcohol function

In order to circumvent solubility problems and inhibit aggregation in the precursor polymer attempts were made to mask the free alcohol group and protect it to obtain a product not able to make hydrogen bonds. The protecting group had to be easy to introduce in the molecule, has to be stable under the applied conditions and if necessary has to be removed in a smooth way. Therefore the tetrahydropyranyl ether was chosen since it normally is stable under basic conditions. This group was introduced according to procedures¹⁸ described in literature data (scheme 13).

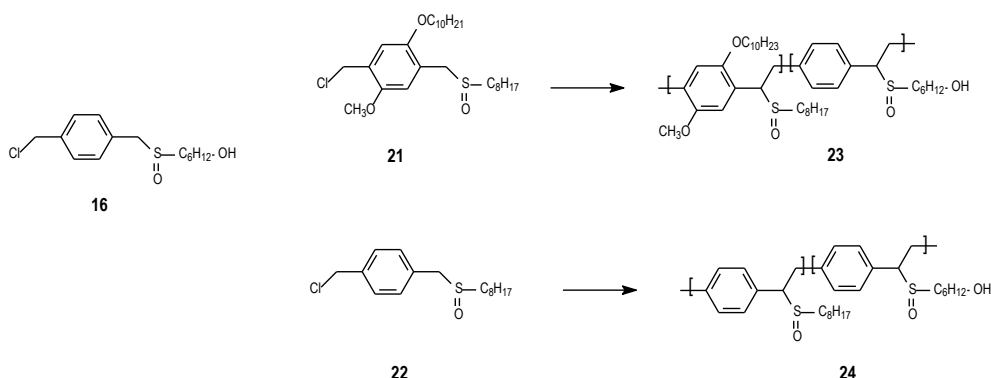
Scheme 13. Synthesis of the protected alcohol monomer. 1 : CH_2Cl_2 , dihydropyran, $\text{TosOH}_{\text{cat}}$, 0°C.

The alcohol monomer **16** is dissolved in dichloromethane and the solution is stirred at 0°C. Subsequently 2 equivalents of dihydropyran and 0.1 equivalents of *p*-toluene sulfonic acid as a catalyst are added and the progress of the reaction is monitored on TLC. When all alcohol has disappeared the mixture is poured into water and after extraction the protected alcohol **20** is obtained in high yield. Polymerisation of the protected alcohol resulted in a soluble precursor polymer in such way that extraction of the precipitated polymer could be achieved without addition of solvents like methanol or 2-butanol. However after drying again an insoluble solid was obtained from which the low molecular weight products could be

dissolved as detected with GPC. Probably the pyranyl ether can be cleaved resulting in some new hydrogen bonds.

2.2.6. Copolymerisation reactions

Another way to solve the insolubility problems of the precursor polymer **17** can be the copolymerisation with a second monomer that ensures a better solubility. Examples of such kind of monomer are the OC₁C₁₀ monomer **21** and the n-octyl sulfinyl monomer **22** respectively (scheme 14). So in our case the alcohol monomer **16** was copolymerised with these two monomers in two different experiments in a 1/1 ratio yielding a soluble precursor polymer **23-24** in both cases. Probably the number of hydrogen bonds is strongly reduced because of the steric hindrance of the alkyl chains and thus subsequent aggregation of the polymer chain is inhibited.



Scheme 14. Synthesis of the precursor copolymers **23-24**

The precursor polymers **23** and **24** were characterised by ¹H-NMR spectroscopy and the conversion into the conjugated material was monitored with in situ UV-Vis spectroscopy. GPC results in THF indicate only formation of low molecular weight material (M_w = 700-1000) and are hence considered to be unreliable, possibly due to interactions between the GPC column and the free alcohol functions. Both copolymers show the typical formation of the conjugated structure. The maximum absorption for the n-octyl copolymer **24** is at 410 nm, typically for the non-substituted PPV (figure 18-19). The maximum absorption for the

other copolymer is 437 nm. This last value was also observed by Gillissen¹⁹ who copolymerised the n-octyl monomer **22** with the OC₁C₁₀ monomer **21** in a 1/1 ratio. The ratio of the comonomers built in the copolymer made by Gillissen was determined to be 68/32 in favour of the n-octyl monomer using quantitative ¹³C-NMR spectroscopy. In our case the ratio of the built in monomers in copolymer **23** was determined to be about 1/1 and 3/2 for copolymer **24** in favour of monomer **22** as determined by ¹H-NMR spectroscopy from the integration of the aromatic and the methylene protons.

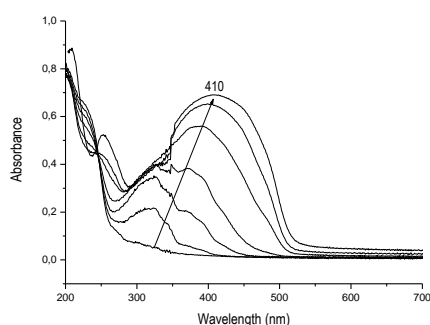


Figure 18. Gradual formation of the conjugated structure of copolymer **24**

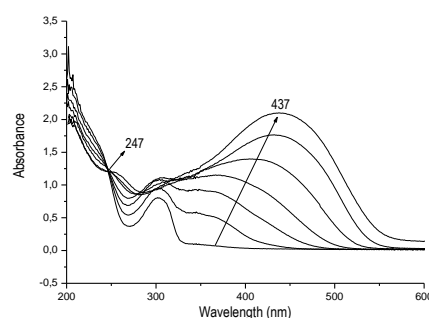
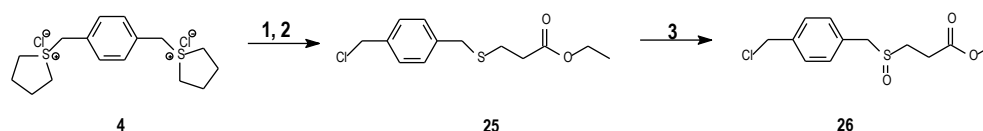


Figure 19. Gradual formation of the conjugated structure of copolymer **23**

2.3. Synthesis of an ester derived polymer

2.3.1. Monomer synthesis

A third monomer was synthesised now bearing an ester function on the sulfinyl tail. The use of the diluted conditions described earlier in this chapter resulted in a high yield of the thioether. The choice of the thiol used here was inspired by its commercial availability. No other ester functionalised thiols are on the market yet.



Scheme 15. Synthesis of monomer **26**. 1 : 3-mercapto ethyl propionate, Na-*t*BuO, 2 : *n*-octane, ΔT , 3 : TeO₂/H₂O₂, MeOH, HCl_{cat}

So a methanol solution of 3-mercapto ethyl propionate and base in a 1/1 ration is added to a stirred solution of the bissulfonium salt (1 equivalent). After four hours the solvent is evaporated and the THT is removed azeotropically. The ethyl ester thioether **25** is oxidised to the corresponding sulfoxide **26** with occurrence of a transesterification to the methyl ester (scheme 15). Esters are very versatile functionalities from synthetic point of view. Simple chemical reaction conditions make conversion of the ester into other functionalities possible. Reduction to the alcohol, transesterification to other ester groups and hydrolysis to the carboxylic acid. This last conversion can be very interesting since it allows water solubility of the end product using very mild basic conditions.

2.3.2. *p*-Quinodimethane formation

The formation of the *p*-quinodimethane system was also investigated for the ester monomer **26** using UV-Vis spectroscopy. A solution of monomer (10^{-4} M) in 2-butanol was brought in a cuvet and an excess of base was added whereupon the continuous scanning of the spectrum started. Unlike the monomers described earlier, no change in the spectrum was observed indicating that there is no formation of a *p*-quinodimethane system (figure 20). Hence no polymerisation should occur and also solvent substitution seemed absent since it has been elucidated that this reaction mainly occurs on the *p*-quinodimethane stage.

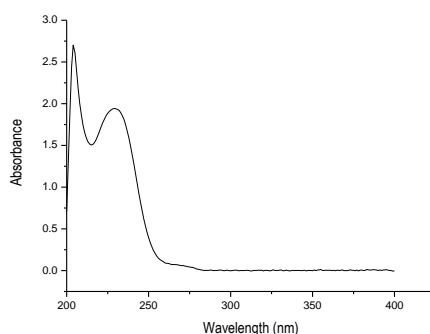
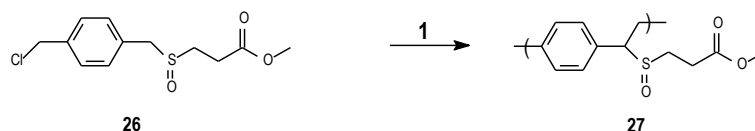


Figure 20. UV-Vis spectrum of monomer **26** upon addition of base excess

2.3.3. Polymerisation of monomer **26**

Scheme 16. Polymerisation of monomer **26**. 1 : 2-BuOH or THF, Na-tBuO (1.3 equivalents), 40°C, N₂

Although no *p*-quinodimethane system was observed for the ester monomer **26** with UV-Vis spectroscopy a real polymerisation reaction was performed using the method of Van Breemen. The only difference is that the polymerisation temperature was raised to 40 °C due to the partial insolubility of the monomer at 30 °C. Upon addition of the base solution to the monomer the solution turned deep red indicating that some reaction occurs. However the colour disappeared immediately after addition of the base solution. This phenomenon never was observed for polymerisation reactions of other sulfinyl monomers. After stirring the solution for one hour it was poured into water whereupon a white solid precipitated that was insoluble in any kind of solvent. Changing the polymerisation solvent from 2-butanol to THF gave an identical insoluble material. According to FT-IR spectroscopy this certainly was no precursor polymer **27** since the typical S=O signal at 1040 cm⁻¹ could not be detected.

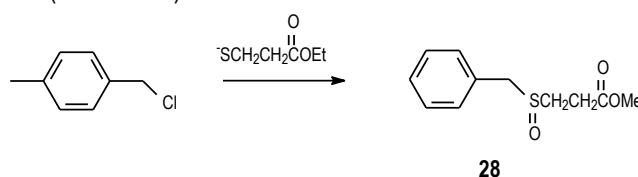
This insolubility seemed quite surprising since unlike the alcohol precursor polymer no hydrogen bonding in the ester polymer can occur. So the idea of incompatibility of an ester function with a sulfinyl group grew and some test reactions were performed.

If the sulfinyl group and an ester function indeed are incompatible functionalities no polymer should be obtained from the polymerisation reaction of the *n*-octyl sulfinyl monomer **22** upon addition of an ester functionalised molecule. So three reactions were performed each one with addition of ethyl acetate as the ester (table 5). In a first reaction ethyl acetate (1 equivalent versus the monomer) is added to the monomer solution. In a second and third reaction respectively one and two equivalent of ethyl acetate are added to the base solution. In all three cases high molecular weight precursor polymer could be obtained, contradicting the hypothesis of incompatibility of the functional groups.

Eq. of EtOAc	Added to	M _w	PD
1	monomer	158.000	6.70
1	base	169.000	3.54
2	base	143.000	3.35

Table 5. Overview of polymerisation results of the polymerisation reactions of *n*-octyl monomer **22** upon addition of ethylacetate

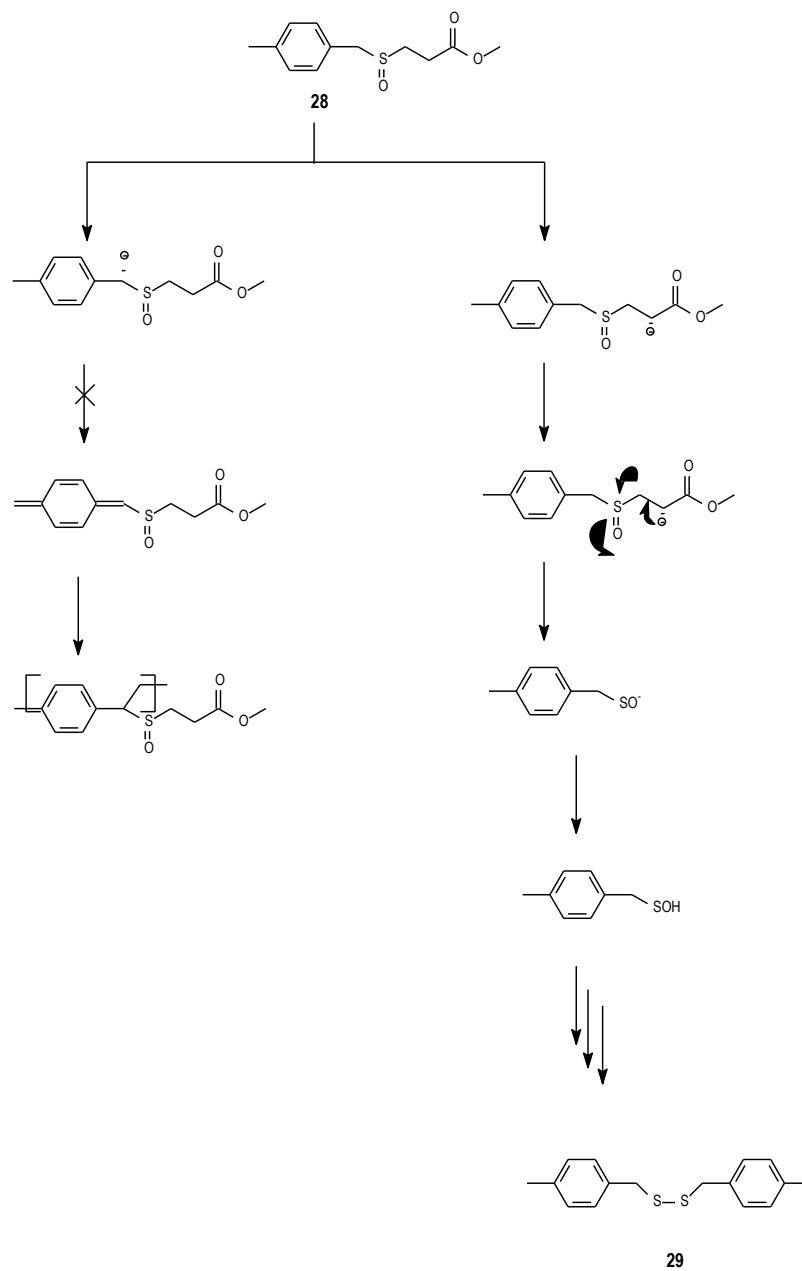
A next attempt to elucidate the processes occurring during polymerisation was the treatment of so called model compounds to mimic the polymerisation. Compound **28** was synthesised using benzyl bromide and a solution of the thiolate. Oxidation of the thioether yields a mutilated monomer (scheme 17).



Scheme 17. Synthesis of the mutilated monomer **28**

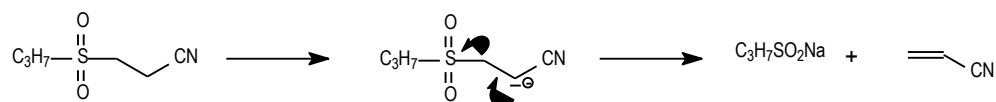
Since this compound has no leaving group at the α' -position no *p*-quinodimethane system can be formed and thus any possible reaction should occur at the sulfinyl tail. The model compound was treated under polymerisation conditions and after work up of the reaction a very complicated mixture was obtained according to TLC. Gas chromatograph analysis revealed a whole range of products among which the disulfide **29** in a major quantity. Also some other products known from the elimination reaction of sulfinyl precursor polymers were present. Such a disulfide is one of the end products from dimerisation and disproportionation reactions of sulfenic acids expelled during elimination and thus a possible reaction mechanism was proposed as depicted in scheme 18. Basic treatment of the ester functionalised model compound does not yield the benzylic anion but an enolate anion, stabilised by the mesomeric effect of the ester carbonyl group. The next step is an E_{1cb} elimination reaction to give a double bond and the expulsion of the conjugated base of

sulfenic acid. After protonation, the corresponding sulfenic acid undergoes dimerisation and disproportionation reactions to give the disulfide **29** as one of the end products. This unwanted elimination reaction hence should be inhibited using a sulfinyl ester chain with one more methylene group between the sulfoxide and the ester. However because of the unavailability of such thiol this approach was not further investigated.



Scheme 18. Possible reactions affording a disulfide **29** from compound **28**. Reaction conditions: THF or 2-BuOH, Na-tBuO (1.3 equivalents), 40°C, N₂

Also in literature¹⁹ such kind of elimination reaction is described with a sulfonyl group as the leaving group and a cyano group to stabilise the anion. The sulfinic acid that is expelled is very unstable and tends to disproportionate to yield a sulfonic acid and a thiosulfonate (scheme 19).



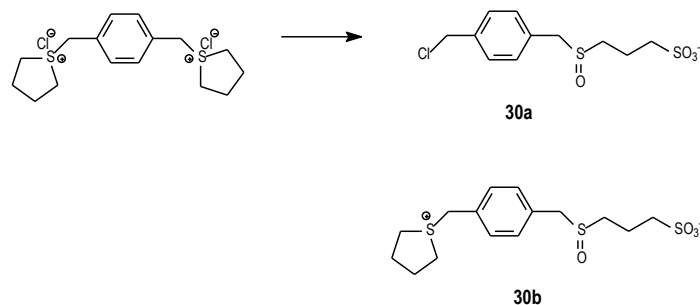
Scheme 19. Base induced elimination of sulfonic acid from a β -sulfonyl nitrile

2.4. Synthesis of a sulfonate derived polymer

As a last synthetic part in this chapter we will discuss the synthesis of an anionic sulfinyl monomer. In this case the ionic group is a sodium sulfonate salt. PPV derivatives bearing a sulfonate functionality are described in literature²⁰ since they can interact with both inorganic and organic cationic species which causes a change in the fluorescence of the polymer. Such polymers can then be used as cation indicators or sensors.

2.4.1. Monomer synthesis

The thiol we used is commercially available and is used without further purification. The thioether synthesis was started as discussed earlier. After evaporation of methanol and removal of THT the residue is dissolved in a minimal amount of water and poured into cold acetone whereupon a white solid precipitated that is collected by filtration. ¹H-NMR analysis of the product revealed that the thioether could be obtained in a high yield but the majority of the benzylic chlorides still was substituted by THT groups. Possibly these sulfonium salts no longer have a chlorine atom as the counter ion but the sulfonate group may take over this role. Hence there are no chlorine ions left to substitute the sulfonium group when n-octane is added.



Scheme 20. Synthesis of monomer **30**. 1 : MeOH, $\text{HSC}_3\text{H}_6\text{SO}_3\text{Na}^+$, Na-tBuO, 2 : n-octane, ΔT

From integration of the benzylic NMR signals it is seen that only twenty percent of these positions is chlorine substituted. Nevertheless the mixture was used in the oxidation step without any further purification. The oxidation step was also performed as described earlier but here no TLC monitoring of the progress of the reaction is possible. After work up of the reaction ^1H NMR revealed that the sulfinyl compound **30** was contaminated with a small amount of sulfon (scheme 20).

2.4.2. *p*-Quinodimethane formation

The monomer **30** was also tested on *p*-quinodimethane formation. However unlike the previous tests for the other monomers water was used as the solvent instead of 2-butanol since it is insoluble in the latter. Also in this case a clear *p*-quinodimethane signal can be detected at 315 nm that increases quickly and subsequently decreases due to reaction with solvent molecules (figure 21-22).

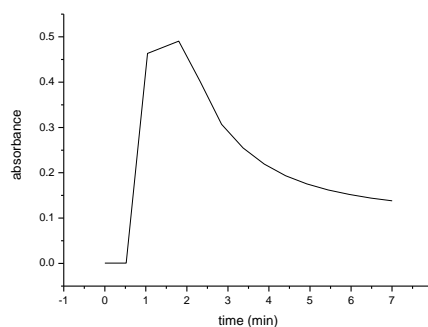
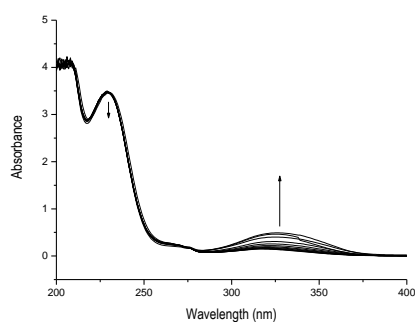
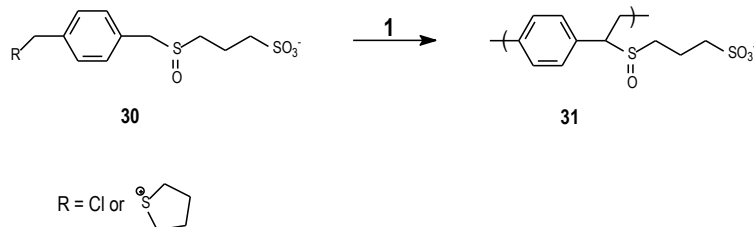


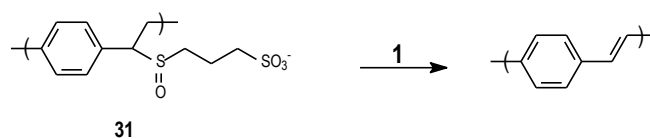
Figure 21. Gradual formation of the *p*-quinodimethane system

Figure 22. Signal at 313 nm versus time.

2.4.3. Polymerisation of monomer **30**Scheme 21. Polymerisation of monomer **30**. 1 : H₂O, Na-*t*BuO, 30°C, N₂

The mixture of sulfoxides was polymerised according to the general procedure only the solvent is changed from 2-butanol to water for solubility reasons. After addition of the base a gel-like precipitate is formed that is insoluble in any solvent. The polymer is collected through filtration and dried in vacuo. Molecular weights were not determined since GPC measurements could not be performed.

2.4.4. Conversion of the polymer into the conjugated polymer

Scheme 22. Conversion of precursor **31** into the conjugated structure

The conversion of the precursor polymer into its conjugated counterpart was analysed using in situ UV-Vis and FT-IR spectroscopy. For the UV-Vis measurements the precursor polymer was dissolved in water and a piece of polymer was wiped over a quartz disc. The disc was placed in the oven described earlier and a heating program of 2°C per minute was applied up to 300°C. A maximum wavelength is obtained at 396 nm, which is somewhat smaller than PPV obtained from other precursor polymers (410 nm). The elimination process starts around 69°C and reaches its maximum only at 193°C, which is much later than the non-charged precursors. Possibly the presence of charged sulfinyl tails inhibits the formation of a favourable transition state for elimination and hence the conversion reaction is slowed down and the effective conjugation length is somewhat shortened.

Chapter 2

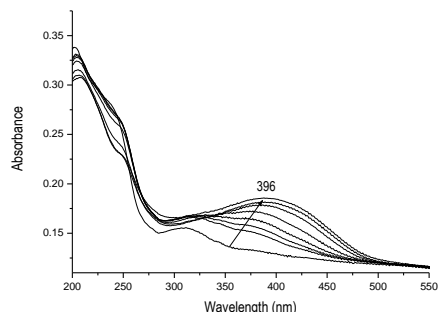


Figure 23. Gradual formation of the conjugated structure.

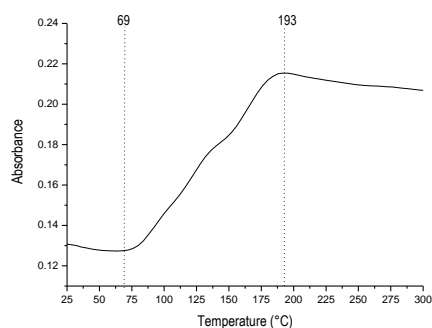


Figure 24. Plot of the absorbance at 396 nm versus temperature

The elimination process was also studied using in situ FT-IR spectroscopy and a KBr pellet was made containing solid particles of the precursor polymer. Again the pellet is placed in the oven and the same heating program is applied. From the data obtained from this experiment we conclude that elimination start also at 70°C which is in good accordance with the data obtained from the UV-Vis experiment.

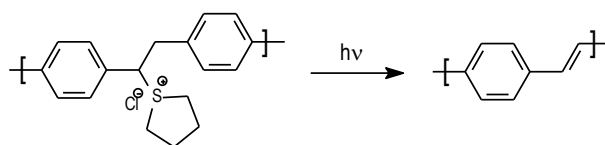
3. Applications of elimination behaviour – elimination induced by infrared absorption.

Since the elimination of the sulfinyl group can be performed in a very mild way, which means at temperatures below 100 °C, one may think of an application of this phenomenon. Not only is it nice to have a soluble precursor polymer that can be spin coated easily. It is also attractive to turn a soluble polymer in its insoluble counterpart just by applying a small thermal treatment.

After laser spectroscopy entered the scientific world a few decades ago, intensive research has been performed in absorbing properties of materials. When irradiating an absorbing material, the material will only absorb certain amounts of energy and after the excitation of the material, a relaxation process occurs setting free an amount of heat. It is this heat that can be used for the assisted elimination of the sulfinyl groups in the precursor polymer to create the conjugated material in situ. The main advantage of the conversion process using

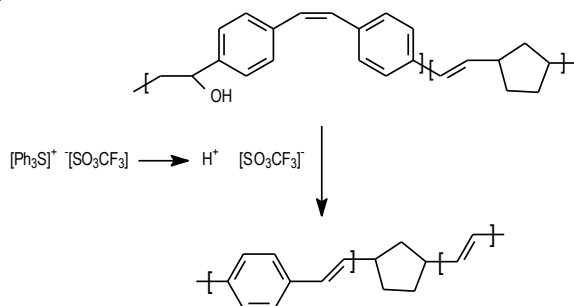
lasers is the possibility of patterning the conjugated polymer via a precursor route. Due to the precise irradiation of the laser lamp very sharp lines can be formed easily.

In literature a few examples of laser induced conversion of precursor PPV derivatives into the conjugated material have been described so far. Paik and coworkers reported on the elimination of sulfonium groups from a Wessling precursor polymer using UV-laser irradiation²¹. Here a solid sample of the PPV precursor polymer is irradiated with a laser. To convert the coated film into PPV, a pulsed-laser beam treatment by a XeCl excimer laser with a wavelength of 308 nm was applied. After 20 seconds conversion was completed and byproducts such as THT or HCl were not found in the polymer film.



Scheme 23. Laser assisted conversion of a Wessling precursor polymer into the conjugated structure.

Another laser assisted elimination of a PPV-like precursor polymer was described by Renak and coworkers²². The precursor polymer was mixed with a photo-acid generator. Upon absorption of light the photoinitiator, triphenyl sulfonium trifluoromethanesulfonate (TPST), produces triflic acid that promotes dehydration of the precursor polymer to its conjugated all-trans analogue.



Scheme 24. Laser assisted conversion using a photo-acid.

A comparable approach was performed now not using a photoinitiator but a set of infrared absorbers. These absorbers were mixed with a polymer solution and subsequently

dropcasted on a PET substrate. Laser irradiation was performed using a diode and a NdYAG laser. Two different polymer solutions were used: the PEO sulfinyl polymer **15** and the n-octyl polymer **22**.

The precursor polymer (1g) is dissolved in 10 ml methylethylketone (MEK) resulting in a 10 % solution. To 3 ml of this solution is added an amount of the infrared absorber (circa 30 mg). After stirring the solution, a film was drop casted on a PET-substrate resulting in a film thickness of 20 μm . Three different infrared absorbers (figure 25) were used.

The films were subsequently placed in the laser beam and treated with different intensities. Two kinds of infrared lasers were used: a diode laser and a NdYAG laser.

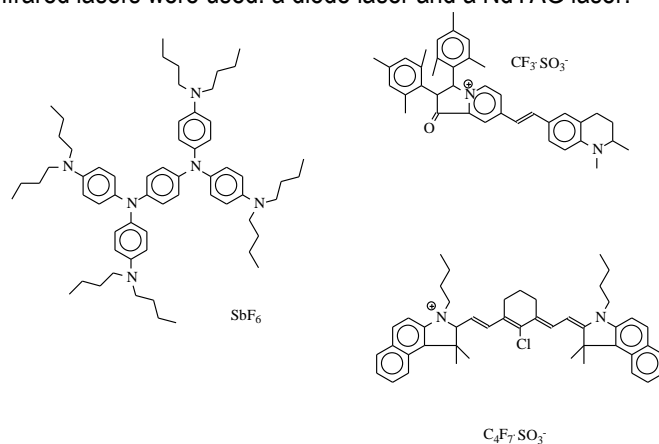


Figure 25. Overview of the applied infrared absorbers

A schematic presentation is depicted in figure 26. Entry **1** shows the precursor polymer and the IR-absorber coated on a PET substrate. In entry **2** the sample is treated with laser light resulting in conjugated segments on the irradiated areas. Since the conjugated polymer is not soluble, the soluble precursor polymer can be removed by washing with an adequate solvent as shown in entry **3**.

The fourth monomer, a sulfonate functionalised monomer, was synthesised making adaptations to the general procedures concerning the solvent and purification. However the monomer could be obtained yet contaminated with traces of sulfon. The use of charged species like a sulfonate salt in the monomer synthesis and polymerisation seems not advisable but no attempts to use a non-charged protected sulfonate were made.

All these experiments clear out that the polymerisation of a functionalised monomer is possible when using small adaptations to the normal procedure. The experience obtained from these experiments will be used for further research on functional PPV derivatives now bearing the functional groups on the phenyl core yielding a functional conjugated PPV derivative.

5. Experimental Section

Materials.

All chemicals were purchased from Aldrich or Acros and used without further purification. Tetrahydrofuran (THF) and 1,4-dioxane were distilled over sodium/benzophenone.

Characterization.

¹H-NMR spectra were obtained in CDCl₃ or D₂O at 300 MHz on a Varian Inova Spectrometer using a 5 mm probe. Chemical shifts (δ) in ppm were determined relative to the residual CHCl₃ absorption (7.24 ppm) or to the residual H₂O absorption (4.6 ppm). The ¹³C-NMR experiments were recorded at 75 MHz on the same spectrometer using a 5 mm broadband probe. Chemical shifts were defined relative to the ¹³C resonance shift of CHCl₃ (77.0 ppm). Molecular weights and molecular weight distributions were determined relative to polystyrene standards (Polymer Labs) with a narrow polydispersity by Size Exclusion Chromatography (SEC). Separation to hydrodynamic volume was obtained using a Spectra series P100 (Spectra Physics) equipped with a pre-column (5 μ m, 50 mm*7.5 mm, guard, Polymer Labs) and two mixed-B columns (10 μ m, 2x300 mm*7.5 mm, Polymer Labs) and a Refractive Index (RI) detector (Shodex) at 40°C. SEC samples are filtered through a 0.45 μ m filter. HPLC grade THF (p.a.) or DMF (p.a.) is used as the eluent at a constant flow rate of 1.0 ml/min. Toluene is used as flow rate marker.

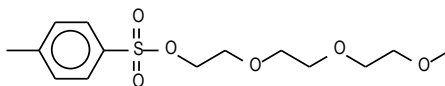
Direct Insert Probe Mass Spectroscopy analysis is carried out on a Finnigan TSQ 70, electron impact mode, mass range of 35-500. Electron energy is 70 eV. A solution of

precursor polymer is applied on the heating element of the direct insert probe. A heating rate of 10°C/min was.

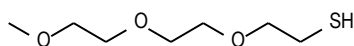
The in situ elimination reactions were performed in a Harrick High Temperature Oven (purchased from Safir), which is positioned in the beam of a Perkin Elmer spectrum one FT-IR spectrometer (nominal resolution 4 cm⁻¹, summation of 16 scans). The temperature of the sample is controlled by a Watlow (serial number 999, dual channel) temperature controller. The soluble precursor polymers were spincoated from solution (6 mg/ml) on a KBr pellet at 500 rpm. The spincoated KBr pellet (diameter 25 mm, thickness 1 mm) is in direct contact with the heating element. All experiments were performed at 2°C/min under a continuous flow of nitrogen. "Timebase software" supplied by Perkin Elmer is used to investigate regions of interest. The insoluble precursor polymers were wiped over the KBr pellet or mixed in the pellet.

In situ UV-Vis measurements were performed on a Cary 500 UV-Vis-NIR spectrophotometer, specially adopted to contain the Harrick high temperature cell (scan rate 600 nm/min, continuous run from 200 to 600 nm). The soluble precursor polymer was spincoated from a CHCl₃ solution (6 mg/ml) on a quartz glass (diameter 25 mm, thickness 3mm) at 700 rpm. The other precursor polymers were wiped over the glass or dropcasted from a aqueous solution. The quartz glass was heated in the same Harrick oven high temperature cell as was used in the FT-IR measurements. The cell was positioned in the beam of the UV-Vis-NIR-spectrophotometer and spectra were taken continuously. The heating rate was 2°C/min up to 300°C. All measurements were performed under a continuous flow of nitrogen. "Scanning Kinetics software" supplied by Varian is used to investigate regions of interest.

The UV-Vis measurements on the *p*-quinodimethane formation were performed on a Cary 500 UV-Vis-NIR spectrophotometer equipped with a stop-flow module allowing very fast measurements. A 10⁻⁴ M monomer solution and a 5 10⁻⁴ M base solution in the same solvent (mostly 2-butanol unless stated otherwise in the text) are injected simultaneously and the monitoring of the regions of interest is started immediately after mixing of the two components. "Scanning Kinetics" and "Kinetics" software supplied by Varian is used to investigate regions or wavelengths of interest.

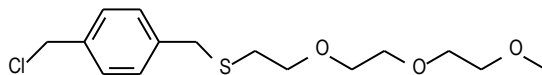
Toluene-4-sulfonic acid 2-[2-(2-methoxy-ethoxy)-ethoxy]-ethyl ester **11**

To a stirred and cooled solution of {2-[2-(2-methoxyethoxy)ethoxy]ethylalcohol **10** (10 g, 0.0613 mol) and triethylamine (12.5 g, 2 equivalents) as a base, is added portionwise *p*-tosylchloride (5.8 g, 0.0306 mol). After 5 minutes the mixture is brought to room temperature and stirred for another three hours while the reaction progress is monitored with TLC. After work up with water, the solution is extracted with chloroform three times and the combined organic fractions are dried over magnesium sulfate. The solvent and the remaining triethylamine are evaporated. A chromatographic purification with ether as the eluent yields the desired toluene-4-sulfonic acid 2-[2-(2-methoxy-ethoxy)-ethoxy]-ethyl ester as an oil (8.5 g, 87.5%). ¹H-NMR (400 MHz, δ , ppm, CDCl₃): 7.60 (d, 2H), 7.17 (d, 2H), 3.96 (t, 2H), 3.49 (t, 2H), 3.42-3.38 (m, 8H), 3.17 (s), 2.25 (s). MS (EI, m/z): 318 (M⁺), 273, 259, 243, 229, 199, 172, 155, 91, 59, 45

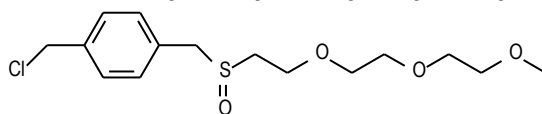
2-[2-(2-Methoxy-ethoxy)-ethoxy]-ethanethiol **13**

In 60 ml acetone is refluxed under nitrogen atmosphere toluene-4-sulfonic acid 2-[2-(2-methoxy-ethoxy)-ethoxy]-ethyl ester **11** (16.7 g, 0.0525 mol) and thiourea (1.1 equivalents, 4.4 g) for sixteen hours. After evaporating the solvent, the residual salt **12** is dissolved in 56 ml water. Subsequently NaHCO₃ (4.8 g, 0.057 mol) is added and the solution is stirred at 70°C for three hours. After cooling, the solution is acidified with HCl (1M) up to pH 3. Extracting the water layer three times with chloroform, drying over magnesium sulfate and a column purification with ether as the eluent yields the pure sulfide **13** as a colorless fluid. (7.52 g, 79%)

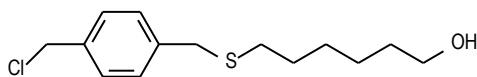
¹H-NMR (400 MHz, δ , ppm, CDCl₃): 3.49-3.30 (m, 12H), 3.14 (s, 3H), 2.91 (s broad, 1H)
MS (EI, m/z): 181, 133, 121, 103, 89, 75, 59, 45

1-Chloromethyl-4-{2-[2-(2-methoxy-ethoxy)-ethoxy]-ethylsulfanyl}methyl-benzene

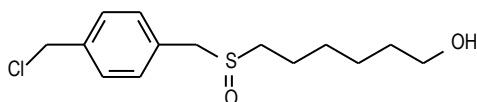
A solution of the 2-[2-(2-methoxy-ethoxy)-ethoxy]-ethanethiol **13** (2.45 g, 0.0135 mol) and sodium *t*-butoxide (1.3 g, 1 equivalent) in 100 ml methanol is stirred for one hour at room temperature. This solution is added dropwise to a stirred solution of 1,4-bis(tetrahydrothio pheniomethyl)xylene dichloride (5 g, 1 equivalent) in 800 ml methanol and the resulting mixture is stirred for sixteen hours at room temperature. After neutralizing the solution with HCl (1M), the solvent is evaporated and *n*-octane is added and evaporated again to remove the THT. This procedure is repeated three times. The residue is dissolved in chloroform and extracted with water. After drying the combined organic layers over magnesium sulfate and a column purification with ether as the eluent, the desired compound is obtained as a yellowish oil (2.75 g, 64 %). ¹H-NMR (400 MHz, δ , ppm, CDCl₃): 7.32+7.26 (dd, 4H), 4.56 (s, 2H), 3.72-3.5 (m, 14H), 3.30 (s, 3H)

1-Chloromethyl-4-{2-[2-(2-methoxy-ethoxy)-ethoxy]-ethylsulfinyl}methyl-benzene **14**

To 1-chloromethyl-4-{2-[2-(2-methoxy-ethoxy)-ethoxy]-ethylsulfanyl}methyl-benzene (1.6 g, 0.005 mol) in 50 ml methanol is added TeO₂ (40 mg, 5 mol %) and H₂O₂ (0.97 g, 2 equivalents). A few drops of concentrated HCl are added to catalyse the reaction. The progress of the reaction is followed on TLC and when all thioether is disappeared, 50 ml of brine is added to stop the reaction. Extraction three times with chloroform, drying over magnesium sulfate and a column purification with ether/methanol as the eluent yields the sulfoxide as a yellow oil which becomes solid upon cooling in the freezer. (1.32 g, 79%). ¹H-NMR (300 MHz, δ , ppm, CDCl₃): 7.38+7.28 (dd, 2H), 4.57, (s, 2H), 4.11+3.98 (dd, 2H), 3.92+3.84 (m, 2H), 3.64 (m, 2H), 3.61 (m, 2H), 3.51 (m, 2H), 3.33 (s, 3H), 2.90+2.70 (m, 2H). MS (EI, m/z): 335, 299, 269, 199

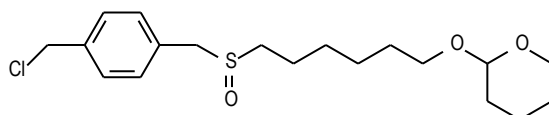
6-(4-Chloromethyl-benzylsulfanyl)-hexan-1-ol

A solution of the 6-mercapto-hexanol (1.81 g, 0.0135 mol) and sodium *t*-butoxide (1.3g, 1 equivalent) in 100 ml methanol is stirred for one hour at room temperature. This solution is added dropwise to a stirred solution of 1,4-bis(tetrahydrothio pheniomethyl)xylene dichloride (5 g, 1 equivalent) in 800 ml methanol and the resulting mixture is stirred for 16 hours at room temperature. After neutralizing the solution with HCl 1M, the solvent is evaporated and *n*-octane is added and evaporated again to remove the THT. This procedure is repeated three times. The residu is dissolved in chloroform and extracted with water. After drying over magnesium sulfate and a column purification with ether as the eluent, the desidred compound is obtained as a yellowish oil (2.7 g, 73%). ¹H-NMR ppm (300MHz, δ , ppm, CDCl₃): 7.27+7.31 (dd, 4H), 4.55 (s, 2H), 3.66 (s, 2H), 3.60, (t, 2H), 2.38 (t, 2H), 2.00(s, br, 1H), 1.52 (m, 8H). MS (EI, m/z): 272, 236, 171, 139

6-(4-Chloromethyl-benzylsulfinyl)-hexan-1-ol 16

To 6-(4-chloromethyl-benzylsulfanyl)-hexan-1-ol (2.7 g, 0.01 mol) in 110 ml of methanol is added TeO₂ (94 mg, 5 mol%) and H₂O₂ (2.3 g, 2 equivalents). A few drops of concentrated HCl are added to catalyze the reaction. The progress of the reaction is followed on TLC and when all thioether is disappeared 100 ml of brine is added to stop the reaction. Extraction with chloroform, drying over magnesium sulfate and column with ether/methanol as the eluent yields the sulfoxide as a white solid (2.16 g, 79%). ¹H-NMR ppm (300MHz, δ , ppm, CDCl₃): 7.26+7.37 (dd, 4H), 4.56 (s, 2H), 3.90+3.96 (dd, 2H), 3.59 (s, br, 2H), 2.55 (t, 2H), 1.72 (m, 6H).

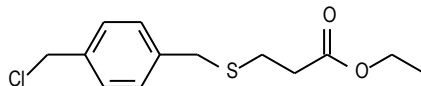
2-[6-(4-Chloromethyl-phenylmethanesulfinyl)-hexyloxy]-tetrahydro-pyran 20



A solution of 6-(4-chloromethyl-benzylsulfinyl)-hexan-1-ol (2.25g, 0.0078 mol) in 135 ml dichloromethane is stirred at room temperature and dihydropyran (1.31 g, 2 equivalents) is added dropwise. A catalytic amount of *p*-toluene sulfonic acid (0.1 equivalent) is added and the mixture is stirred until no free alcohol is left on TLC. The reaction mixture is poured into 200 ml water and extracted three times with dichloromethane. The organic phase is dried over magnesium sulfate and the solvent is evaporated. A chromatographic purification with ether as the eluent yields the 2-[6-(4-chloromethyl-phenylmethanesulfinyl)-hexyloxy]-tetrahydro-pyran as a white solid (87%).

¹H-NMR ppm (300MHz, δ , ppm, CDCl₃): 7.36+7.26 (dd, 4H), 4.55 (s, 2H), 4.52 (t, 1H), 3.97+3.92 (dd, 2H), 3.81 (m, 1H), 3.69 (dt), 3.45m, 1H), 3.33 (dt, 1H), 2.56 (m, 2H), 1.80-1.36 (m, 14H). MS (DIP-MS/CI) : 373, 289, 139, 105

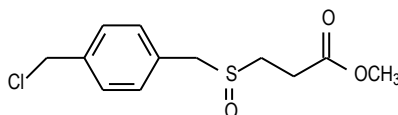
3-(4-Chloromethyl-benzylsulfanyl)-propionic acid ethyl ester 25



A solution of 3-mercapto-ethylpropionate (1.86 g, 0.0138 mol) and sodium *t*-butoxide (1.3 g, 1 equivalent) in 100 ml methanol is stirred for one hour at room temperature. This solution is added dropwise to a stirred solution of 1,4-bis(tetrahydrothio pheniomethyl)xylene dichloride (5 g, 1 eq) in 800 ml methanol and the resulting mixture is stirred for 16 hours at room temperature. The solvent is evaporated and *n*-octane is added and evaporated again to remove the THT. This procedure is repeated three times. The residu is dissolved in chloroform and extracted with water. After drying over magnesium sulfate and a column with CH₂Cl₂ as the eluent, the desired compound is obtained as a colorless oil (2.75g, 72%).

¹H-NMR ppm (300MHz, δ , ppm, CDCl₃): 1.21 (t, 3H), 2.51 (t, 2H), 2.63 (t, 2H), 3.68 (s, 2H), 4.11 (q, 2H), 4.52 (s, 2H), 7.28 (dd, 4H). MS (EI): 272 ([M]⁺), 236, 227 171

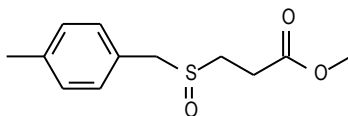
3-(4-Chloromethyl-benzylsulfanyl)-propionic acid methyl ester 26



To 3-(4-chloromethyl-benzylsulfanyl)-propionic acid ethyl ester (0.68 g, 0.0025 mol) in 35 ml methanol is added TeO_2 (20 mg, 5 mol%) and H_2O_2 (0.485 g, 2equivalents). A few drops of concentrated HCl are added to catalyse the reaction. The progress of the reaction is followed on TLC and when all thioether is disappeared 35ml of brine is added to stop the reaction. Extraction with chloroform, drying over magnesium sulfate and column with CH_2Cl_2 /methanol as the eluent yields the desired sulfoxide as a white solid (0.63 g, 89%).

$^1\text{H-NMR}$ ppm (300MHz, δ , ppm, CDCl_3): 7.27 + 7.37 (dd, 4H), 4.54 (s, 2H), 4.12(q, 2H), 3.97 (s, 2H), 2.77 +2.93 (m, 4H), 1.22 (t, 3H). MS (CI, m/z): 289, 253, 151, 139, 105

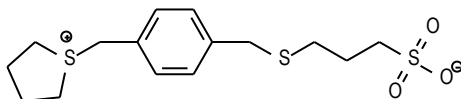
3-Benzylsulfanyl-propionic acid methyl ester 28



To a stirred solution of α -chloro-*p*-xylene (2g) in 20 ml methanol is added 3-mercaptoethylpropionate (2 g, 0.0138 mol) and sodium *t*-butoxide (1.45 g, 1 equivalent). The reaction is stirred at room temperature until no chloroxylene is left on TLC. The reaction is poured into water and the aqueous layer is extracted with dichloromethane three times. Drying over magnesium sulfate, evaporation of the solvent and a short column purification with dichloromethane as the eluent yields the desired product as a white solid. (2.69g, 84%). the thioether is oxidized using the common reaction conditions described earlier and the reaction is stopped when all thioether is disappeared on TLC.

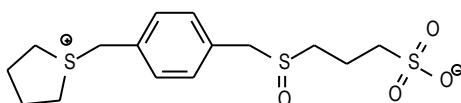
$^1\text{H-NMR}$ ppm (300MHz, δ , ppm, CDCl_3): 7.22 (s, 4H), 4.02+3.93 (dd, 2H), 3.64 (s, 3H), 2.93-2.72 (m, 4H), 2.32 (s, 3H)

Thioether compound of monomer 30



A solution of the 3-mercaptopropanesulfonic acid sodium salt (0.55 g, 0.003 mol) and sodium *t*-butoxide (290 mg, 1 eq) in 30 ml methanol is stirred for one hour at room temperature. This solution is added dropwise to a stirred solution of 1,4-bis(tetrahydrothio pheniomethyl)xylene dichloride (1.04 g, 1 eq) in 160 ml methanol and the resulting mixture is stirred for 16 hours at room temperature. After neutralizing the solution with HCl 1M, the solvent is evaporated and *n*-octane is added and evaporated again to remove the THT. This procedure is repeated three times. The resulting mixture is dissolved in a small amount of methanol and precipitated in ice cooled acetone. This yields the thioether as a mixture of chloride and sulfonium salt. ¹H-NMR (300MHz, δ, ppm, D₂O): 7.52+7.36 (s, 4H), 4.47+4.41 (2s, 2H), 3.67 (s, 2H), 3.35 (m, 4H), 2.80 (t, 2H), 2.46 (t, 2H), 2.17 (m, 4H), 1.82 (m, 2H)

Synthesis of monomer 30



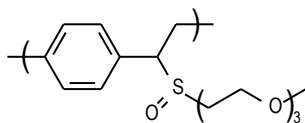
To (2.7g, mol) in 120 ml methanol is added TeO₂ (102 mg, 5mol%) and H₂O₂ (3 g, 2 equivalents). A few drops of concentrated HCl are added to catalyze the reaction. The reaction is stirred for 2 hours at room temperature. The solvent is filtered to remove solid substances and evaporated and the crude mixture is redissolved in a small amount of methanol and precipitated in ice cooled acetone to yield the sulfoxide yet contaminated with traces of sulfon.

¹H-NMR (300MHz, δ, ppm, D₂O): 7.59 + 7.55 , 4.59+4.56 (2s, sulfon), 4.52+4.50 (2s, 2H), 4.32+4.30+4.28+4.25+4.13+4.11+4.09+4.07 (2dd, 2H), 3.41 (m, 4H), 3.04 (m, 2H), 2.85 (m, 2H), 2.19 (m, 6H)

Polymerisation of the monomers

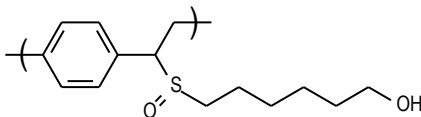
All precursor polymers were synthesised according to a general procedure. Solutions of the monomers (0.14 M) and base (Na-*t*-BuO, 1.3 equivalents) were prepared and degassed for one hour by a continuous flow of nitrogen at 30 °C unless stated otherwise. The base solution was added in one portion to the stirred monomer solution. During the reaction the temperature was maintained at 30 °C and the passing of nitrogen was continued. After one hour the reaction mixture was poured into well stirred water whereupon some precursor polymer precipitated. The water layer was extracted with chloroform or dichloromethane to ensure that all polymer and residual fraction was collected, and the combined organic fractions were concentrated *in vacuo*. The polymer was precipitated in a non-solvent, depending on the polymer composition, collected by filtration and dried *in vacuo*. The residual fraction was concentrated *in vacuo*.

Poly[*p*-phenylene(1-{2-[2-(2-methoxyethoxy)ethoxy]ethyl}sulphinyl)ethylene] 15



This compound was synthesised in 2-butanol according to the general procedure starting from 1g of monomer to give the precursor polymer as a white solid (638 mg, 72%) Mw= 499.000 and PD = 2.58. ¹H-NMR (300 MHz, δ , ppm, CDCl₃): 7.3-6.75 (4H, br), 3.9-3.7+3.7-3.52 (2H, br), 3.52-3.42 (2H, br), 3.35-3.25 (3H, br), 3.25-2.75 (1H), 2.65-2.3+2.1-1.95 (2H, br). ¹³C-NMR (75 MHz, δ , ppm, CDCl₃): 138.2, 132.0, 131.6, 129.2, 128.7, 71.7, 70.3, 69.7, 65.4, 64.1, 63.3, 58.9, 49.5, 36.0. FT-IR (KBr), ν (cm⁻¹): 2955, 2926, 2855, 1104, 1041

Poly[*p*-phenylene(1-{6-hydroxyhexyloxy}sulphinyl)ethylene] 17



This compound was synthesised according to the general procedure to give the precursor polymer as a white solid that was insoluble in common organic solvents such as chloroform, dichloromethane, THF, acetone etcetera allowing no characterisation in solution. In situ UV-

Vis and FT-IR measurements were performed by wiping a piece of the polymer in methanol over the discs.

FT-IR (KBr), ν (cm^{-1}): 3400 (OH), 2955, 2926, 2855, 1480, 1022 (S=O)

Copolymer 23

This compound was synthesised according to the general procedure starting from a mixture of 486 mg of octyl OC₁C₁₀ monomer and 288 mg of monomer 2 in 14 ml sec-BuOH and 250 mg base in 6 ml to give the precursor polymer as a white solid (502 mg). ¹H-NMR: 7.1-6.4, 4.0-3.4, 3.2, 2.6-2.0, 1.8-1.4, 1.4-1.0, 0.8

Copolymer 24

This compound was synthesised according to the general procedure starting from a mixture of 300 mg of octyl PPV monomer and 288 mg of monomer 2 in 14 ml 2-BuOH and 250 mg base in 6 ml to give the precursor polymer as a white solid (470 mg). ¹H-NMR: 7.1, 6.8, 4.0-3.4, 3.2, 3.1, 2.4-2.0, 1.8-1.1, 0.8

6. References

- ¹ Kim, K. S.; Hwang, H. J.; Cheong, C. S.; Hahn, C. S. *Tetrahedron Lett.* 31, **1990**, 2893.
- ² Margreet De Kok, *PhD dissertation*, Limburgs Universitair Centrum, Diepenbeek, **1998**. Kesters Els, *PhD dissertation*, Diepenbeek, **2002**.
- ³ a) Tagaki, W. in: *Organic Chemistry of Sulphur* Oae, S. Ed., Plenum Press, London, **1977**, 231-302.
b) Herriot, A. W. *Synthesis* **1975**, 447.
- ⁴ van Breemen, A.; Vanderzande, D.; Adriaensens, P.; Gelan, J. *J. Org. Chem.* 64, **1999**, 3106. van Breemen, A. *Ph.D. Dissertation*, **1999**, Limburgs Universitair Centrum, Diepenbeek, Belgium
- ⁵ a) Wessling, R.A.; Zimmerman, R.G. U.S. pat., 1968, 3401152. b) Wessling, R.A. J; *Polym. Symp.*, 1985, 75, 55
- ⁶ Pinto, M.R.; Schanze, K.S., *Synthesis*, 9, **2002**, 1293.
- ⁷ Akcelrud, L. *Prog. Polym. Sci.*, 28, **2003**, 875. Pron, A. *Prog. Polym. Sci.*, 27, **2002**, 135. Shi, S.; Wudl, F. *Macromolecules*, 23, **1990**, 2119. Wang, J.; Wang, D.; Miller, E.K.; Moses, D.; Bazan, G.C.; Heeger, A.J. *Macromolecules*, 33, **2000**, 5153. Fan, C.; Plaxco, K.W.; Heeger, A.J. *J. Am. Chem.*

Chapter 2

Soc., 124, **2002**, 5642. Gaylord, B.S.; Wang, S.; Heeger, A.J.; Bazan, G.C. *J. Am. Chem. Soc.*, **2001**, 18. Hong, J.W.; Gaylord, B.S.; Bazan, G.C. *J. Am. Chem. Soc.*, 124, **2002**, 11868. Wallace, G.G.; Kane-Maguire, L.A.P. *Adv. Mater.*, 14, **2002**, 13.

⁸ Huang, C.; Huang, W.; Guo, J.; Yang, C.Z.; Kang, E.T. *Polymer*, 42, **2001**, 3929. Li, F.; Coa, Y.; Gao, J.; Wang, D.; Yu, G.; Heeger, J.A. *Synth. Met.*, 99, **1999**, 243. He, G.; Yang, C.; Wang, R.; Li, Y. *Displays*, 21, **2000**, 69. Garay, R.O.; Mayer, B.; Karasz, F.E.; Lenz, R.W. *Journal of the polymer Science*, 33, **1995**, 525. Morgado, J.; Cacialli, F.; Friend, R.H.; Chuah, B.S.; Rost, H.; Holmes, A.B. *Macromolecules*, 34, **2001**, 3094. Yang, C.; He, G.; Sun, Q.; Li, Y. *Synth. Met.*, 124, **2001**, 449. Tasch, S.; Holzer, L.; Wenzl, F.P.; Gao, J.; Winkler, B.; Dai, L.; Mau, A.W.H.; Sotgiu, R.; Sampietro, M.; Scherf, U.; Müllun, K.; Heeger, A.J.; Leising, G. *Synth. Met.*, 102, **1999**, 1046. Holzer, L.; Winkler, B.; Wenzl, F.P.; Tasch, S.; Dai, L.; Mau, A.W.H.; Leising, G. *Synth. Met.*, 100, **1999**, 71. Morgado, J.; Friend, R.H.; Cacialli, F.; Chuah, B.S.; Rost, H.; Moratti, S.C.; Holmes, A.B. *Synth. Met.*, 122, **2001**, 111. Sun, Q.J.; Wang, H.Q.; Yang, X.G.; Wang, C.H.; Liu, D.S.; Li, Y.F. *Thin Solid Films*, 417, **2002**, 14. Huang, C.; Huang, G.; Guo, J.; Huang, W.; Kang, E.T.; Yang, C.Z. *Polymer preprints*, 43, **2002**, 574.

⁹ Cho, B.R.; Kim, Y.K.; Han, M.S. *Macromolecules* **1998**, 31, 2098.

¹⁰ *Principles of polymerization*, Odian G.; John Wiley and sons, inc., 3rd edition, New York, **1991**.

¹¹ Issaris Anna, *PhD Dissertation*, Limburgs Universitair Cantrum, Diepenbeek, **1998**.

¹² *Organische scheikunde*, D. Vanderzande, Diepenbeek, **1995**.

¹³ Pal, K.; Murty, K.; Mal, D., *Synt. Comm.*, 23, **1993**, 1555.

¹⁴ *Practical Organic Chemistry*, Furniss, B.S.; Hannaford, A.J.; Smith, P.W.G.; Tatchell, A.R., 5th edition, 1989.

¹⁵ Cho, B. R. *Prog. Polym. Sci.* 27, **2002**, 307. Denton, F.R.; Sarker, A.; Lahti, P. M.; Garay, R. O.; Karasz, F. E. *J. Polym. Sci. Part A: Polym. Chem.* 30, **1992**, 2233. TCNQ: a) Iwatsuki, S.; Itoh, T.; Horiuchi, K. *Macromolecules* 11, **1978**, 997. b) Iwatsuki, S.; Kamiya, H. *Macromolecules* 7, **1974**, 732.

¹⁶ Ajayagosh, A.; George, S.J. *J. Am. Chem. Soc.*, 123, **2001**, 5148.

¹⁷ Benjamin, I.; Hong, H.; Avny, Y.; Davidov, D.; Neumann, R. *J. Mater. Chem.*, 8, **1998**, 919.

¹⁸ Yu, J.; Orfino, F.P.; Holdcroft, S. *Chem. Mater.*, 13, **2001**, 526. Murray, K.A.; Moratti, S.C.; Baigent, D.R.; Greenham, N.C.; Pichler, K.; Holmes, A.B.; Friend, R.H. *Synth. Met.*, 69, **1995**, 395. Yu, J.; Holdcroft, S. *Macromolecules*, 33, **2000**, 5073.

¹⁹ *Organosulfur Chemistry* Gordon H. Whitham, Oxford Science Publications, New York, USA, **1995**, 44-45.

²⁰ Shi, S.; Wudl, F. *Macromolecules*, **23**, **1990**, 2119. Wang, J.; Wang, D.; Miller, E.K.; Moses, D.; Bazan, G.C.; Heeger, A.J. *Macromolecules*, **33**, **2000**, 5153. Fan, C.; Plaxco, K.W.; Heeger, A.J. *J. Am. Chem. Soc.*, **124**, **2002**, 5642. Gaylord, B.S.; Wang, S.; Heeger, A.J.; Bazan, G.C. *J. Am. Chem. Soc.*, **2001**, **124**, 11868.

²¹ Paik, S. Y.; Kwon, S. H.; Kwon, O. J.; Yoo, J. S.; Han, M. K. *Synth Met.* **129**, **2002**, 101. Wéry, J.; Dulieu B.; Launay E. ; Bullo J. ; Baïtoul M.; Buisson J.P. *Synth Met.* **84**, **1997**, 277.

²² Renak, M. L. ; Bazan, G. C.; Roitman, D. *Synth. Met.* **97**, **1998**, 17.

Chapter 3

PPV derivatives with polar or functional groups on the phenyl core

1. Introduction

In chapter 3 the synthesis and characterisation of PPV derivatives with a polar or functional chain on the phenyl core will be discussed. As mentioned before the motivation for this kind of research is twofold. First we want to examine whether the versatile sulfinyl precursor route is also applicable for any kind of PPV derivative, including polar and functional ones. A second reason is the fact that these polar derivatives may have interesting properties to act as active layer in plastic photovoltaic cells, light emitting electrochemical cells and chemical sensors. At present functional PPV derivatives are more like a curiosity in literature. However the possible applications of such materials seem very promising. Some of these functional PPV derivatives with water-soluble properties were reviewed by Pinto and throughout this chapter some examples will be depicted¹. Also, such functional polymers may be interesting for their self-assembling properties.

In the present chapter four different monomers and polymers were synthesised all with different functionalities on the phenyl core of the polymer backbone. Although the synthetic procedure used for every monomer is very similar, the synthesis of each monomer will be discussed separately. The knowledge obtained from the experiments described in chapter 2 will turn out to be very useful to solve several synthetic problems in the present chapter. Hence also note the similarity between the functional groups introduced in this chapter and the ones described in chapter 2.

2.1. Synthesis of triethylene glycol derived polymers 1 and 2

The first polar PPV derivatives synthesised through the sulfinyl precursor route are the ones with a triethylene glycol derived chain on the phenyl core. We synthesized the monomer and polymers with one and two of such side chains respectively (figure 1). The synthesis of both conjugated polymers is well described in literature using the Gilch and the Wessling precursor route².

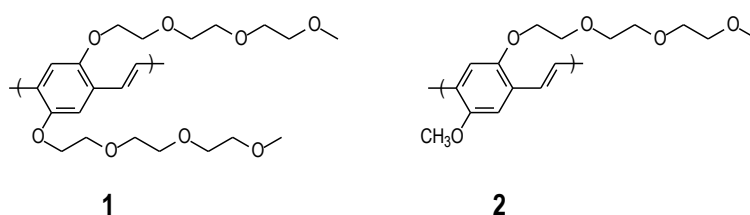


Figure 1. Presentation of the chemical structures of polymer 1 and 2

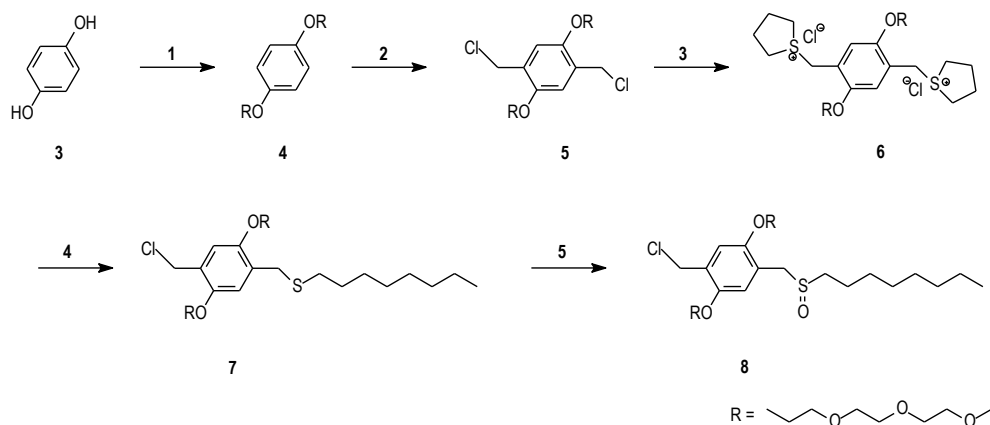
These polymers show interesting properties for use as active layer in light emitting electrochemical cell devices³ and sensors⁴. The number of articles devoted to these products is still increasing. The use of the sulfinyl precursor route may provide these products in a more defined and defect poor approach compared to the other precursor routes. Moreover the low reactivity of the chains probably excludes the interference with other functionalities and makes these materials a worthwhile tool to develop the skills in handling this class of materials.

2.1.1. Monomer synthesis

Synthesis of the monomers is depicted in schemes 1 and 3 and starts in both cases with a Williamson ether synthesis using dihydroquinon **3** or p-hydroxy-anisol as the nucleophile towards the tosylate ester described in chapter 2. The reaction is performed in ethanol with sodium t-butoxide acting as a base. The second step is a chloromethylation reaction of the phenyl core **4**. In literature commonly used is formaldehyde and HCl in a HCl saturated 1,4-dioxane solution⁵. However we used the route developed by Becker and co workers where high yields of the desired dichloride **5** can be obtained⁶. The reaction is performed in a mixture of acetic anhydride and HCl with p-formaldehyde under a nitrogen atmosphere at

70°C. After workup of the reaction with water the dichloro compound **5** is obtained in a good yield.

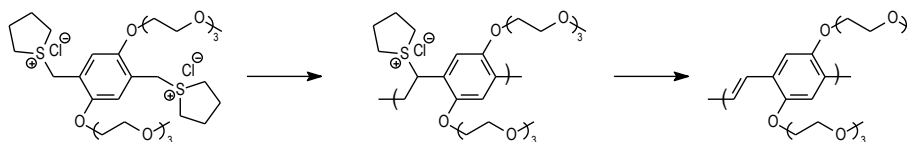
Subsequently the dichloride is treated with an excess of THT in methanol to yield the corresponding bissulfonium salt **6**. These reactions are well documented in literature. The salt is precipitated in a non-polar aprotic solvent like ether or tetrahydrofuran and collected through filtration. The desired bissulfonium salt is obtained in moderate yields. The reason for these rather low yields was not determined but probably the ion complexing properties of the chain may attribute to this phenomenon. The pure salt is collected and dried in vacuo. In the next step the thioether **7** is obtained by treating the bissulfonium salt using the method developed by van Breemen *et al.*



Scheme 1. Synthesis of monomer **8** 1: EtOH, KOH, tosylate ester, 2: *p*-formaldehyde, HCl, Ac₂O, 3: MeOH, THT, 4: MeOH, *n*-octanethiol, Na-*t*BuO, 5: 1,4-dioxane, TeO₂, H₂O₂, HCl *cat*

However when using the same concentrations as used for non-polar derivatives like OC₁C₁₀ PPV, only low yields of the thioether **7** can be obtained. The solution of the bissulfonium salt turns yellow upon adding the thiolate solution probably due to Wessling polymerisation of the bissulfonium salt. (scheme 2)

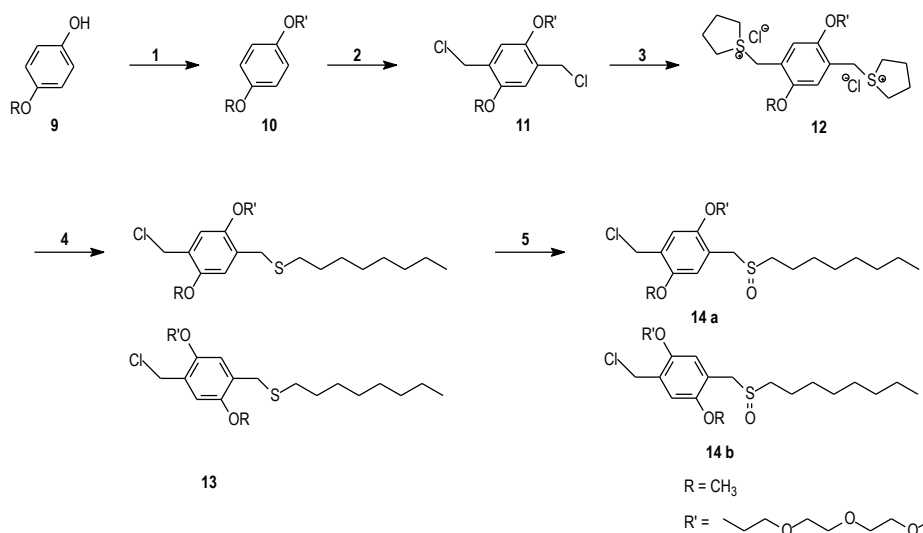
Chapter 3



Scheme 2: Unwanted Wessling polymerisation reaction of the bissulfonium salt **6**

When diluting the reaction five times and with slow addition of the thiolate solution no polymerisation occurs and the thioether **7** is obtained in high yields because the initiation of this Wessling polymerisation will be inhibited as mentioned in chapter 2. We also noticed that under these conditions almost no dithioether was formed which eases purification afterwards. The pure thioether is readily oxidized to the sulfinyl analogue **8** using the mild reaction conditions described earlier, however to avoid solvent substitution 1,4-dioxane is used as the solvent instead of methanol.

The reaction scheme for monomer **14** with only one of such oligo ethylene oxide chain is analogous to the previous, now starting from *p*-hydroxy-anisol **9** instead of dihydroquinon. The only difference is the formation of two regioisomers on the thioether level **13** due to a non-symmetrical substituted phenyl core.



Scheme 3. Synthesis of monomer **14** 1: EtOH, KOH, tosylate ester, 2: *p*-formaldehyde, HCl, Ac₂O, 3: MeOH, THT, 4: MeOH, *n*-octanethiol, Na-*t*BuO, 5: 1,4-dioxane, TeO₂, H₂O₂, HCl_{cat}

2.1.2. Characterisation of the monomers

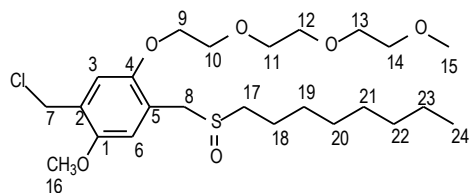
Both monomers **8** and **14** are characterised using different analytical techniques such as ^1H and ^{13}C -NMR spectroscopy, mass spectroscopy (DIP-MS) and FT-IR spectroscopy. For the non-symmetrically substituted monomer **14** several Nuclear Overhauser Enhancement (NOE) experiments and both a long and short range two-dimensional HETCOR experiment were performed to assign all NMR-signals and to determine the ratio of both regio isomers.

2.1.2.1. Nuclear Overhauser Enhancement (NOE)

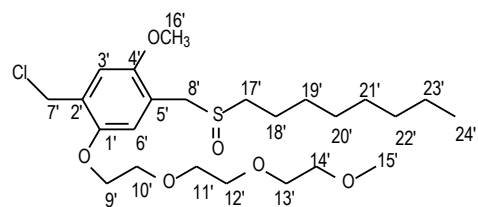
It is generally known that magnetic nuclei can also interact through space. This interaction does not lead to coupling but irradiation of one nucleus at its resonance frequency leads to a more intense or weaker signal than usual for the nuclei on a distance of 2-4 angström of the irradiated nucleus⁷. This through space dependence can be a powerful tool in characterising the stereochemistry of a compound. Five different Nuclear Overhauser Enhancement experiments were performed to start the determination of the exact and complete assignment of the different regio-isomers of monomer **14**. Since a column separation of the two isomers was not possible, the mixture of the two compounds **14a** and **14b** was used for these experiments.

For each NOE experiment two different spectra were recorded. A first spectrum was recorded with a specific pre-irradiation at the resonance frequency of the nucleus of interest. A second spectrum (control spectrum) was recorded without this pre-irradiation. By computational subtraction of these two spectra a so called difference spectrum is obtained where only the signals that have changed their intensity upon irradiation are observed. The resulting spectra of the different experiments are depicted below. For each experiment the upper spectrum is the difference spectrum, the middle is the NOE spectrum and the control spectrum is depicted at the bottom.

Chapter 3



14a (present in excess)



14b

Irradiation at the resonance frequency of the chlorobenzyl proton (nucleus H₇ and H_{7'}) in two different experiments yields a NOE enhancement at 6.92 ppm and 6.88 ppm for isomer **14a** and isomer **14b** respectively as depicted in figure 2 and 3. All the other signals remain unaffected and hence they are completely disappeared in the difference spectrum.

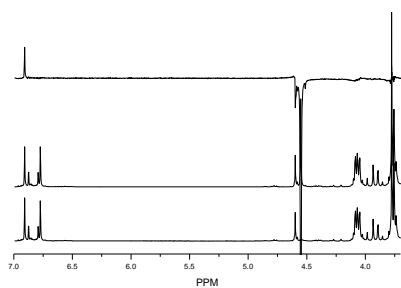


Figure 2. NOE spectrum after irradiation at H₇

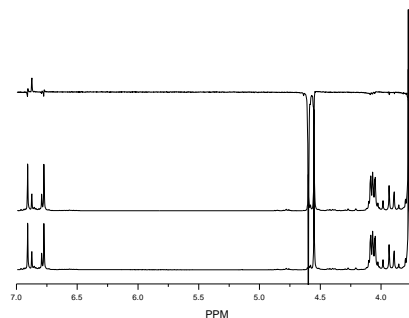


Figure 3. NOE spectrum after irradiation at H_{7'}

Saturation of H₁₆ only creates an enhancement of the signal at 6.79 ppm. Saturation of H_{16'} gives an enhanced signal at 6.88 ppm. (Figure 4-5)

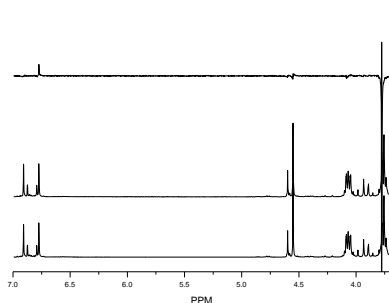


Figure 4. NOE spectrum after irradiation at H_{16}

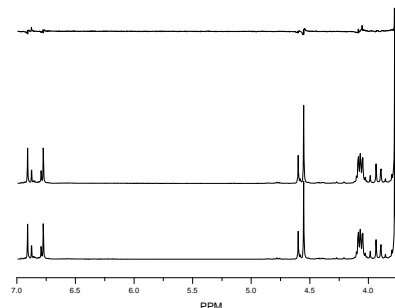


Figure 5. NOE spectrum after irradiation at H_{16}'

Saturation of H_8 and H_8' affords an enhancement of the signals at 6.79 and 6.81 ppm (figure 6). From the irradiation experiments at H_7 and H_{16}' it can be seen that the proton H_3' at 6.88 ppm is spatially situated between the methoxy group and the chloro methylene group. From the experiments where nuclei H_{16} and H_8 are irradiated it is concluded that H_6 is spatially situated between the methoxy group and the sulfinyl substituted benzylic position. Hence, on this basis, a clear distinction is made between the two isomers.

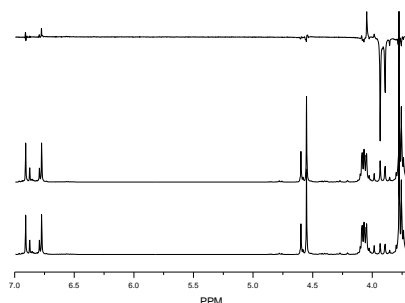


Figure 6. NOE spectrum after irradiation at H_8 and H_8'

2.1.2.2. Direct coupling HETCOR experiment

In order to obtain a full assignment of the other ^1H and ^{13}C NMR signals two different HETCOR (heteronuclear chemical shift correlation) experiments were performed. A direct coupling HETCOR ($J=140$ Hz) indicates which proton is attached to the corresponding carbon atom. So a clear distinction between all proton resonances can be made. The

obtained spectrum is depicted in figure 7 and the exact values of the resonances are mentioned in table 1

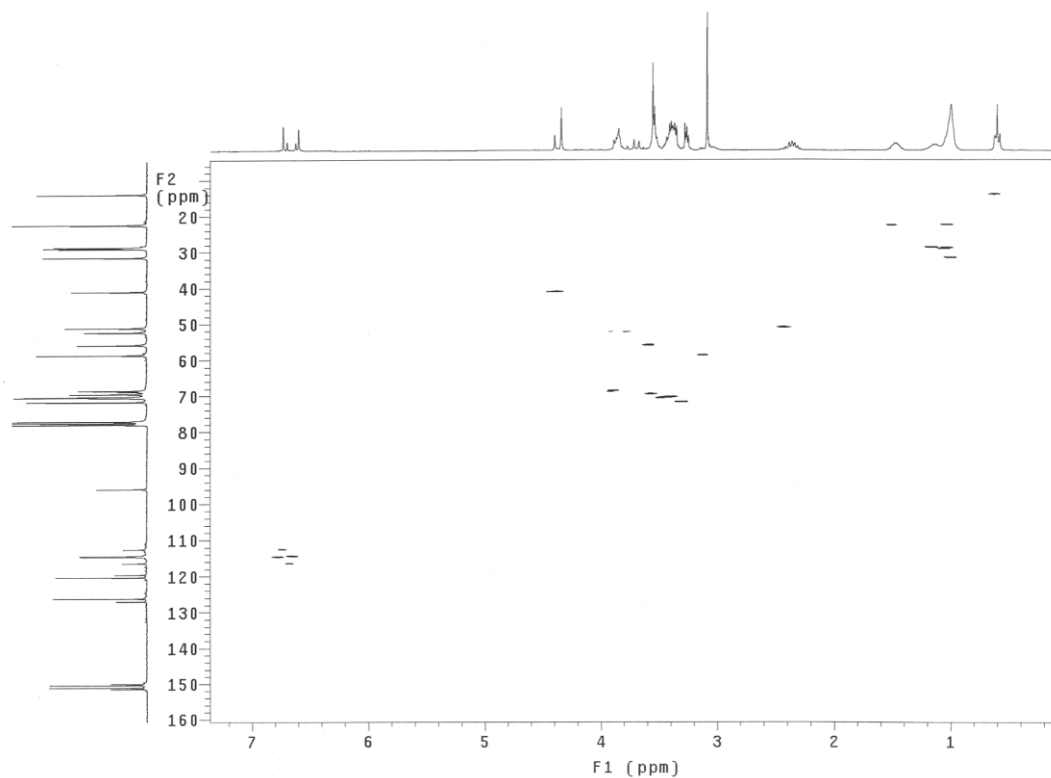


Figure 7. Direct HETCOR spectrum of monomer **14** (mixture of 14a and 14b)

2.1.2.3. Long range HETCOR (J=8Hz)

For the determination and assignment of the quaternary carbon resonances a long range coupling HETCOR experiment was set up. In such experiment a correlation is made between a carbon atom shift and a proton shift 2 and/or 3 bonds further. The spectra obtained from such an experiment are depicted in figure 8. The exact values of the proton and carbon resonances obtained from these experiments are also listed in table 1.

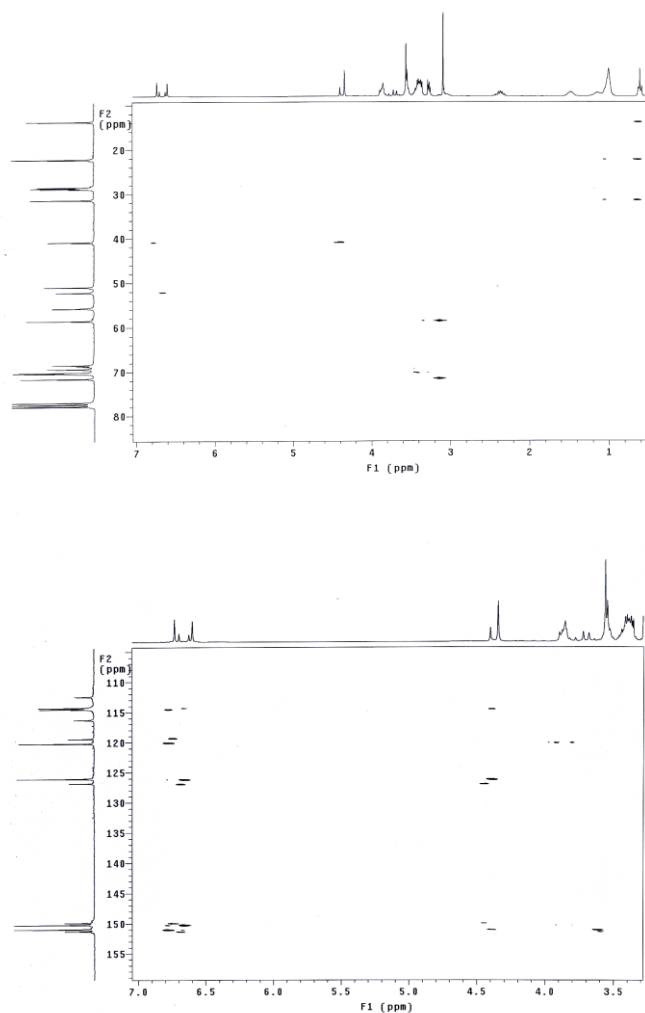


Figure 8 Long range HETCOR spectrum of monomer **14** (mixture of **14a** and **14b**). Full proton spectrum and aliphatic ¹³C region (above) and proton region from 3.0-7.0 ppm and aromatic ¹³C region (bottom)

After these experiments a complete assignments can be performed and the ratio of the two isomers was calculated from the proton resonances at 4.59 and 4.61 ppm. A ratio of 57/43 was determined in favour of monomer **14a**.

14a			14b		
	¹ H	¹³ C		¹ H	¹³ C
1	/	150.93	1'	/	149.87
2	/	126.03	2'	/	126.81
3	6.92	114.47	3'	6.88	112.43
4	/	150.18	4'	/	151.25
5	/	120.19	5'	/	119.41
6	6.79	114.24	6'	6.81	116.26
7	4.59	40.82	7'	4.61	40.82
8	3.98+3.90	52.14	8'	3.98+3.90	52.14
9	4.09	68.39	9'	4.09	68.71
10	3.60	69.29	10'	3.60	69.29
11	3.60		11'	3.60	
12	3.60	70.30	12'	3.60	70.30
13	3.60		13'	3.60	
14	3.50	71.72	14'	3.50	71.50
15	3.32	58.49	15'	3.31	58.49
16	3.79	55.70	16'	3.76	55.59
17	2.61	50.92	17'	2.61	50.92
18	1.73	22.29	18'	1.73	22.29
19	1.36	28.48	19'	1.36	28.48
20		28.85	20'		28.85
21		28.64	21'		28.64
22	1.21	31.35	22'	1.21	31.35
23		22.44	23'		22.44
24	0.82	13.73	24'	0.82	13.73

Table 1. Overview of ¹H and ¹³C NMR signals of monomer **14a** and **14b**

2.1.3. p-Quinodimethane formation

Prior to the polymerisation reactions of both monomers **8** and **14** the possibility of p-quinodimethane formation was studied using stop-flow UV-Vis spectroscopy. After mixing the monomer (1×10^{-4} M) with an excess of base in the sample cell both for monomer **8** and **14** a new band at 320 nm is observed that increases quickly. The signal declines again indicating the formation of solvent substituted product. The formation of the p-quinodimethane system of monomer **8** is depicted in figure 9 and in figure 10 the absorption at 320 nm is plotted versus time.

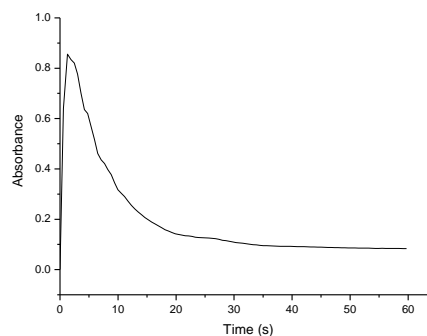
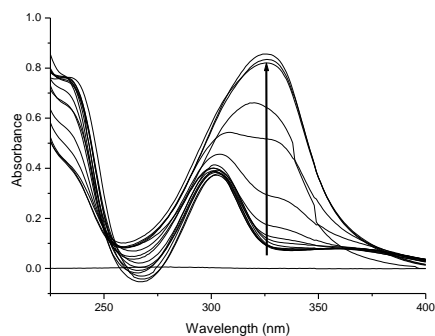
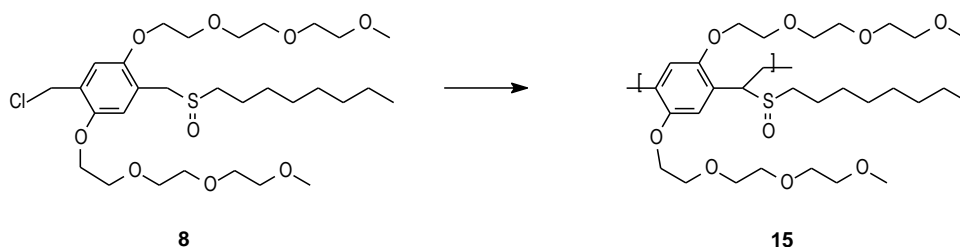


Figure 9. UV-Vis spectra of the gradual p-quinodimethane formation from monomer **8** Figure 10. Plot of absorbance at 320 nm versus time

2.1.4. Polymerisation of monomer **8**

Monomer **8** was polymerised in different solvents according to the standard procedure developed in our group by van Breemen. A solution of monomer and a solution of sodium t-butoxide (1.3 equivalents to correct for losses during addition) in the same solvent are degassed by a continuous flow of nitrogen. The base solution is added to the monomer in one portion and the reaction was stirred for one hour at 30°C while passing nitrogen through the solution. Subsequently the reaction mixture is poured in water and extracted three times with chloroform or dichloromethane. The combined organic layers are evaporated and precipitated in a non-solvent to yield the precursor polymer **15** (scheme 4). The filtrate is evaporated to yield the rest fraction.



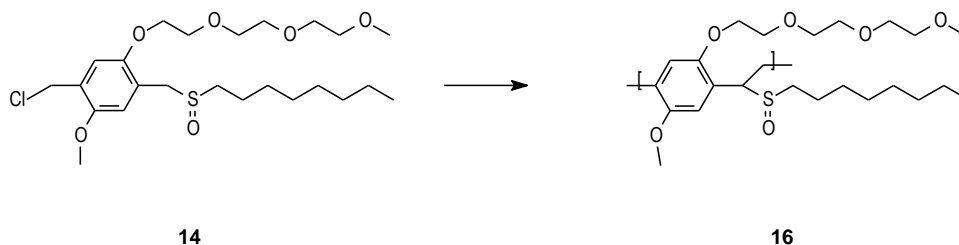
Scheme 4. Synthesis of precursor polymer **15**. 1: Na-*t*BuO (1.3 eq)

GPC measurements both on the precursor and conjugated polymers were performed versus polystyrene standards using DMF as the eluent. Molecular weights and polydispersities for the polymerisation reactions in the different solvents are summarized in table 2. Note that the molecular weight and yield of the polymerisations are only determined after the conversion to the conjugated analogue in toluene (see elimination in solution). The molecular weight of the precursor polymer obtained from polymerisation in 2-BuOH ($M_w = 77.000$) was determined versus polystyrene standards with DMF as the eluent.

solvent	yield (%)	M_w ($\times 10^{-3}$)	PD
2-BuOH	50	435	5.02
THF	46	280	2.84
CH ₂ Cl ₂	46	331	3.07
DMF	36	96	1.51
MMF	33	151	2.84

Table 2. Overview of the results of polymerisation reactions of monomer **8** in different solvents

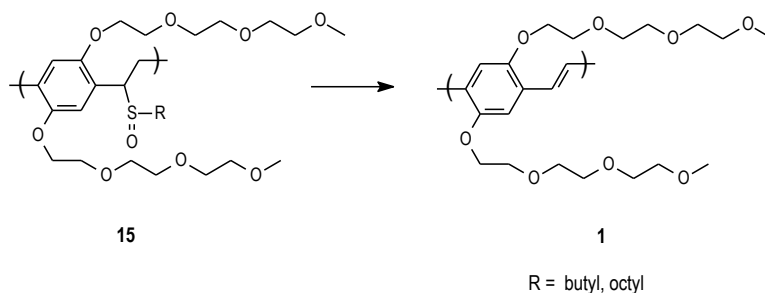
From table 2 it is concluded that in 2-BuOH the highest yield and molecular weight are obtained while polymerisation in a more polar and aprotic solvent like DMF affords lower yields and M_w . These observations are in total accordance with polymerisation data from other non-substituted monomers⁸.

2.1.5. Polymerisation of monomer **14** (mixture of **14a** and **14b**)Scheme 5. Synthesis of precursor polymer **16**. 1: Na-*t*BuO (1.3 eq)

Monomer **14** was polymerised in 2-butanol and THF according to the standard procedure described above. Results of the polymerisation are listed in table 3. In both cases high molecular weights are obtained with good yields. For the polymerisation of monomer **14** in 2-BuOH GPC results both of the precursor polymer and the conjugated material are listed. For the polymerisation in THF the GPC results after conversion are depicted. The significant difference in yield between the polymerisation in 2-butanol of monomer **8** and **14** can be related to the scale on which the polymerisation reactions are performed. Mass losses when started from a smaller amount of monomer affect the yield relatively more than higher amounts. As can be seen from table 3, the value of the molecular weights for the precursor polymer increase upon conversion as chain stiffness and possible solvent interaction increase and thus the hydrodynamic volume increases.

Solvent	Yield (%) ^a	M _w ^{b,c}	PD ^{b,c}	M _w ^{a,d}	PD ^{a,d}
2-BuOH	63	214.000	3.74	299000	3.19
THF	40	/	/	216000	4.43

Table 3. Overview of the polymerisation results of monomer **14**. ^a = determined after conversion, ^b = determined for the precursor polymer, ^c = GPC eluent is THF, ^d = GPC eluent is DMF

2.1.6. Thermal conversion of precursor polymer **15** to the conjugated structure

Scheme 6. Thermal conversion of precursor polymer **15** into the fully conjugated structure.

The final step in the sulfinyl precursor route is the thermal elimination of the sulfinyl group to yield the double bond (scheme 6). As mentioned in chapter 1 and 2 this elimination is an expulsion of sulfenic acid and the formation of a double bond on the polymer backbone. The double bonds formed are all trans due to increased steric hindrance in the transition state which leads to cis double bonds. Numerous techniques can be applied to monitor the elimination process. The ones used here are in situ UV-Vis spectroscopy, in situ FT-IR spectroscopy and direct insertion probe mass spectroscopy (DIP-MS).

UV-Vis spectroscopy measurements were carried out on a film of the precursor polymer, spin-coated on a quartz disc. An experimental set-up was used which allowed in situ monitoring of the elimination process as described in chapter 2.

Before heating, the precursor polymer shows strong absorptions below 250 nm. As the heating program progresses, new absorption bands appear that gradually redshift with increasing temperature. Finally the maximal conjugated polymer **1** with an absorption maximum around 473 nm is obtained. This maximum is slightly lower compared to the maximum of other alkoxy-substituted PPV derivatives like OC₁C₁₀ PPV. However the elevated temperature causes this blueshift. This phenomenon is described further on in this chapter.

The gradual formation of the conjugated structure is shown in figure 11. When the absorption at this assumed maximum wavelength (473 nm) is plotted versus temperature, the elimination and stability behaviour of the polymer becomes clear. (figure 12). Also the effect of the eliminable group on the elimination behaviour was tested by performing the

thermal heating experiment on the butyl precursor polymer. This polymer was synthesised analogous to the octyl compound and the corresponding monomers were prepared as described under the experimental section. There seems to be no significant difference between the three polymers concerning their elimination temperature. Elimination starts around 75°C. At temperatures above 123°C a strong decline in the maximum is observed.

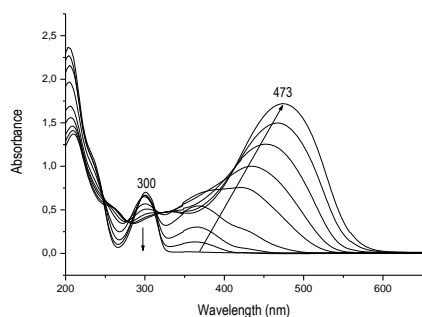


Figure 11. Gradual formation of the conjugated structure.

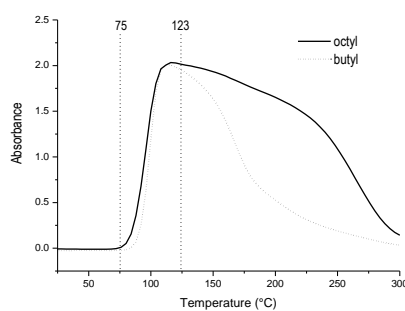


Figure 12. Absorption at 473 nm versus temperature

This observation could correspond to a quick degradation of the conjugated structure at these elevated temperatures. However this phenomenon can also be explained by the thermochromic^{9,10} effect that is discussed later in this chapter. Together with the decline in maximum absorbance a small blue shift of the absorption maximum is observed, which may be explained by a shortening of the conjugated segments in the polymer backbone.

A second technique that was used to study the thermal elimination and stability of the sulphonyl precursor was *in situ* FT-IR. In this technique an identical experimental set-up was used as in the *in situ* UV-Vis measurements. Because of the identical experimental set-up the results derived from both techniques complement each other and a very detailed picture of the elimination process is obtained. *In situ* FT-IR measurements were also performed on a film of the precursor polymer, spin coated on a KBr disc and a dynamic heating program of 2°C/min up to 300°C, under a continuous flow of nitrogen, was used. The most important and distinct absorption bands in the FT-IR spectrum, which are changed during the elimination process, are those of the sulfinyl group at 1046 cm⁻¹ and that of the vinylene double bond at 962 cm⁻¹ (figure 13).

The relative trends in both elimination and stability behavior of the two precursor polymers (octyl and butyl) become clear when the intensity of these two absorption bands is plotted

versus temperature. (Figure 14) From the FT-IR data we can conclude that the formation of the fully conjugated system is formed in the temperature domain starting from 75 °C. This result is in accordance with the data obtained from the in situ UV-Vis measurements. Figure 14 also demonstrates a difference in evaporation behaviour between the butyl and octyl analogue, probably caused by a higher boiling point of the elimination products derived from the octyl sulfinyl group.

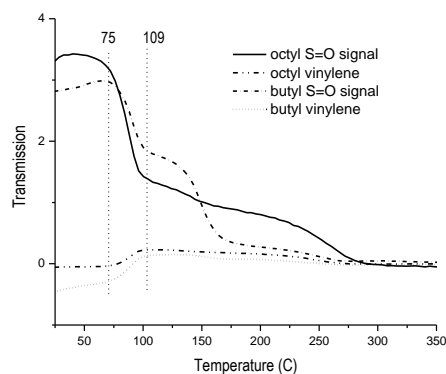
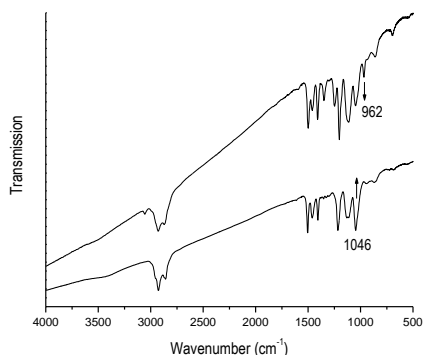


Figure 13. IR spectrum of the octyl precursor polymer before (below) and after conversion (upper) Figure 14. Absorption at 962 and 1046 cm^{-1} versus temperature for the octyl and butyl precursor polymer

The elimination and stability behaviour of the octyl precursor polymer was also studied with DIP-MS, to allow the analysis of the elimination products. In this technique the precursor polymer is placed directly on the heating element of the probe and measurements are performed under high *vacuum*. The heating rate used was 10°C/min and the sample was heated till 650°C. By plotting the total ion current versus temperature, the thermal stability of both precursor and conjugated polymer can be visualised. (Figure 15) As expected two signals can be observed in the thermogram. The first at a maximum of 132 °C, based on the fragments detected, corresponds to the elimination and evaporation of the sulfinyl groups to yield the double bonds. These temperatures are higher than those obtained from the UV-Vis and IR measurements and are caused by the differences in heating rate. The second signal, between 400 and 500°C corresponds to the evaporation of the degradation products of the conjugated structure.

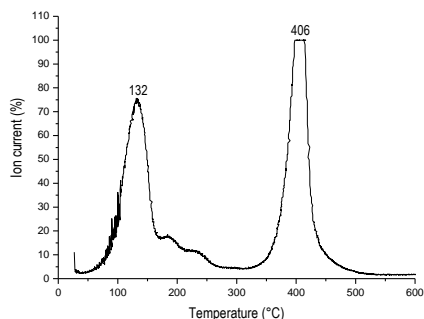


Figure 15. Thermogram of the octyl precursor polymer 15

DIP-MS (132°C)	
Fragment	m/z
$C_8H_{17}SSC_8H_{17}$	290
$SS(O)C_8H_{17}$	194
$S(O)C_8H_{17}$	161
SC_8H_{17}	145

Table 4. Mass fragments of the elimination products.

2.1.7. Thermal conversion of precursor polymer 16 into the conjugated structure

The same analytical techniques as used for the elimination behaviour of precursor polymer 8 were used here. Figure 16 shows the UV-Vis spectra recorded at different temperatures and a plot of the maximum absorption (466 nm) versus the temperature is depicted in figure 17. Formation of the conjugated system is started at 71°C. At higher temperatures a large decline in the maximum absorption is observed which can also be explained by the thermochromic effect that will be discussed later. Also the elimination behaviour of the butyl analogue was investigated and no significant difference was observed compared to the octyl precursor polymer 16.

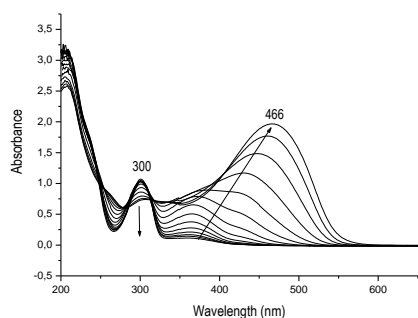


Figure 16. Gradual formation of the conjugated structure.

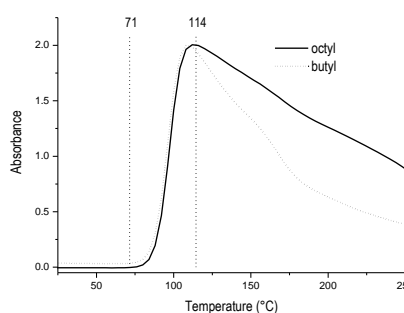


Figure 17. Absorption at 473 nm versus temperature

Chapter 3

The elimination behaviour of the octyl precursor polymer **16** was also studied using FT-IR spectroscopy. Like precursor polymer **15** two signals are of interest and both the signals at 1042 and 962 cm^{-1} are plotted versus the temperature (figure 18). Elimination starts at about 66°C (figure 19).

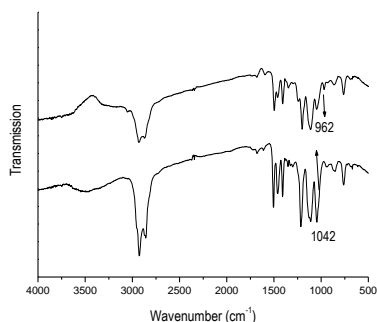


Figure 18. IR spectrum before (below) and after conversion (upper)

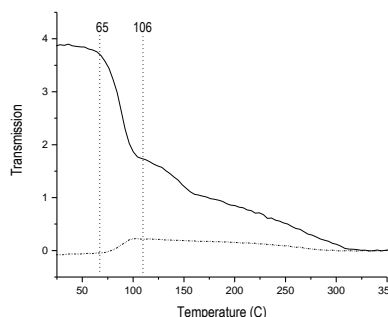


Figure 19. Absorption at 962 and 1042 cm^{-1} versus temperature

Also DIP-MS was used for the analysis of the elimination products. Again two distinct signals are clear from figure 20. The first signal at 141°C is assigned to the formation of the elimination products (table 5). The second peak corresponds to the total degradation of the conjugated structure.

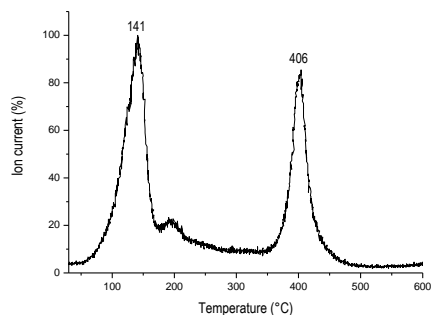


Figure 20. Thermogram of the sulphanyl precursor polymer

DIP-MS (141°C)	
Fragment	m/z
$\text{C}_8\text{H}_{17}\text{SSC}_8\text{H}_{17}$	290
$\text{SS(O)}\text{C}_8\text{H}_{17}$	194
$\text{S(O)}\text{C}_8\text{H}_{17}$	161
SC_8H_{17}	145

Table 5. Mass fragments of the elimination products.

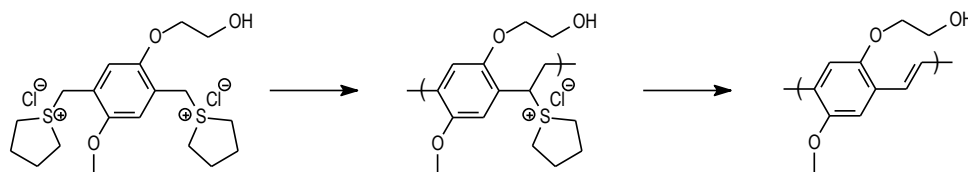
2.1.8. Elimination of the precursor polymers in solution

Since we obtain a completely soluble conjugated polymer (**1-2**) after elimination, the elimination reaction can also be performed in solution using the following protocol. The precursor polymer (0.5 g) is dissolved in toluene (50 ml) and the resulting solution is stirred at 110 °C under an inert atmosphere. The stirring is continued for three hours and then the solution is cooled down to room temperature. The solvent is evaporated and a red gel like polymer is obtained. This polymer is dissolved in a minimal amount of chloroform and the solution is precipitated in a well-stirred amount of hexanes, affording the desired polymer as red wires. The polymer fraction is obtained through filtration and the residue is washed with the same non-solvent. The polymer is dried in vacuo. The filtrate is collected and evaporated to yield the rest fraction of the polymerisation reaction.

2.2. Synthesis of an alcohol derived polymer

A third monomer with a polar chain on the phenyl core is the one with an alcohol function. Alcohol functions may exhibit interesting properties because they can be easily converted to other functional groups allowing eventual post-polymerisation functionalisation of the polymer. Also their self-assembling behavior is of major interest for research groups all over the world¹¹. The presence of the polar side chains can be used to fabricate self-assembled multilayer films based on strong hydrogen bonding.

Up till now very little alcohol bearing PPV derivatives have been synthesized and described in literature. Benjamin and coworkers describe the synthesis of an alcohol functionalized PPV derivative and the copolymerization reactions with plain PPV using the Wessling route (scheme 7). The precursor homopolymer was insoluble due to hydrogen bonding¹².

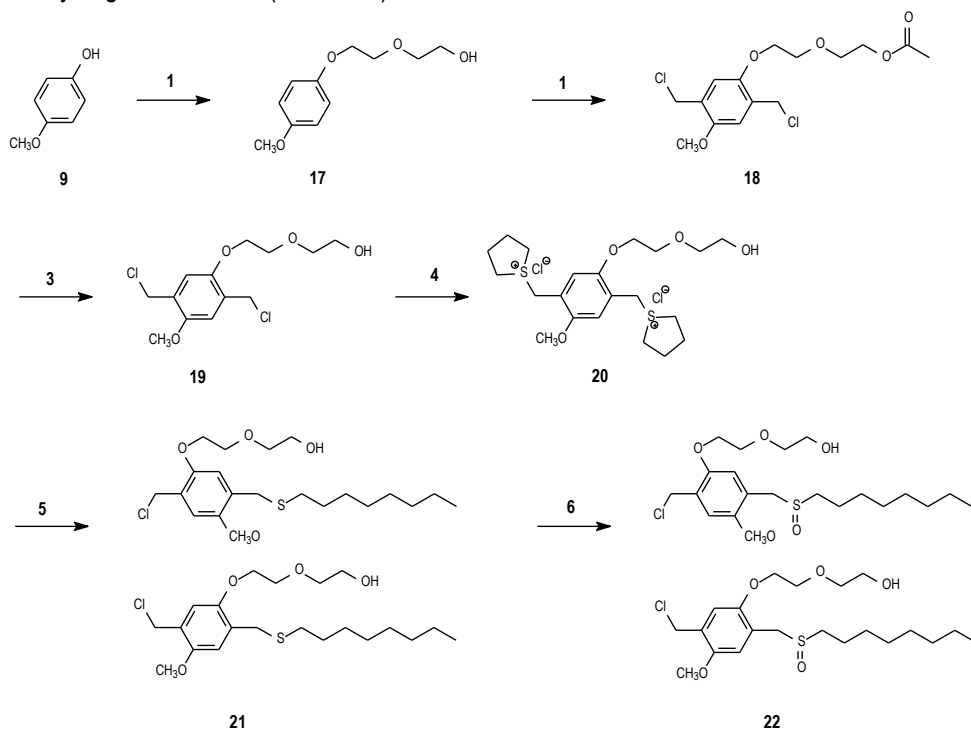


Scheme 7. Synthesis of an alcohol functionalised PPV derivative through the Wessling precursor route according to Benjamin and co workers

2.2.1. Monomer synthesis

The first synthetic step is a Williamson ether synthesis starting from *p*-hydroxy anisol **9** and the commercially available 2-chloro-2-ethoxy ethanol in ethanol at reflux. Sodium *t*-butoxide acts as the base in this reaction and a small amount of sodium iodide is added to catalyze the reaction. The next step, the chloromethylation reaction, does not yield the desired product **19** but the pure acetylated product **18** is obtained in high yield.

The protected alcohol **18** can be hydrolyzed quantitatively by treating the product with an aqueous K_2CO_3 solution. The bisulfonium salt **20** can be obtained through reaction of the dichloro alcohol with an excess of THT in methanol. Also here only very moderate yields can be obtained. The next step generates two regio isomers **21**, which can not be separated using simple column chromatography. Mild oxidation conditions yield a mixture of the sulfinyl regio isomers **22** (scheme 8).



Scheme 8. Synthesis of monomer **22** 1: EtOH, Na-OEt, 2-(chloro-ethoxy)ethanol, 2: *p*-formaldehyde, HCl, Ac₂O, 3: K₂CO₃, H₂O/MeOH, 4: MeOH, THT, 5: MeOH, *n*-octanethiol, Na-*t*BuO, 6: 1,4-dioxane, TeO₂, H₂O₂, HCl_{cat}

that elimination starts at 71°C (figure 22). The maximum wavelength after conjugation is 474 nm (figure 21), comparable to the ones of polymer **1** and **2**.

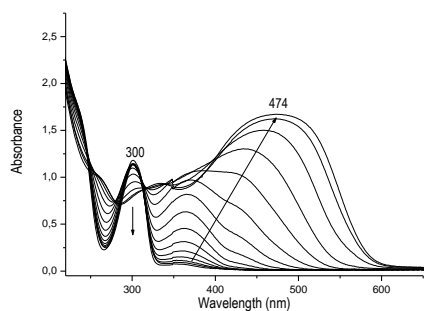


Figure 21. Gradual formation of the conjugated structure.

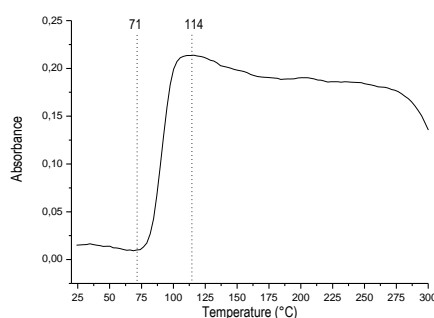


Figure 22. Absorption at 474 nm versus temperature

In situ FT-IR spectroscopy shows the same trends as UV-Vis spectroscopy when the signals at 1034 and 960 cm^{-1} are plotted versus temperature. Also the signal at 3400 cm^{-1} declines with increasing temperature (figure 23). Elimination starts at 67°C (figure 24).

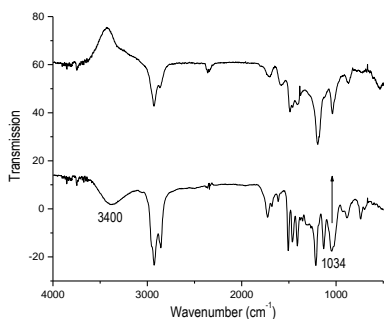


Figure 23. IR spectrum before (below) and after conversion (upper)

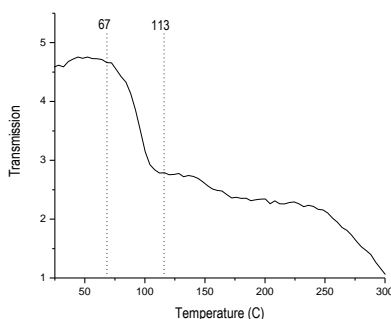


Figure 24. Absorption at 1034 cm^{-1} versus temperature

The DIP-MS thermogram (figure 25) shows the same trends as described for the polymers **15** and **16**. A first peak at 121°C corresponds to the elimination and evaporation of the sulfenic acid and its derivatives (table 6). The second signal corresponds for the evaporation of the degradation products of the conjugated polymer.

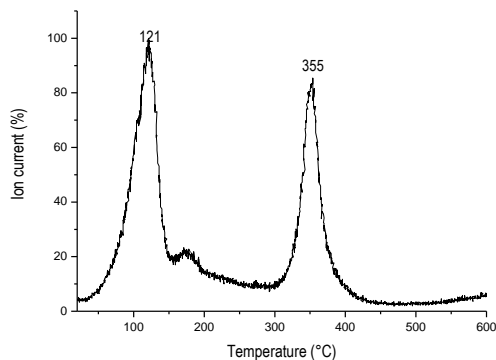


Figure 25. Thermogram of the sulphinyl precursor polymer

DIP-MS (121°C)	
Fragment	m/z
$C_8H_{17}SSC_8H_{17}$	290
$SS(O)C_8H_{17}$	194
$S(O)C_8H_{17}$	161
SC_8H_{17}	145

Table 6. Mass fragments of the elimination products.

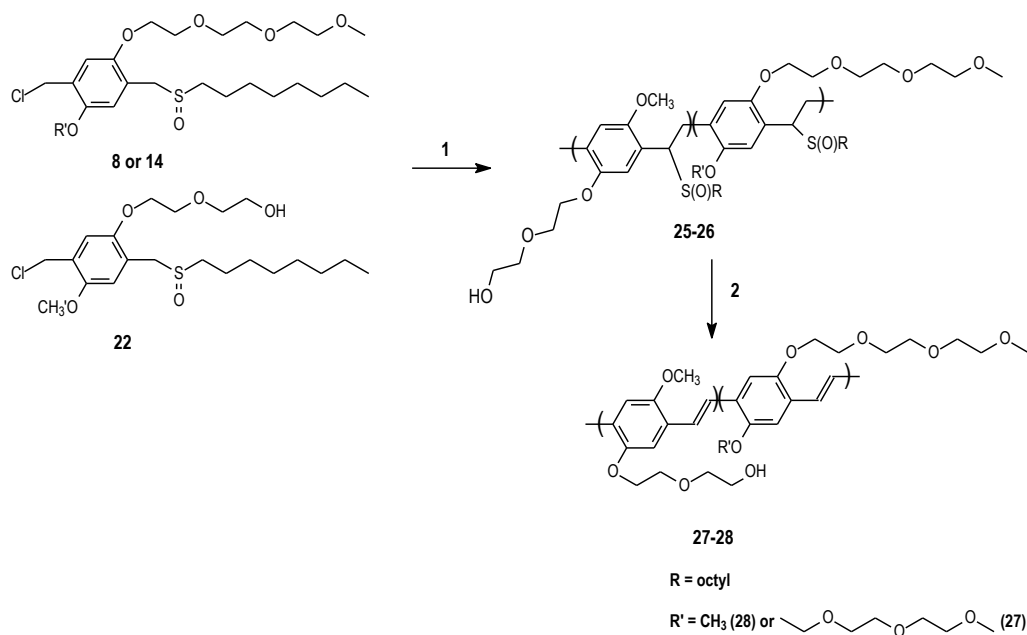
2.2.4. Elimination in solution

The elimination behaviour in solution of polymer **23** was somewhat complicated. Again the precursor polymer is brought in toluene and the resulting mixture is stirred for three hours at reflux (110°C). However compared to the polymers **1** and **2** an insoluble product was formed during the reaction that precipitated from the toluene solution. This phenomenon made normal characterisation in solution (GPC, NMR-spectroscopy etc..) impossible and hence very little characterisation is described here. However the elimination behaviour of the precursor polymer in film could be studied using the techniques described before.

2.2.5. Copolymerisation reactions

To circumvent the solubility problems with the homo-alcohol polymer, two copolymerisation reactions were performed using both monomer **8** and **14** as one of the comonomers (scheme 11). A 3/1 mixture of monomer **8** (or **14**) and monomer **22** were polymerised according to the standard procedure. These polymerizations yielded a soluble copolymer after elimination. The relative fractions of the comonomers built in into the copolymer **27** were determined using ^{13}C -NMR. The integration values of the signal at 58 ppm (aliphatic methoxy) and at 56 ppm (aromatic methoxy) were determined to be 3/1.

Chapter 3



Scheme 11. Copolymerisation reactions of monomer **8** and **14** with monomer **22**. 1: Na-*t*BuO (1.3 eq), 2: toluene 110°C

For the copolymerisation with monomer **8** a molecular weight of 358.000 (polydispersity = 6.33) was obtained for the precursor polymer **25** and 357.000 (polydispersity = 6.52) for the converted product **27**. For the reaction involving monomer **14** a molecular weight of 151.000 was obtained for polymer **26** with a polydispersity of 3.21.

2.2.6. Elimination behaviour of the copolymers 25-26

The elimination behaviour of the copolymers was also analysed with in situ UV-Vis spectroscopy (figure 26), in situ FT-IR spectroscopy and DIP-MS. All three techniques reveal the same trends in elimination temperature as obtained from the homopolymers. Elimination starts at 71°C. In figure 27 and 28 the signals of interest for copolymer **25** are plotted versus temperature.

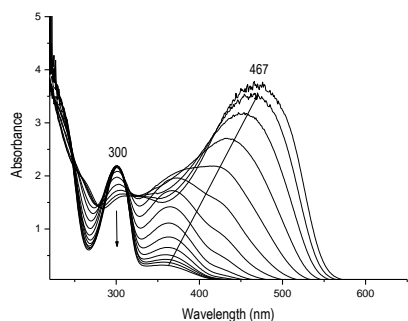


Figure 26. UV-Vis spectra of the gradual formation of copolymer **27**

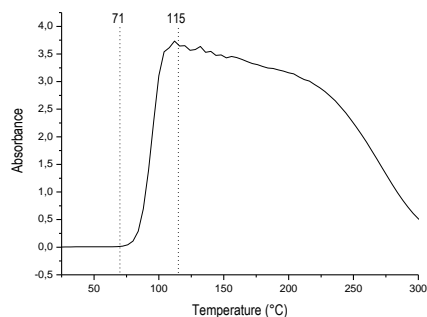


Figure 27. Plot of the absorbance at 461 nm versus temperature

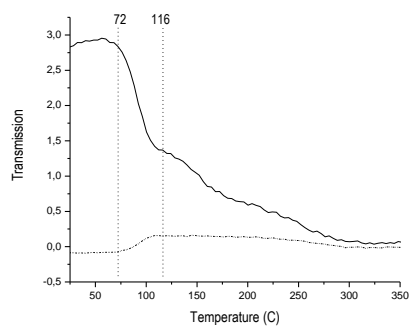


Figure 28. Plot of the signal at 1040 cm^{-1} and 960 cm^{-1} versus temperature for copolymer **25**

Using DIP-MS yields also a thermogram similar to the ones obtained for the homopolymers. The same fragments can be detected indicating the evaporation of elimination products. In figure 29 the thermogram for copolymer **25** is depicted with the assignment of the according fragments.

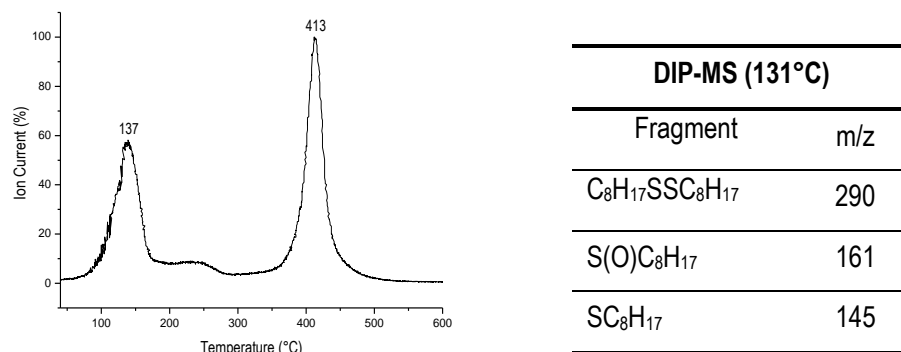
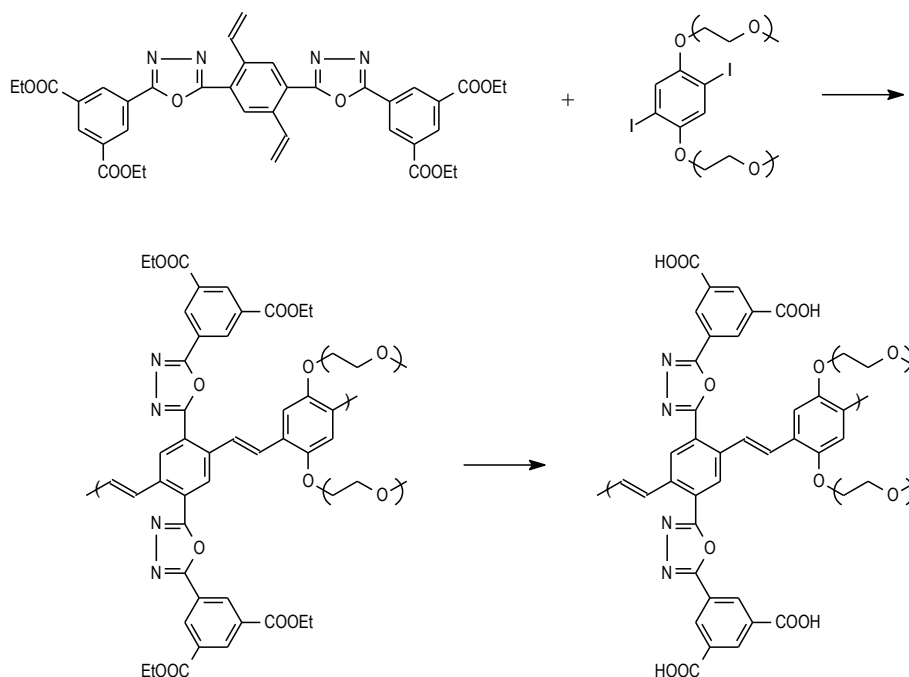


Figure 29. DIP-MS thermogram for precursor *Table 7*. Mass fragments of the elimination polymer **25** products.

2.3. Synthesis of an ester derived polymer

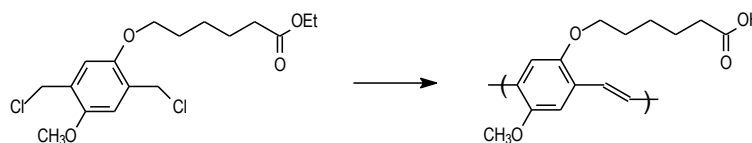
A fourth monomer with a functionalised side chain on the phenyl core is the one with an ester function. Ester bearing PPV derivatives are very rare in literature. Only a few of such derivatives have been described so far but none of them was synthesised using a precursor route. Peng and coworkers¹³ designed an ester functionalised copolymer using a palladium catalysed Heck reaction (scheme 12). Basic hydrolysis yields a water-soluble PPV derivative.

Synthesis of functional PPV derivatives



Scheme 12. Synthesis of an ester functionalised PPV derivative through a Heck coupling reaction according to Peng.

Fujii and coworkers¹⁴ designed a PPV derivative functionalised with carboxylic acid side groups using the Gilch route starting from an ester functionalised Gilch monomer (scheme 13). Because of the strongly basic conditions in this route, the ester functions are readily hydrolysed to the corresponding carboxylic acids during work up of the reaction mixture.

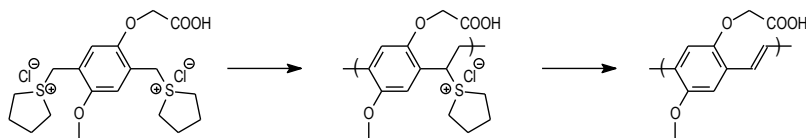


Scheme 13. Synthesis of a carboxylic acid functionalised PPV derivative through the Gilch precursor route starting from an ester functionalised monomer

The use of the sulfinyl precursor route for the synthesis of the ester polymer may offer some advantages over the approach used by Fujii. The smoother polymerisation conditions offer a

chance to obtain the ester without hydrolysis to the acid. This step can then be accomplished in a later more controlled stage.

Such a carboxylic acid functionalised PPV derivative was also developed by Benjamin and coworkers¹⁵ using the Wessling precursor route (scheme 14). Similarly with the alcohol analogue an insoluble precursor polymer was obtained due to aggregation. However this phenomenon could be avoided by performing some co-polymerisation reactions.



Scheme 14. Synthesis of a carboxylic acid functionalised PPV derivative through the Wessling precursor route .

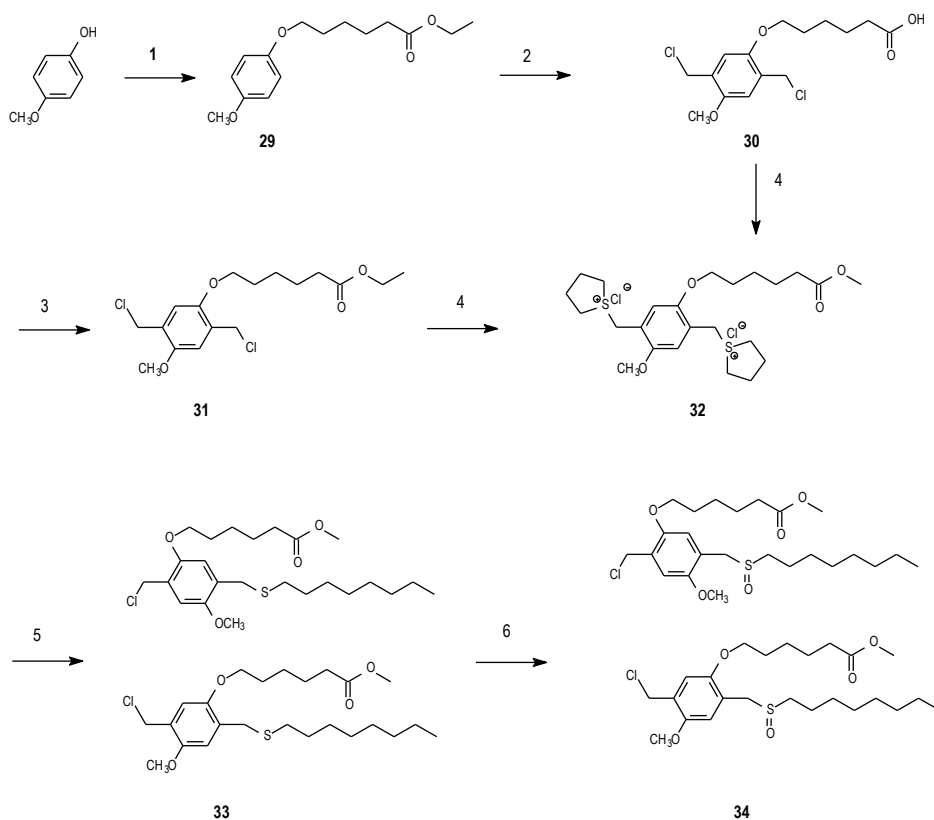
2.3.1. Monomer synthesis

The first synthetic step is a Williamson ether synthesis starting from p-hydroxy-anisole and the commercially available 6-bromo-ethyl hexanoate in ethanol at reflux. Sodium t-butoxide acts as the base in this reaction. The next step, the chloromethylation reaction, does not yield the desired corresponding ester 31 but the pure hydrolysed product 30 is obtained in high yield. The free carboxylic acid 30 can be converted into the ester 31 using acidic esterification conditions i.e. dissolving the acid in an excess of alcohol with sulfuric acid as the catalyst at reflux.

The bisulfonium salt 32 was obtained through reaction of the dichloro ester 31 with an excess of THT in methanol. The next step, the thioether synthesis, also generates two regio isomers 33, which cannot be separated using simple column chromatography. Mild oxidation conditions yield a mixture of the sulfinyl regio isomers 34 (scheme 15).

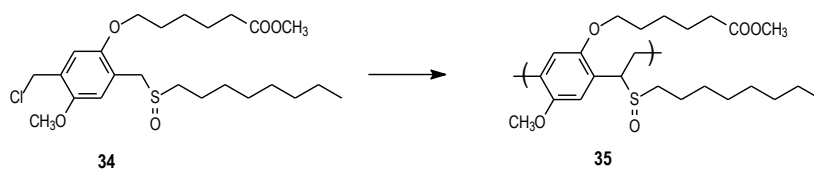
Attempts to make a bisulfonium salt from the free acid 30 failed. Nevertheless this failure is a very interesting feature since the ester bisulfonium salt 32 was obtained in high yields so the esterification reaction can be avoided resulting in a large increase of the overall yield.

Synthesis of functional PPV derivatives



Scheme 15. Synthesis of monomer **34** 1: EtOH, Na-tBuO, 6-bromo-ethyl hexanoate 2: *p*-formaldehyde, HCl, Ac₂O, 3: EtOH, H₂SO₄ cat, 4: MeOH, THT, 5: MeOH, *n*-octanethiol, Na-tBuO, 6: MeOH, TeO₂, H₂O₂, HCl cat

2.3.2. Polymerisation of the ester monomer

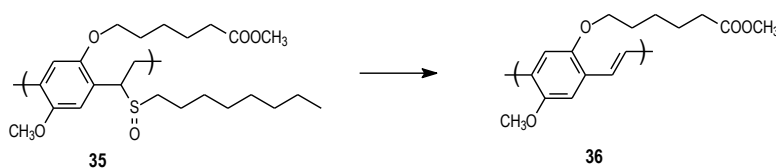


Scheme 16. Synthesis of precursor polymer **35**. 1: Na-tBuO (1.3 eq)

The ester monomer **34** was also polymerized according to the standard procedure (scheme 16). The ester group was not affected by the polymerization conditions as noticed from FT-

IR spectroscopy where the signal at 1729 cm^{-1} remains unaffected. A precursor polymer **35** in a yield of 64% and with a molecular weight of 250.000 is obtained according to GPC analysis in THF.

2.3.3. Conversion of precursor polymer **35** to the conjugated structure



Scheme 17. Thermal conversion of precursor polymer **35** into the fully conjugated structure.

The three common in situ techniques are used to study the elimination behaviour of the ester precursor polymer **35**. With increasing temperature there is a gradual redshift to a maximum wavelength of 470 nm (figure 29). Formation of the conjugated structure is started at 65°C and is completed at 110°C (figure 30). After this temperature a large decline is observed caused by the thermochromic effect as will be analysed and described later on in this chapter.

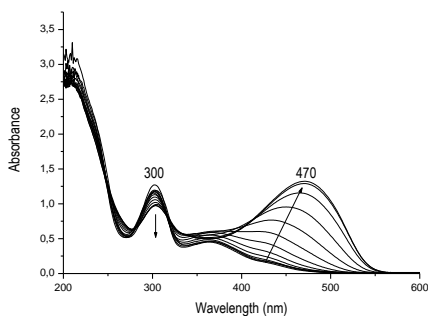


Figure 29. Gradual formation of the conjugated structure **36**

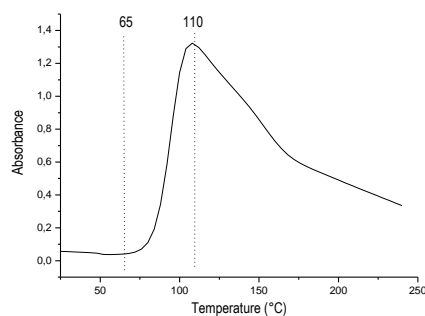


Figure 30. Absorption at 470 nm versus temperature

In situ FT-IR spectroscopy shows the same trends as UV-Vis spectroscopy. The vinylene signal at 960 cm^{-1} starts to show at 64°C and reaches its maximum value at 108°C (figure

32). The ester function is not affected when applying elevated temperature since the signal at 1729 cm^{-1} remains unaffected by the temperature program (figure 31).

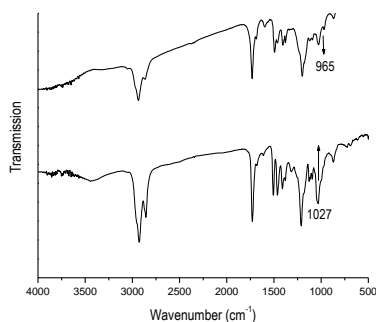


Figure 31. FT- IR spectrum before (below) and after conversion (upper)

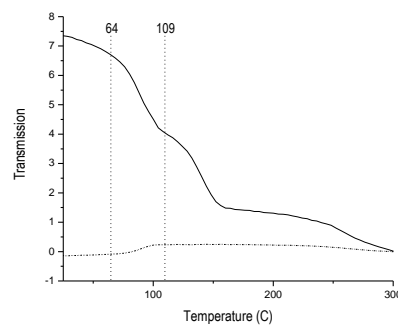
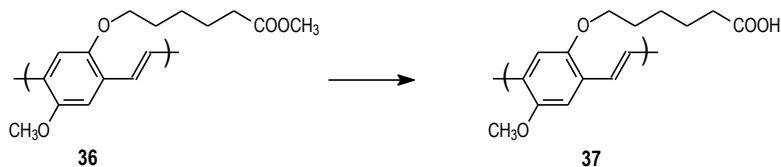


Figure 32. Absorption at 960 and 1042 cm^{-1} versus temperature

2.3.4. Hydrolysis of the ester function



Scheme 18. Hydrolysis of the ester function. 1,4-dioxane, $t\text{-BuO}^- / \text{H}_2\text{O}$

The ester function can readily be hydrolyzed to the free carboxylic acid using basic conditions (scheme 18). The conjugated polymer **36** is brought in 1,4-dioxane and the mixture is stirred at reflux under an inert atmosphere. Subsequently an excess of sodium-*t*-butoxide in water is added and the mixture is maintained at reflux temperature. After cooling down the reaction to room temperature water is added and the aqueous solution is acidified with a concentrated HCl solution whereupon the polymer **37** precipitated. The product was obtained through filtration and washed with water. FT-IR analysis showed a new typical peak at 1702 cm^{-1} and the initial C=O stretching band at 1728 cm^{-1} was completely disappeared. In figure 33 the infrared spectra of both ester and carboxylic acid polymer are

depicted. The hydrolysed polymer is soluble in organic solvents like THF and ethanol and in basic water.

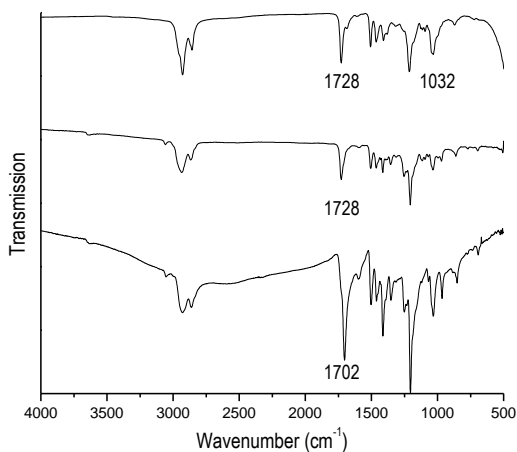
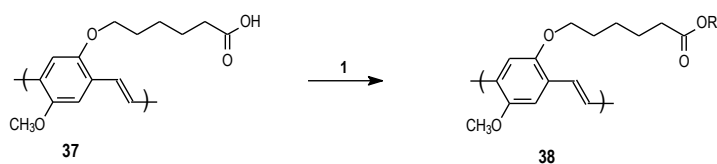


Figure 33. FT-IR spectra of the precursor polymer **35** (upper), conjugated polymer **36** (middle) and hydrolysed polymer **37** (below)

2.3.5. Functionalisation of the carboxylic acid

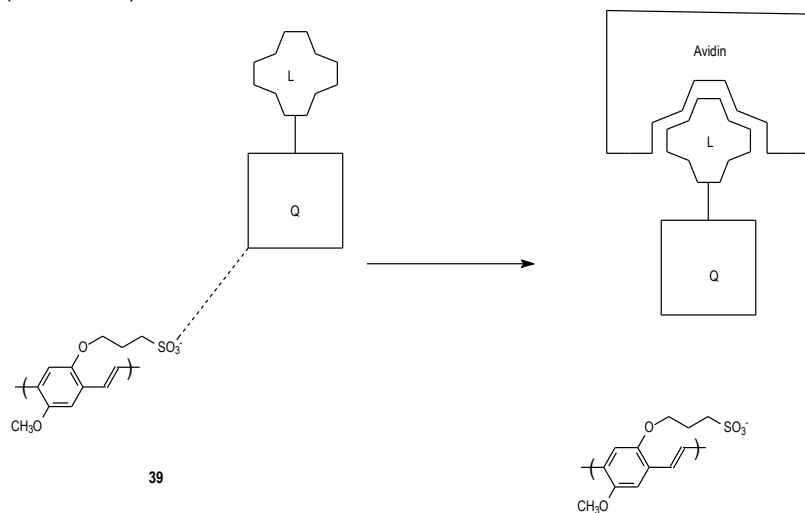
Functional groups such as alcohols or carboxylic acid are very grateful to chemists since they can easily be converted into other groups using simple chemical reactions. Polymers exhibiting this feature can be used for post-polymerization functionalisation reactions. In our group dra. Ineke Van Severen performed such functionalisation reactions on the polymer stage using Mitsunobu conditions, which yielded the ester functionalized polymers **38** in high yields¹⁶ (scheme 19). The polymers were characterized using FT-IR spectroscopy where the C=O stretching signal at 1709 cm⁻¹ has disappeared and a new ester band at 1729 cm⁻¹ is observed. The exact reaction conditions are beyond the scope of this study and will be published elsewhere¹⁷.



Scheme 19. Conversion of the carboxylic acid into an ester using Mitsunobu conditions. 1: Et₂O, PPh₃, DEAD, 0°C, R-OH

2.4. Synthesis of a sulfonate derived polymer

In literature much attention has been paid to the synthesis and properties of a poly-anionic PPV derivative **39**¹⁸. This compound can be used as an indicator or highly sensitive fluorescence-based sensor for chemical and biochemical targets. The fluorescence of the polymer **39** is quenched with very low concentrations of cationic quenchers like N,N'-dimethylviologen (MV²⁺). This quenching effect arises from ion-pairing between the poly-anion and the quencher. When this quencher is attached covalently to a ligand, the fluorescence quenching is inhibited as soon as the ligand binds to for instance avidin (scheme 20).

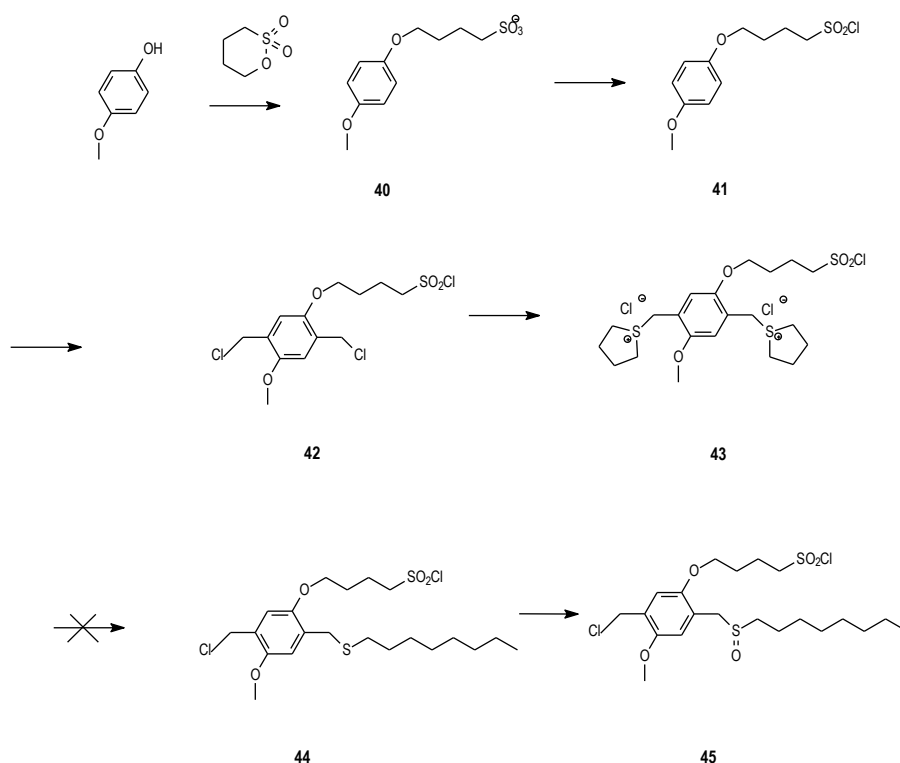


Scheme 20. Principle of fluorescence quenching. Left: Fluorescence of polymer **39** is quenched due to interaction with the quencher(Q)/ligand (L). Right: When the ligand L binds to a receptor (avidin), the quencher-polymer interaction is discontinued and fluorescence of the conjugated polymer will be observed.

Attempts were made to create this known polymer through the sulfinyl precursor route because its ease to control the occurring chemistry compared to the Wessling or Gilch route. Moreover we wanted to synthesize a non-charged precursor and conjugated material that could be hydrolyzed afterwards to yields the ionic structure. Several attempts failed probably due to the reactivity of the functional group present in the monomer.

A first attempt was made using the protected sulfonyl chloride instead of the free sulfonic acid (scheme 21). For every synthetic step high yields of the desired products were achieved. The use of the non-charged sulfonyl chloride has the advantage that every reaction product can be purified using organic solvents for extraction and simple column chromatography for the subsequent purification. So the first step involves again an ether synthesis using p-hydroxy anisol, sodium t-butoxide as the base and δ -1,4-butanedisulfone in ethanol to yield compound **40**. The mixture is poured into cold acetone whereupon the desired product precipitated. The product is readily obtained through filtration and dried in vacuo. The next step is the conversion of the sulfonate group into the sulfonyl chloride using an excess of thionyl chloride in DMF. After column purification product **41** is obtained as a white solid. Chloromethylation of compound **41** yields the dichloride **42** without affecting the functional group. Subsequently the dichloride is treated with an excess of THT in methanol and the bisulfonium salt is precipitated in ether, collected through filtration and dried in vacuo. Treatment of the bisulfonium salt **43** with an equimolar amount of n-octyl thiolate did not result in the desired thioether **44**, probably due to the high reactivity of the sulfonyl chloride function under these reaction conditions.

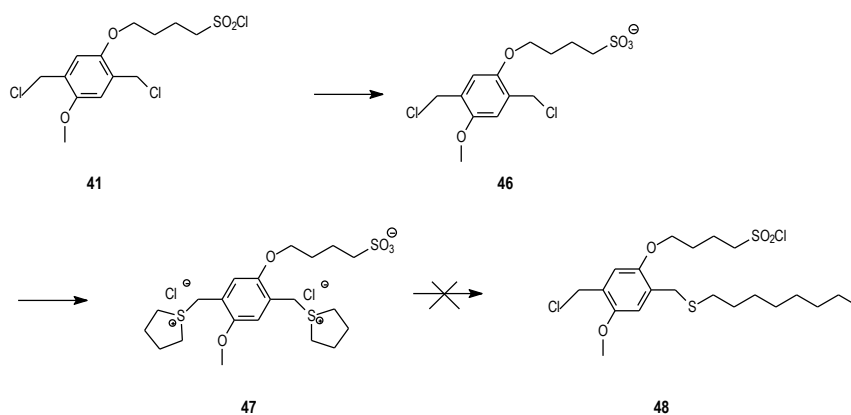
Synthesis of functional PPV derivatives



Scheme 21. Representation of attempts to synthesise monomer **45**

In another attempt to achieve this interesting polymer, the sulfonyl chloride function in the dichloride **42** was hydrolysed using basic conditions and the resulting sulfonate salt **46** could be precipitated in acetone in high yield (scheme 22). This salt was then treated to yield the bisulfonium salt **47** using an excess of THT in methanol. Precipitation in acetone yielded the salt which was collected through filtration and dried in vacuo. Again thioether **48** formation starting from the salt was not successful since no reaction did occur due to the insolubility of the salt in methanol. Further attempts were not performed but still it may be worthwhile to study the formation of the planned monomer or its derivatives in detail to obtain some interesting materials with application in the growing field of sensor devices.

Chapter 3



Scheme 22. Representation of attempts to synthesise compound 48

3. Thermochromic effect – Thermal stability of the polymers 1, 2, 24 and 36.

When heating a solid sample of precursor polymer with a heating gun, the colour of the sample turns from colourless into yellow and little later it becomes deep red. This phenomenon is ascribed to the conversion of the precursor into the conjugated polymer. Further heating resulted in a colour change from deep red into bright yellow. Upon cooling the sample turns red again, however when the heating time is too long, degradation occurs and the sample turns brown. These observations are likely caused by the thermochromic effect.

In literature a lot of papers discuss the thermochromic effect of both organic and inorganic compounds and their application in several devices. Thermochromic means a colour change induced by a change in temperature and hence materials exhibiting this property may act as heat sensors or indicators. Several thermochromic conjugated polymers have been described so far but very little is known about the thermochromic properties of PPV or its derivatives. The most known thermochromic conjugated polymer up to date is the alkyl substituted poly(thiophene)¹⁹ (figure 34).

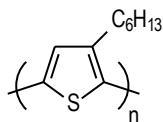


Figure 34. Chemical structure of poly(2,5-(3'-hexyl)thiophene)

This thermochromic process in polymers **1**, **2**, **24** and **36** is reversible to a certain point and it is demonstrated by several heating-cooling experiments at different temperatures applying in situ UV-Vis and FT-IR measurements. Upon heating a conjugated polymer sample, the maximum wavelength in the UV-Vis spectrum is blueshifted because the mobility of the polymer chains increases and hence the torsion angle increases. This implies a less effective conjugation length resulting in a shift to a lower wavelength in the UV-Vis spectrum. When cooling down the heated sample the UV-Vis spectrum is redshifted again. The value of the shifts to a lower wavelength is dependent of the temperature applied. At higher temperatures this shift is larger than at lower temperatures. Besides the blueshift of the spectrum, also a decrease in absorbance occurs due to the lower extinction coefficient. In FT-IR spectroscopy, the same temperature program is applied to the sample and the same behaviour is observed. When monitoring the double bond signal at 960 cm^{-1} a decrease is detected when temperature increases up to $150\text{ }^{\circ}\text{C}$. As the temperature drops down again, the signal increases again to its initial value. This is in total accordance with the data obtained from the in situ UV-Vis measurements. No other significant changes in the FT-IR spectrum can be observed.

3.1. Heating-cooling experiments

A solution of the conjugated polymer eliminated in solution (toluene reflux, 3 hours) in CHCl_3 is spincoated at 1000 rpm on a quartz disc. This disc is subsequently heated at $2^{\circ}\text{C}/\text{min}$ up to different temperatures and is cooled down to room temperature three times, under a continuous flow of nitrogen. Polymer **23** was spincoated in its precursor form and eliminated prior to the heating-cooling experiment because of the insolubility of the conjugated polymer **24**.

For polymer **1** three different heating-cooling experiments were performed: heating up to 120°C , 150°C and 200°C at two degrees per minute and cooling down to room temperature (20°C) in three cycles. The results of the different experiments performed on polymer **1**, **2**, **24** and **36** are listed in table 8.

Sample	Temp (°C)	initial wavelength (nm)	minimal wavelength (nm)	difference (nm)
Polymer 1	120	504	473	31
Polymer 1	150	504	458	46
Polymer 1	200	504	448	56
Polymer 2	120	504	468	36
Polymer 24	120	500	475	25
Polymer 36	130	510	478	32

Table 8: overview of minimal wavelength and wavelength after three heating-cooling runs of polymers 1, 2, 24 and 36

From figure 35 it can be seen that the initial wavelength is only little affected after three heating-cooling runs. This indicates that the polymer is stable when higher temperature are applied and that the significant decrease of the maximum wavelength in the UV-Vis elimination experiments is not indicating a weak stability of the polymer but is due to this thermochromic effect. The decrease of the absorption value at maximum wavelength after the first heating run is attributed to small rearrangements in the sample resulting in a smaller thickness of the sample and hence a smaller absorption value. In heating run two and three no significant decrease in maximum absorption is observed for each of the three temperatures. We can conclude that the conjugated materials are at least stable till 200°C and that the results from the elimination reaction are somewhat misleading.

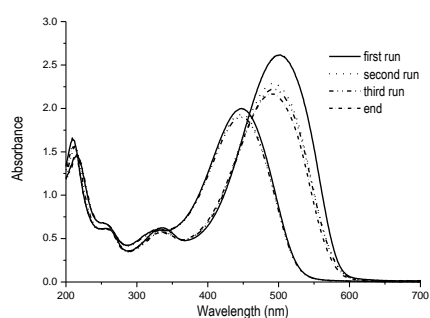


Figure 35. UV-Vis spectra of polymer 1 during a heating-cooling experiment

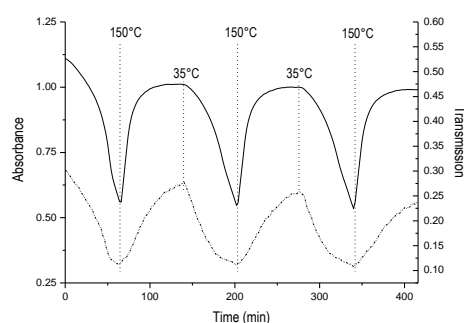


Figure 36. Plot of absorbance at 510 nm versus time (full line) and 960 cm^{-1} (dashed line) for polymer 1

The occurrence of this significant wavelength shift looked quite surprising to us since the same experiments were also performed on the conjugated aliphatic OC₁C₁₀ PPV. With in situ UV-Vis spectroscopy only a very small blueshift is observed when applying consecutive heating-cooling runs⁹. For example heating a sample of OC₁C₁₀ polymer up to 100°C results in a blueshift from 517 nm to 501 nm. Only after 200°C a significant decrease in the maximum wavelength is observed.

4. Electrochemical characterisation of the conjugated polymers

The conjugated polymers described in this chapter were electrochemically analysed using cyclic voltammetry. Cyclic voltammetry (CV) is the most widely used technique for acquiring qualitative information about electrochemical reactions. Cyclic voltammetry is often the first experiment performed in an electro-analytical study. In particular, it offers a rapid location of redox potentials of the electroactive species, and convenient evaluation of the effect of media upon the redox process. Cyclic voltammetry consists of scanning linearly the potential of a stationary working electrode, using a triangular potential waveform. Depending on the information sought, single or multiple cycles can be used. During the potential sweep, the potentiostat measures the current resulting from the applied potential. The resulting plot of current vs. potential is termed a cyclic voltammogram.

The electrochemical properties of the polymers were studied in order to determine the electrochemical band gap and to estimate the energy levels of its LUMO and HOMO.

The energy values of the LUMO and HOMO for the synthesised polymers were determined from the onset potentials of both n- and p-doping and were calculated using the ferrocene value of - 4.8 eV below the vacuum level. The onset potentials are determined from the intersection of the two tangents drawn at the rising current and baseline charging current of the CV traces.

The correlation can be expressed as:

$$E_{\text{LUMO}} = - (4.8 + E_{\text{onset red}}) \text{ eV}$$

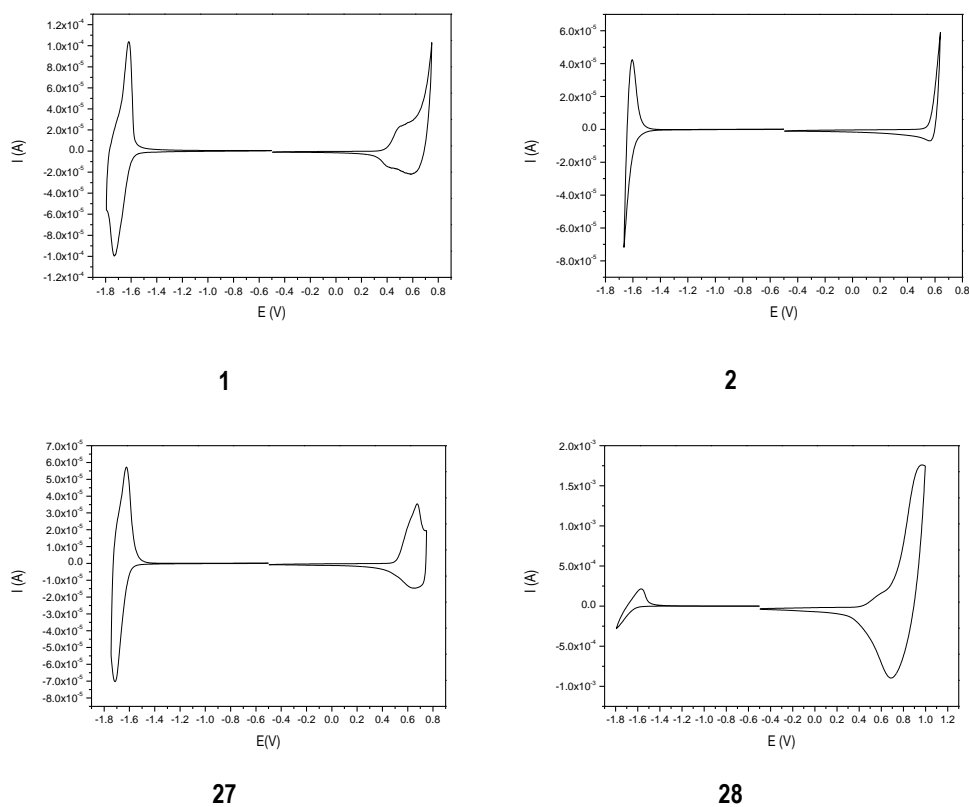
$$E_{\text{HOMO}} = - (4.8 + E_{\text{onset ox}}) \text{ eV}$$

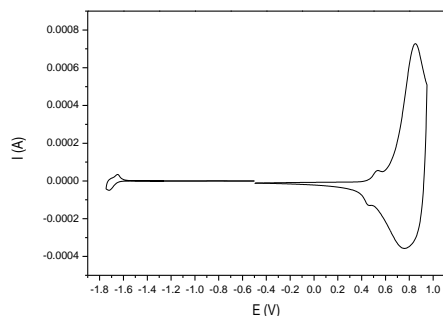
From the onset potentials of oxidation and reduction, it can be estimated that the band gap of the polymers is somewhat different from the value obtained from the optical absorption spectra. The interface barrier between the polymer films and the electrode surface may

Chapter 3

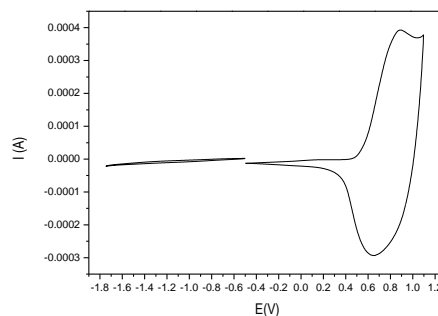
cause these differences. The optical value corresponds to the pure band gap between the valence band and the conduction band, while the electrochemical data may be the result of the optical band gap coupled with the interface barrier of charge injection. For polymer **1**, **2**, **27** and **28**, both p-doping/dedoping and n-doping/dedoping are reversible and the peak current value for p-doping is similar to that for n-doping. The CV trace of all the synthesized conjugated polymers is presented in figure 37. Scans over the oxidative and reductive region are combined in one plot, although two separate experiments were performed and the working electrode was cleaned between two experiments. Polymer **24** showed instability during consecutive CV runs.

Upon reduction a clear anodic peak is observed for polymers **1** and **2**. For The ester functionalised polymer **35** only a very small anodic peak is observed.

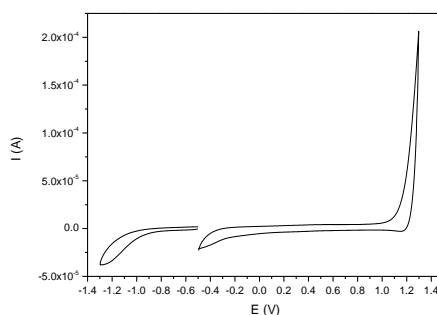




35



36



24

Figure 37. CV plots of conjugated polymers 1, 2, 24, 27, 28, 35 and 36

4.1. Determination of the optical band gap and comparison with electrochemical results

In addition to the electrochemical determination of the band gap of the conjugated polymers we determined the optical band gap of the respective polymers using UV-Vis spectroscopy. From the UV-Vis spectrum the optical band gap is determined through the intersection of the tangent of the absorption peak at the lowest energy side with the x-axis (figure 38). The transformation of the data from wavelength (nm) to eV was obtained through the equation below. The results from the measurements are listed in table 9. From these data it is seen that the result of both electrical and optical band gap are in good accordance except for the free carboxylic acid polymer 36. Here the electrical band gap is determined to be 1.42 and

this is probably due to irreversible chemical transformations at the functional group during a CV run.

$$E_g = 1242/\text{wavelength (nm)}$$

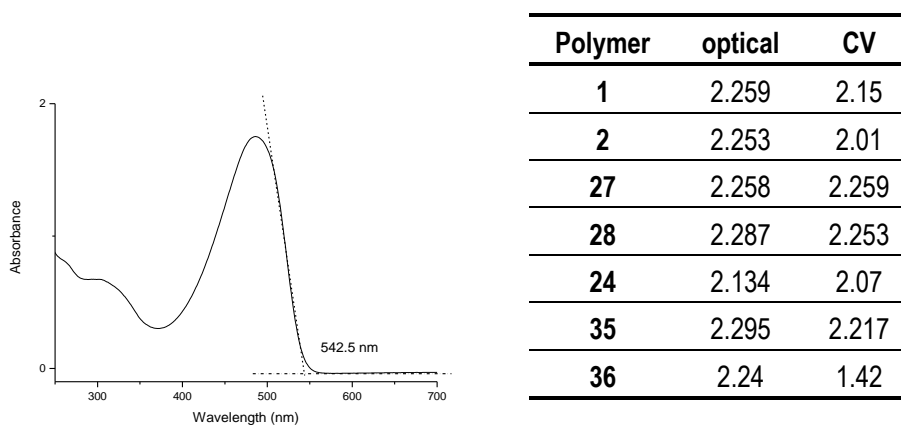


Figure 38. Principle of optical band-gap determination

Table 9. Overview of the optical and electrochemical band-gaps

5. Conclusion

Throughout this chapter it was demonstrated that the sulfinyl precursor route is a very versatile route and that some functional PPV derivatives can be obtained when some precautions are taken into account. The normal standard conditions for monomer synthesis have to be adapted for the concentrations inhibiting premature and unwanted Wessling polymerisation. For the polymerisation reactions high yields of the precursor polymers can be obtained. There seems to be no incompatibility between the functional groups present in the respective monomers. The characterisation of both monomers and polymers could be performed using different analytical techniques. The elimination behaviour of the precursor polymers was studied revealing that there is no significant influence of the nature of the aliphatic sulfinyl chain. From the thermal measurements a strong thermochromic effect was observed for each of the conjugated polymers. For the alcohol functionalised conjugated polymer the same problems occurred as described in chapter 2. Due to hydrogen bonding

one ends up with an insoluble product. However, copolymerisation reactions demonstrate the possibility of a soluble alcohol PPV derivative. The ester derivative can also be obtained in high yield and subsequent hydrolysis affords a soluble carboxylic acid that can be subject for post-polymerisation functionalisation reactions. The synthesis of a poly anionic PPV derivative through the sulfinyl precursor route failed despite several different attempts.

6. Experimental Section

Materials. All chemicals were purchased from Aldrich or Acros and used without further purification. Tetrahydrofuran (THF) was distilled over sodium/benzophenone.

Characterization. ¹H-NMR spectra were obtained in CDCl₃ or D₂O at 300 MHz or 400 MHz on a Varian Inova Spectrometer using a 5 mm probe. Chemical shifts (δ) in ppm were determined relative to the residual CHCl₃ absorption (7.24 ppm) or to the residual H₂O absorption (4.6 ppm). The ¹³C-NMR experiments were recorded at 75 MHz on the same spectrometer using a 5 mm broadband probe. Chemical shifts were defined relative to the ¹³C resonance shift of CHCl₃ (77.0 ppm). Molecular weights and molecular weight distributions were determined relative to polystyrene standards (Polymer Labs) with a narrow polydispersity by Size Exclusion Chromatography (SEC). Separation to hydrodynamic volume was obtained using a Spectra series P100 (Spectra Physics) equipped with a pre-column (5 μ m, 50 mm*7.5 mm, guard, Polymer Labs) and two mixed-B columns (10 μ m, 2x300 mm*7.5 mm, Polymer Labs) and a Refractive Index (RI) detector (Shodex) at 40°C. SEC samples are filtered through a 0.45 μ m filter. HPLC grade THF (p.a.) or DMF (p.a.) is used as the eluent at a constant flow rate of 1.0 ml/min. Toluene is used as flow rate marker.

Direct Insert Probe Mass Spectroscopy analysis is carried out on a Finnigan TSQ 70, electron impact mode, mass range of 35-500. Electron energy is 70 eV. A CHCl₃ solution of precursor polymer is applied on the heating element of the direct insert probe. A similar heating rate of 10°C/min was used to ensure a good comparison with TGA data.

The in situ elimination reactions were performed in a Harrick High Temperature Oven (purchased from Safir), which is positioned in the beam of a Perkin Elmer spectrum one FT-IR spectrometer (nominal resolution 4 cm⁻¹, summation of 16 scans). The temperature of the sample is controlled by a Watlow (serial number 999, dual channel) temperature controller.

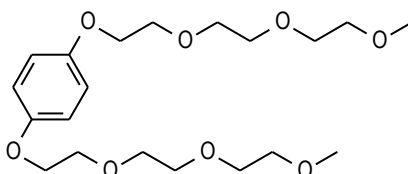
Chapter 3

The precursor polymer was spincoated from a CHCl_3 solution (6 mg/ml) on a KBr pellet at 500 rpm. The spincoated KBr pellet (diameter 25 mm, thickness 1 mm) is in direct contact with the heating element. All experiments were performed at $2^\circ\text{C}/\text{min}$ under a continuous flow of nitrogen. "Timebase software" supplied by Perkin Elmer is used to investigate regions of interest.

In situ UV-Vis measurements were performed on a Cary 500 UV-Vis-NIR spectrophotometer, specially adapted to contain the Harrick high temperature cell (scan rate 600 nm/min, continuous run from 200 to 600 nm). The precursor polymer was spincoated from a CHCl_3 solution (6 mg/ml) on a quartz glass (diameter 25 mm, thickness 3mm) at 700 rpm. The quartz glass was heated in the same Harrick oven high temperature cell as was used in the FT-IR measurements. The cell was positioned in the beam of the UV-Vis-NIR-spectrophotometer and spectra were taken continuously. The heating rate was $2^\circ\text{C}/\text{min}$ up to 300°C . All measurements were performed under a continuous flow of nitrogen. "Scanning Kinetics software" supplied by Varian is used to investigate regions of interest.

Cyclic voltammetry (CV) is performed with an Autolab PGSTAT 20 potentiostat from Eco Chemie B.V. equipped with General Purpose Electrochemical System (GPES) software for CV and Frequency Response Analyzer System (FRA2) software (version 4.9 for windows) for EIS. The electrochemical set-up consists of a cell including a Ag/AgCl reference electrode, a platinum counter electrode and a platinum disk (area = 1.6mm^2) with a thin drop-casted film as working electrode immersed in 0.1 M $\text{Bu}_4\text{NClO}_4/\text{acetonitrile}$ electrolyte. The experiments are carried under N_2 atmosphere. The potentials were calibrated using the ferrocene redox couple.

1,4-Bis-{2-[2-(2-methoxy-ethoxy)-ethoxy]-ethoxy}-benzene 4

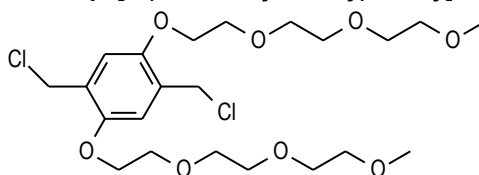


Hydroquinone (11g, 0.1 mol) and potassium hydroxide (13g, 2.2 equivalents) are dissolved in 300 ml ethanol and stirred for one hour at room temperature. Toluene-4-sulfonic acid 2-[2-(2-methoxy-ethoxy)-ethoxy]-ethyl ester is added (67g, 2.1 equivalents) and the resulting mixture is stirred overnight at reflux. The mixture is poured into 300 ml water and the

aqueous layer is extracted three times with dichloromethane. The organic layer is dried over magnesium sulfate and the solvent is evaporated. A chromatographic purification with ether as the eluent yields 1,4-bis-{2-[2-(2-methoxy-ethoxy)-ethoxy]-ethoxy}-benzene as a light yellow liquid. (29g, 72.5%)

¹H-NMR (300MHz, ppm, CDCl₃): 6.73 (s, 4H), 3.98 (t, 4H), 3.74 (t, 4H), 3.63 (t, 4H), 3.55 (m, 8H), 3.44 (t, 4H), 3.29 (s, 6H)

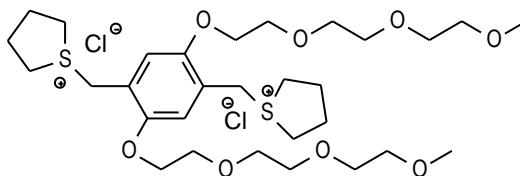
1,4-Bis-chloromethyl-2,5-bis-{2-[2-(2-methoxy-ethoxy)ethoxy]ethoxy}-benzene 5



To 1,4-bis-{2-[2-(2-methoxy-ethoxy)ethoxy]ethoxy}benzene **4** (14g, 0.035 mol) and *p*-formaldehyde (2.87 g, 2.75 equivalents) is added dropwise and under nitrogen atmosphere 17 ml of concentrated HCl. Afterwards 34 ml of acetic anhydride is added at such a rate that the temperature does not exceed 70°C. The solution is stirred at 70°C for three hours and then poured into water. Extraction with chloroform, drying over magnesium sulfate and a column purification with ether as the eluent yields the dichloride **5** as an oil (12.5 g, 72%).

¹H-NMR (300MHz, ppm, CDCl₃): 3.25 (s, 6H), 3.45, 3.55, 3.65 (m, 12H), 3.78 (t, 4h, J=5.4Hz), 4.05 (t, 4H, J=5.4Hz), 4.55 (s, 4H), 6.85 (s, 2H)

1,4-tetrahydrothiophenylmethyl-2,5-bis-{2-[2-(2-methoxy-ethoxy)-ethoxy]-ethoxy}-benzyl) dichloride 6



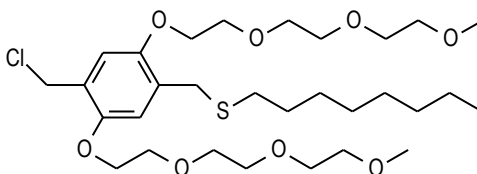
1,4-Bis-chloromethyl-2,5-bis-{2-[2-(2-methoxy-ethoxy)-ethoxy]-ethoxy}-benzene (12.5g, mol) is dissolved in 120 ml methanol and 13 ml tetrahydrothiophene. The clear solution is stirred at room temperature for three days and the obtained bisulfoniumsalt is precipitated in cold

Chapter 3

ether or THF (800 ml) and filtered off to yield a white solid. The solid is collected and dried at room temperature under reduced pressure (60 %).

¹H-NMR (300MHz, ppm, D₂O): 2.21 (m, 8H), 3.25 (s, 6H), 3.48-3.67 (m, 8H), 3.84 (m, 4H), 4.19 (m, 4H), 4.45 (s, 4H), 7.13 (s, 2H)

1-Chloromethyl-2,5-bis-{2-[2-(2-methoxy-ethoxy)-ethoxy]-ethoxy}-4-octyl-sulfanyl-methyl-benzene 7

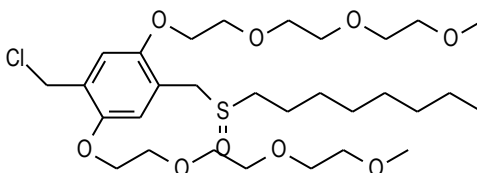


Octane thiol (0.78g, 5.34 mmol) and sodium *t*-butoxide (0.512g, 1 equivalent) are dissolved in methanol (40ml) and stirred at room temperature for one hour. This solution is added dropwise to 1,4-tetrahydrothiophenylmethyl-2,5-bis-{2-[2-(2-methoxy-ethoxy)-ethoxy]-ethoxy}-benzyl) dichloride 6 (3.6 g, 1 equivalent) in 100 ml methanol. The resulting solution is stirred for another 4 hours and neutralized if necessary. The solvent is evaporated and *n*-octane is added and evaporated again to remove the THT. This procedure is repeated three times. The residue is dissolved in chloroform and extracted with water. After drying over magnesium sulfate and a column purification with ether as the eluent, the desired compound is obtained as a yellowish oil (2.66 g, 79%)

¹H-NMR (300MHz, ppm, CDCl₃): 0.79 (t, 3H, J=6.3Hz), 1.14-1.28 (m, 10H), 1.48 (m, 2H), 2.37 (t, 2H, J=7Hz), 3.29 (s, 6H), 3.48 (m, 4H), 3.54-3.69 (m, H), 3.75 (m,4H), 4.06 (m, 4H), 4.56 (s, 4H), 6.80 (s, 1H), 6.83 (s, 1H)

FT-IR (NaCl), ν (cm⁻¹): 2925 (s), 2871 (s), 1509 (s), 1456 (s), 1420 (s), 1215 (s), 1109 (s), 1043 (s), 953 (s)

1-Chloromethyl-2,5-bis-[2-[2-(2-methoxy-ethoxy)-ethoxy]-ethoxy]-4-(octane-1-sulfinyl-methyl)-benzene 8



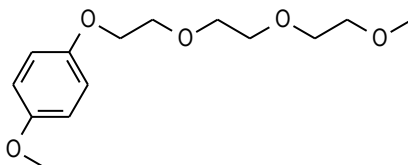
To the thioether (2.66g, mol) in 50 ml dioxane is added TeO_2 (40 mg, 5 mol%) and H_2O_2 (1.04 g, 2 equivalents). A few drops of concentrated HCl are added to catalyse the reaction. The progress of the reaction is followed on TLC and when all thioether is disappeared 60 ml of brine is added to stop the reaction. Extraction with chloroform, drying over magnesium sulfate and column with ethylacetate/methanol as the eluent yields the sulfoxide as a yellow oil (2g, 75%)

$^1\text{H-NMR}$ (300MHz, ppm, CDCl_3): 0.80 (t, 3H, $J=6.6\text{Hz}$), 1.19-1.38 (m, 10H), 1.67 (m, 2H), 2.58 (t, 2H, $J=7.8\text{Hz}$), 3.32 (s, 6H), 3.56 (m, 4H), 3.60-3.70 (m, H), 3.74-3.77 (m, 4H), 3.96 (d, 1H, $J=12.6\text{Hz}$), 4.02-4.08 (m, 5H), 4.58 (s, 2H), 6.80 (s, 1H), 6.91 (s, 1H)

$^{13}\text{C-NMR}$ (75MHz, ppm, CDCl_3): 150.2, 149.8, 126.5, 119.7, 115.7, 113.9, 71.2, 70.1, 70.0, 69.9, 69.8, 68.9, 68.9, 68.3, 68.0, 58.2, 51.7, 50.4, 40.5, 31.0, 28.5, 28.4, 28.2, 22.0, 21.9, 13.5

FT-IR (NaCl), ν (cm^{-1}): 2925, 2872, 1507, 1455, 1413, 1212, 1110, 1062, 952

Methoxy-4-[2-[2-(2-methoxy-ethoxy)-ethoxy]-ethoxy]-benzene 10



4-hydroxy anisol (2 g, 0.016 mol) and potassium hydroxide (1.05g, 1.1 equivalents) are dissolved in 50 ml ethanol and stirred for 1 hour at room temperature. Toluene-4-sulfonic acid 2-[2-(2-methoxy-ethoxy)-ethoxy]-ethyl ester is added (6g, 1.2 equivalents) and the resulting mixture is stirred overnight at reflux. The mixture is poured into 50ml water and the aqueous layer is extracted three times with dichloromethane. The organic layer is dried over

Chapter 3

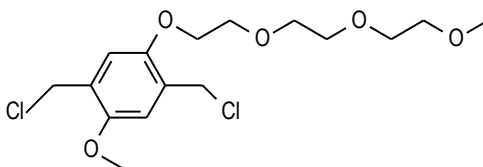
magnesium sulfate and the solvent is evaporated. A chromatographic purification with ether as the eluent yields 1-methoxy-4-{2-[2-(2-methoxy-ethoxy)-ethoxy]-ethoxy}-benzene as a light yellow liquid. (3.8 g, 78%)

$^1\text{H-NMR}$ ppm (300MHz, CDCl_3): 6.69 (s, 4H), 3.92 (t, 2H), 3.69 (t, 2H), 3.60 (m, 5H), 3.51 (m, 4H), 3.43 (m, 2H), 3.24 (s, 3H)

MS (EI, m/z, relative intensity (%)): 270, 151, 147, 136, 124, 109, 92, 77, 59

1,4-Bis-chloromethyl-2-methoxy-5-{2-[2-(2-methoxy-ethoxy)-ethoxy]-ethoxy}-benzene

11

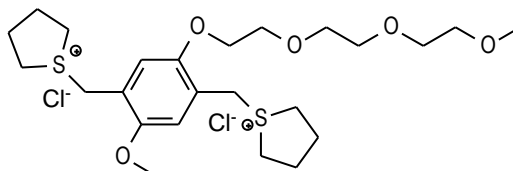


To 1-methoxy-4-{2-[2-(2-methoxy-ethoxy)-ethoxy]-ethoxy}-benzene (8.8g, 0.032 mol) and *p*-formaldehyde (1.98g, 2.75 equivalents) is added dropwise and under nitrogen atmosphere 12 ml of concentrated HCl. Afterwards 25 ml of acetic anhydride is added at such a rate that the temperature does not exceed 70°C. The solution is stirred at 70°C for three hours and then poured into water. Extraction with chloroform, drying over magnesium sulfate and a column purification with ether as the eluent yields the 1,4-bis-chloromethyl-2-methoxy-5-{2-[2-(2-methoxy-ethoxy)-ethoxy]-ethoxy}-benzene as an oil (7 g, 60%).

$^1\text{H-NMR}$ (300MHz, ppm, CDCl_3): 6.91+6.88 (2s, 2H), 4.61+4.57 (2s, 4H), 4.12 (t, 2H), 3.81 (t, 2H), 3.70-3.54 (m, 11H), 3.33 (s, 3H)

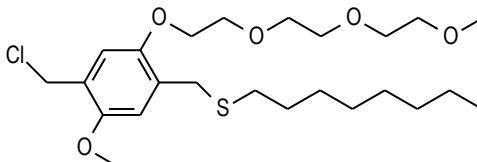
MS (EI, m/z): 368, 332, 266, 231, 149, 103, 89, 69, 59

1,4-tetrahydrothiophenylmethyl-2-methoxy-5-{2-[2-(2-methoxy-ethoxy)-ethoxy]-ethoxy}-benzyl) dichloride 12



1,4-Bis-chloromethyl-2-methoxy-5-{2-[2-(2-methoxy-ethoxy)-ethoxy]ethoxy}benzene (7 g, 0.019 mol) is dissolved in 120 ml methanol and 13 ml tetrahydro-thiophene. The clear solution is stirred at room temperature for three days and the obtained bisulfoniumsalt is precipitated in cold ether (800 ml) or THF and filtered off to yield a white solid. The white solid is then collected and dried at room temperature under reduced pressure (7 g, 69.2%).
¹H-NMR (300MHz, δ, ppm, D₂O): 2.21 (m, 8H), 3.24 (s, 3H), 3.36 (m, 8H), 3.45-3.64 (3m, 8H), 3.80 (s, 3H), 3.83 (m, 2H), 4.18 (m, 2H), 4.40-4.45 (2s, 4H), 7.10 (s, 2H)

1-Chloromethyl-2-methoxy-5-{2-[2-(2-methoxy-ethoxy)-ethoxy]ethoxy}-4-(octane-1-sulfanylmethyl)-benzene and 1-chloromethyl-5-methoxy-2-[2-[2-(2-methoxy-ethoxy)-ethoxy]-ethoxy]-4-(octane-1-sulfanylmethyl)-benzene 13

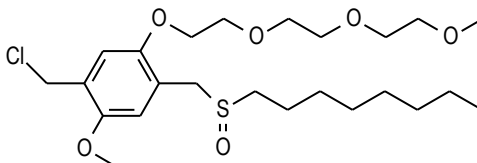


Octane thiol (1.08g, 0.0074 mol) and sodium *t*-butoxide (0.708 g, 0.0074 mol) are dissolved in methanol (50ml) and stirred at room temperature for one hour. This solution is added dropwise to the 1,4-tetrahydrothiophenylmethyl-2-methoxy-5-{2-[2-(2-methoxy-ethoxy)-ethoxy]-ethoxy}-benzyl) dichloride (4g, 1 equivalent) in 150 ml methanol. The resulting solution is stirred for another 4 hours and neutralized if necessary. The solvent is evaporated and *n*-octane is added and evaporated again to remove the THT. This procedure is repeated three times. The residue is dissolved in chloroform and extracted with water. After drying the organic layer over magnesium sulfate and a column purification with ether as the eluent, the desired compound is obtained as a yellowish oil (2.45g, 70 %)

¹H-NMR (300MHz, ppm, CDCl₃): 0.81 (t, 3H, J=6.3Hz), 1.14-1.28 (m, 10H), 1.52 (m, 2H), 2.42 (t, 2H, J=7Hz), 3.34 (s, 2H), 3.48 (m, 2H), 3.54-3.69 (m, H), 3.75 (m, 2H), 4.08 (m, 2H), 4.58 +4.61 (2s, 4H), 6.82-6.83-6.84-6.87 (4s, 2H)

FT-IR (NaCl), ν (cm⁻¹): 2926, 2857, 2246, 1681, 1509, 1463, 1413, 1215, 1109, 1045, 911

1-Chloromethyl-2-methoxy-5-{2-[2-(2-methoxy-ethoxy)-ethoxy]-ethoxy}-4-(octane-1-sulfinylmethyl)-benzene and 1-chloromethyl-5-methoxy-2-{2-[2-(2-methoxy-ethoxy)-ethoxy]-ethoxy}-4-(octane-1-sulfinylmethyl)-benzene 14



To 1-chloromethyl-2-methoxy-5-{2-[2-(2-methoxy-ethoxy)-ethoxy]-ethoxy}-4-(octane-1-sulfinylmethyl)-benzene (2.7 g, mol) in 60 ml dioxane is added TeO_2 (60 mg, 5 mol%) and H_2O_2 (1.43 g, 2 equivalents). A few drops of concentrated HCl are added to catalyze the reaction. The progress of the reaction is followed on TLC and when all thioether is disappeared 60 ml of brine is added to stop the reaction. Extraction with chloroform, drying over magnesium sulfate and a column purification with ethylacetate/methanol as the eluent yields the sulfoxide as a yellow oil (2 g, 80%).

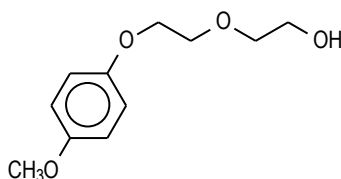
$^1\text{H-NMR}$ ppm (300MHz, CDCl_3): 0.79 (t, 3H, $J=6.6\text{Hz}$), 1.30-1.55(m, 10H), 2.62 (t, 2H, $J=7.8\text{Hz}$), 3.32 (s, 3H), 3.51-3.62 (m, 4H), 3.84 + 3.93 (dd, 2H, $J=12.6\text{Hz}$), 3.76+3.79 (s, 3H), 4.0 (t, 3H), 4.59 + 4.61 (s, 2H), 6.79 + 6.81 + 6.89 + 6.92 (s, 2H),

$^{13}\text{C-NMR}$ (75MHz, ppm, CDCl_3): 13.7-22.2-22.3-28.5-28.6-28.9-31.4-40.8-50.9-52.1-55.6-55.7-58.5-68.4-68.7-69.3-70.1-70.2-70.3-70.4-71.5-112.4-114.2-114.5-116.3-119.4-120.2-126.0-126.8-149.9-150.2-150.9-151.3

FT-IR (NaCl), ν (cm^{-1}): 2926, 2857, 1510, 1464, 1407, 1217, 1110, 1044, 931

MS (DIP, m/z): 549, 493, 457, 295, 218, 197

2-[2-(4-Methoxy-phenoxy)-ethoxy]-ethanol 17



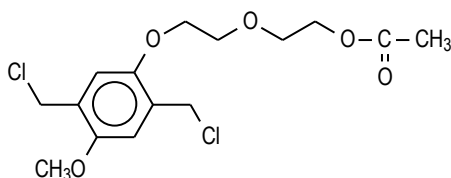
In 125 ml ethanol are dissolved *p*-hydroxy-anisol (15 g, 0.12 mol) and sodium ethoxide (6.85g, 2 equivalents) and the mixture is stirred at room temperature for one hour. A catalytic amount of sodium iodide and the chloride (12.5g, 1 equivalent) are added and the

solution is refluxed under nitrogen atmosphere for 16 hours. The mixture is poured into water. Extraction with chloroform, drying over magnesium sulfate and a column purification with ether as the eluent yields 2-[2-(4-Methoxy-phenoxy)-ethoxy]-ethanol as an oil (17.6 g, 69%).

¹H-NMR (300MHz, ppm, CDCl₃): 3.23 (s, 1H), 3.54 (t, 2H, J=4.8Hz), 3.65 (t + s, 5H), 3.72 (t, 2H, J=4.8Hz), 3.97 (t, 2H, J=4.5Hz), 6.74 + 6.76 (dd, 4H, J=9.3 Hz)

MS (EI, m/z): 212, 151, 124, 109

Acetic acid 2-[2-(2,5-bis-chloromethyl-4-methoxy-phenoxy)-ethoxy]-ethyl ester 18



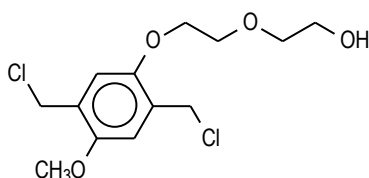
To 2-[2-(4-methoxy-phenoxy)-ethoxy]-ethanol (6g, 0.028 mol) and *p*-formaldehyde (2.34 g, 2.75 equivalents) is added dropwise and under nitrogen atmosphere 14 ml of concentrated HCl. Afterwards 30 ml of acetic anhydride is added at such a rate that the temperature does not exceed 70°C. The solution is stirred at 70°C for three hours and then poured into water. Extraction with chloroform, drying over magnesium sulfate and a column purification with ether as the eluent yields the acetic acid 2-[2-(2,5-bis-chloromethyl-4-methoxy-phenoxy)-ethoxy]-ethyl ester as an oil (3.5 g, 72%).

¹H-NMR (300MHz, ppm, CDCl₃): 2.07 (s, 3H), 3.77 (t, 2H, J=4.8Hz), 3.83 (s, 3H), 3.84 (t, 2H, J=4.8Hz), 4.15 (t, 2H, J=4.5Hz), 4.23 (t, 2H, J=4.8Hz), 4.60+4.64 (2s, 4H), 6.90+6.94 (2s, 2H)

FT-IR (NaCl), ν (cm⁻¹): 2915, 1735, 1639, 1514, 1249, 1225, 1180, 1141, 1058, 1040

MS (EI, m/z): 350, 314, 220, 184, 87, 43

2-[2-(2,5-Bis-chloromethyl-4-methoxy-phenoxy)-ethoxy]-ethanol 19

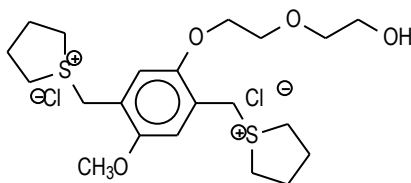


Chapter 3

The acetic acid 2-[2-(2,5-bis-chloromethyl-4-methoxy-phenoxy)-ethoxy]-ethyl ester (2g, mol) is dissolved in 25 ml methanol. A 10% K_2CO_3 solution in water is added until the begin product is completely disappeared on TLC. Extraction with chloroform and drying over magnesium sulfate yields the free alcohol as an oil.

1H -NMR (300MHz, ppm, $CDCl_3$): 2.22 (s, br, 1H), 3.66 (t, 2H, $J=4.8Hz$), 3.74 (s, 3H), 3.83 (s, 3H), 3.85 (t, 2H, $J=4.8Hz$), 4.15 (t, 2H, $J=4.5Hz$), 4.60+4.63 (2s, 4H), 6.89+6.94 (2s, 2H)
MS (EI, m/z): 310, 273, 237, 220, 184, 77, 45

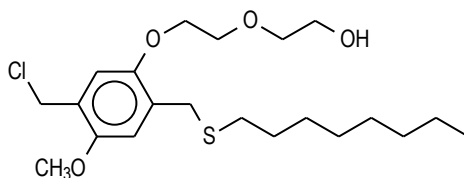
1,4-tetrahydrothiopheniummethyl-2-methoxy-5-[2-(2-hydroxy-ethoxy)-ethoxy]-benzyl dichloride 20



2-[2-(2,5-Bis-chloromethyl-4-methoxy-phenoxy)-ethoxy]-ethanol (2g, 5.7 mmol) is dissolved in 100 ml methanol and 8 ml tetrahydrothiophene. The clear solution is stirred at room temperature for one day and the obtained bisulfonium salt is precipitated in cold ether (300 ml) and filtered off to yield a white solid (1.5 g, 55%).

1H -NMR (300MHz, ppm, D_2O): 2.20 (m, 8H), 3.22 (s, 1H), 3.36 (m, 8H), 3.61 (d, 2H), 3.79 (s, 3H), 3.82 (m, 2H), 4.16 (m, 2H), 4.39-4.44 (2s, 4H), 7.08-7.09 (2s, 2H)

2-[2-(2-Chloromethyl-4-methoxy-5-octylsulfanylmethyl-phenoxy)-ethoxy]-ethanol 21



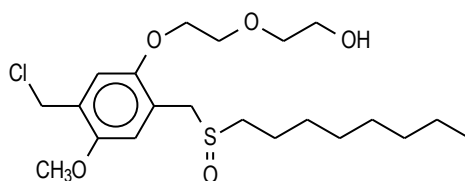
Octane thiol (0.146g, 0.01 mol) and sodium tertiary butoxide (0.096g, 0.01 mol) are dissolved in methanol (10ml) and stirred at room temperature for one hour. This solution is added dropwise to the bissulfonium salt (0.49g, 0.01 mol) in 20 ml methanol. The resulting solution is stirred for another 4 hours and neutralized if necessary. The solvent is evaporated and *n*-octane is added and evaporated again to remove the THT. This procedure is repeated three times. The residue is dissolved in chloroform and extracted with water. After drying over magnesium sulfate and a column with ether as the eluent, the desired compound is obtained as a yellowish oil (g, 68%)

¹H-NMR (300MHz, ppm, CDCl₃): 6.84+6.83+6.78+6.77 (4s, 2H), 4.58+4.54 (2s, 2H), 4.04 (m, 2H), 3.78-3.53 (m, 9H), 2.40 (m, 2H), 1.52 (m, 2H), 1.18-1.33 (m, 10H), 0.79 (t, 3H)

MS (EI, m/z): 382, 237, 207

2-{2-[5-Chloromethyl-4-methoxy-2-(octane-1-sulfinylmethyl)-phenoxy]-ethoxy}-ethanol

22

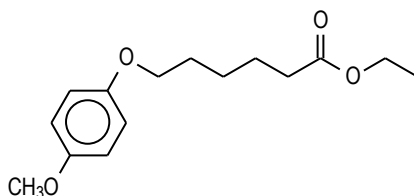


To 2-[2-(2-chloromethyl-4-methoxy-5-octylsulfanylmethyl-phenoxy)-ethoxy]-ethanol (g, mol) in 20 ml dioxane is added TeO₂ (20 mg, 5 mol%) and H₂O₂ (0.36 g, 2 equivalents). A few drops of concentrated HCl are added to catalyze the reaction. The progress of the reaction is followed on TLC and when all thioether is disappeared 20 ml of brine is added to stop the reaction. Extraction with chloroform, drying over magnesium sulfate and column purification with dichloromethane/methanol as the eluent yields the sulfoxide as a yellow oil (

¹H-NMR (300MHz, ppm, CDCl₃): 0.79 (t, 3H), 1.18-1.33 (m, 10H), 1.70 (m, 2H), 2.58 (m, 2H), 3.37 (s, 1H), 3.56 (m, 2H), 3.59 (m, 2H), 3.74-3.77 (m, 5H), 3.98-4.11 (m, 4H), 4.54-4.58 (2s, 2H), 6.73-6.85-6.89-6.91 (4s, 2H)

¹³C-NMR (75MHz, ppm, CDCl₃): 151.4, 151.2, 150.4, 150.1, 127.0, 126.4, 120.3, 119.4, 117.8, 115.0, 114.1, 112.5, 72.5, 69.5, 68.8, 61.3, 55.8, 52.6, 51.1, 41.2, 31.5, 29.9, 22.4, 13.8

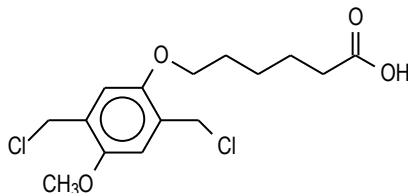
6-(4-Methoxy-phenoxy)-hexanoic acid ethyl ester 29



In 125 ml ethanol is dissolved *p*-hydroxy-anisol (15g, 0.12 mol) and sodium ethoxide (6.85g, 1.2 equivalents) and the mixture is stirred at room temperature for one hour. A catalytic amount of sodium iodide and the 6-bromohexanoate (32.5g, 1.2 equivalents) are added and the solution is refluxed under nitrogen atmosphere for 4 hours. The mixture is poured into water. Extraction with chloroform, drying over magnesium sulfate and a column purification with ether as the eluent yields product 6-(4-methoxy-phenoxy)-hexanoic acid ethyl ester as an oil (29 g, 92%).

$^1\text{H-NMR}$ (300MHz, ppm, CDCl_3): 3.23 (s, 1H), 3.54 (t, 2H, $J=4.8\text{Hz}$), 3.65 (t + s, 5H), 3.72 (t, 2H, $J=4.8\text{Hz}$), 3.97 (t, 2H, $J=4.5\text{Hz}$), 6.74 + 6.76 (dd, 4H, $J=9.3\text{ Hz}$)

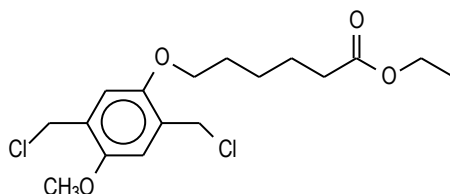
6-(2,5-Bis-chloromethyl-4-methoxy-phenoxy)-hexanoic acid 30



To 6-(4-methoxy-phenoxy)-hexanoic acid ethyl ester (7.2g, 0.027 mol) and *p*-formaldehyde (0.825 g, 2.75 equivalents) is added dropwise and under nitrogen atmosphere 13 ml of concentrated HCl. Afterwards 26 ml of acetic anhydride is added at such a rate that the temperature does not exceed 70°C . The solution is stirred at 60°C for three hours and cooled down to room temperature and the solid formed is then poured into water. After filtration, the solid product is dissolved in dichloromethane and dried over magnesium sulfate. Evaporation of the solvent yields the carbocyclic acid as a white solid. (7.49 g, 76%)

$^1\text{H-NMR}$ (300MHz, ppm, CDCl_3): 6.89+6.88 (2s, 2H), 4.61+4.60 (2s, 4H), 3.97 (t, 2H), 3.83 (s, 3H), 3.39 (t, 2H), 1.81 (m, 2H), 1.72 (m, 2H), 1.58 (m, 2H)

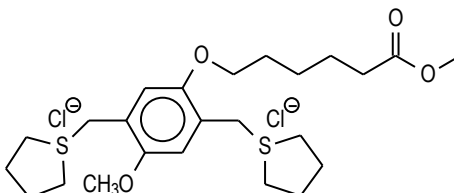
6-(2,5-Bis-chloromethyl-4-methoxy-phenoxy)-hexanoic acid ethyl ester 31



The carboxylic acid is dissolved in absolute ethanol and a trace of H_2SO_4 is added as a catalyst. The solution is stirred at $50\text{ }^\circ\text{C}$ until all acid has disappeared on TLC. After cooling the solution, dichloromethane is added and the solution is washed with NaHCO_3 solution until neutral pH. A short chromatographic purification with silica and dichloromethane as eluent yields the pure ester as a white solid. (55%)

$^1\text{H-NMR}$ (300MHz, ppm, CDCl_3): 6.89+6.88 (2s, 2H), 4.60+4.59 (2s, 4H), 4.10 (q, 2H), 3.96 (t, 2H), 3.82 (s, 3H), 2.31 (t, 2H), 1.80 (m, 2H), 1.66 (m, 2H), 1.53 (m, 2H), 1.23 (t, 3H)

Synthesis of bissulfonium salt 32



The 6-(2,5-Bis-chloromethyl-4-methoxy-phenoxy)-hexanoic acid ethyl ester (3g, 9 mmol) is dissolved in 30 ml methanol and 4 ml THT is added to the solution. The solution is stirred at $50\text{ }^\circ\text{C}$ for 14 hours and cooled to room temperature. The solvent is evaporated a little at room temperature under reduced pressure and the remaining product is precipitated in cold ether. The precipitate is filtered off and dried in vacuo, to yield the pure bissulfonium salt as a white solid. The ethyl ester is converted into a methyl ester function. (69%)

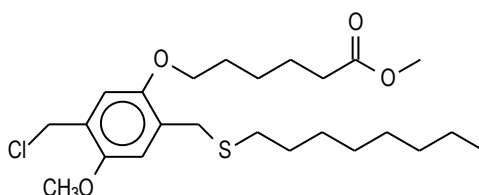
$^1\text{H-NMR}$ (300MHz, ppm, D_2O): 7.12+7.11 (2s, 2H), 4.44+4.43 (2s, 4H), 4.03 (t, 2H), 3.81 (s, 3H), 3.58 (s, 3H), 3.40 (m, 8H), 2.34 (t, 2H), 2.24 (m, 8H), 1.75 (m, 2H), 1.59 (m, 2H), 1.42 (m, 2H)

or

6-(2,5-Bis-chloromethyl-4-methoxy-phenoxy)-hexanoic acid (3g, 9 mmol) is dissolved in 30 ml methanol and 4 ml THT is added to the solution. The solution is stirred at $50\text{ }^\circ\text{C}$ for 14

hours and cooled to room temperature. The solution is evaporated a little at room temperature and the remaining is precipitated in cold ether. The precipitate is filtered off and dried in vacuo, to yield the pure bisulfonium salt as a white solid. $^1\text{H-NMR}$ spectrum is identical to the previous route described

6-(5-Chloromethyl-4-methoxy-2-octylsulfanylmethyl-phenoxy)-hexanoic acid methyl ester and 6-(2-Chloromethyl-4-methoxy-5-octylsulfanylmethyl-phenoxy)-hexanoic acid methyl ester 33

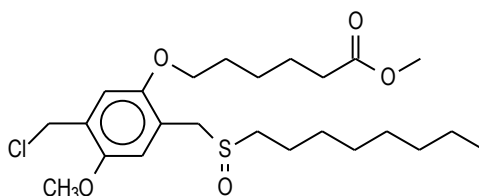


Octane thiol (1g, 7 mmol) and sodium tertiary butoxide (0.67 g, 1 equivalent) are dissolved in methanol (40 ml) and stirred at room temperature for one hour. This solution is added dropwise to the bisulfonium salt (3.8 g, 1 equivalent) in 130 ml methanol. The resulting solution is stirred for another two hours and neutralized if necessary. The solvent is evaporated and *n*-octane is added and evaporated again to remove the THT. This procedure is repeated three times. The residue is dissolved in chloroform and extracted with water. After drying over magnesium sulfate and a column with dichloromethane as the eluent, the desired compound is obtained as a yellowish oil (2.8 g, 88%)

$^1\text{H-NMR}$ (300MHz, ppm, CDCl_3): 4.61+4.60 (2s, 2H), 3.94 (m, 2H), 3.83+3.81 (2s, 3H), 3.79 +3.78 (2s, 3H), 3.69+3.68 (2s, 2H), 2.44 (t, 2H), 2.33 (t, 2H), 1.79 (m, 2H), 1.71 (m, 2H), 1.52 (m, 2H), 1.30-1.23 (m, 12H), 0.85 (t, 3H)

Mass (GC-MS, EI): 458, 423, 329, 313, 277, 185, 129

6-(5-Chloromethyl-4-methoxy-2-octylsulfinylmethyl-phenoxy)-hexanoic acid methyl ester 34

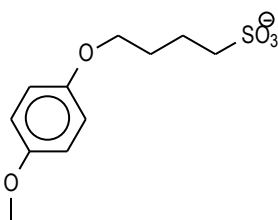


To the thioether (2.8 g, 6 mmol) in 50 ml 1,4-dioxane is added TeO_2 (60 mg, 5 mol%) and H_2O_2 (1.2 g, 2equivalents). One drop of concentrated HCl is added to catalyze the reaction. The progress of the reaction is followed on TLC and when all thioether is disappeared 50 ml of brine is added to stop the reaction. Extraction with chloroform, drying over magnesium sulfate and a column purification with dichloromethane/methanol as the eluent yields the sulfoxide as an orange oil (2.6g, 93%)

$^1\text{H-NMR}$ (300MHz, ppm, CDCl_3): 6.88-6.86-6.85-6.84 (4s, 2H), 4.56+4.55 (2s, 2H), 4.13+4.11+4.20+4.00 (2dd, 2H, $3J=12.6\text{Hz}$), 3.91(m, 2H), 3.77+3.75 (2s, 3H), 3.60 (s, 3H), 2.67 (m, 2H), 2.29 (t, 2H), 1.78-1.61 (m, 6H), 1.49-1.18 (m, 11H), 0.81 (t, 3H)

$^{13}\text{C-NMR}$ (75MHz, ppm, CDCl_3): 173.7, 173.6, 151.0, 150.7, 150.5, 150.2, 126.4, 126.2, 119.7, 119.6, 115.5, 114.5, 113.6, 112.7, 68.4, 68.2, 55.9, 55.8, 52.7, 52.3, 51.3, 51.2, 41.1, 41.0, 33.7, 33.6, 31.5, 30.6, 28.9, 28.7, 28.6, 28.5, 25.4, 25.3, 24.4, 22.3, 13.8,

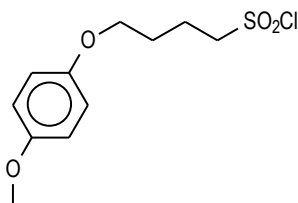
4-(4-Methoxy-phenoxy)-butane-1-sulfonic acid sodium salt 40



4-Hydroxy anisol (1g, 8 mmol) and sodium *t*-butoxide (0.929 g, 1.2 equivalents) are dissolved in 20 ml ethanol and stirred for one hour at room temperature. 1,4-Butanesultone is added (1 ml) and the resulting mixture is stirred overnight. The white solid is filtered off and dried to yield the sodium salt (1.7g, 75%)

$^1\text{H-NMR}$ (300MHz, ppm, D_2O): 1.72 (m, 4H), 2.85 (t, 2H, $J=6.4\text{Hz}$), 3.66 (s, 3H), 3.84 (t, 2H, $J=6.4\text{Hz}$), 6.8 (s, 4H)

4-(4-Methoxy-phenoxy)-butane-1-sulfonyl chloride 41

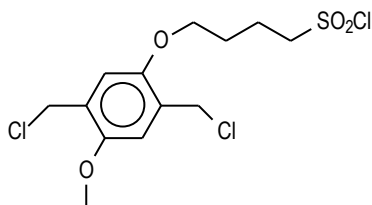


Chapter 3

The 4-(4-methoxy-phenoxy)-butane-1-sulfonic acid sodium salt (9g, 0.03 mol) is dissolved in 40 ml dimethylformamide (DMF) and the solution is placed in an ice bath. Thionylchloride (12 ml) is added dropwise and the solution turns yellow. The solution is brought to roomtemperature and stirred for one hour and then poured into water. The aqueous layer is extracted with ether and the resulting organic layer is washed with water (4 times 100 ml), dried over magnesium sulfate and concentrated in vacuo to yield an oil which becomes solid upon cooling (7.5g, 89%).

$^1\text{H-NMR}$ (300MHz, ppm, CDCl_3): 1.97 (m, 2H), 2.24 (m, 2H), 3.76 (t+s, 5H), 3.96(t, 2H, $J=5.7\text{Hz}$)

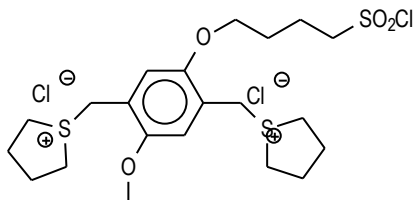
4-(2,5-Bis-chloromethyl-4-methoxy-phenoxy)-butane-1-sulfonyl chloride 42



To 4-(4-methoxy-phenoxy)-butane-1-sulfonyl chloride (2.78 g, 0.01 mol) and *p*-formaldehyde (0.825 g, 2.75 equivalents) is added dropwise and under nitrogen atmosphere 5 ml of concentrated HCl. Afterwards 10 ml of acetic anhydride is added at such a rate that the temperature does not exceed 70°C . The solution is stirred at 60°C for hours and then poured into water. Extraction with chloroform, drying over magnesium sulfate and a column purification with ether as the eluent yields the dichloride as an oil (2.8 g, 74%).

$^1\text{H-NMR}$ (300MHz, ppm, CDCl_3): 2.03 (m, 2H), 2.33 (m, 2H), 3.80 (s+t, 5H), 4.06 (t, 2H, $J=6.4\text{Hz}$), 4.59 (s, 2H), 4.61 (s, 2H), 6.87 (s, 1H), 6.90 (s, 1H)

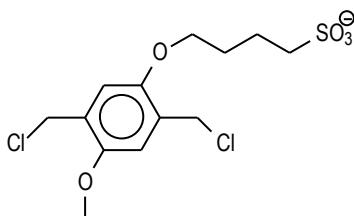
1,4-tetrahydrothiophenylmethyl-2-methoxy-5-[(3-chlorosulfonylpropyloxy)-benzyl] dichloride 43



Dichloride (1g, 2.66 mmol) is dissolved in 4 ml acetone, 7 ml methanol and 5 ml tetrahydrothiophene. The clear solution is stirred at room temperature for 40 hours and the obtained bissulfonium salt is precipitated in cold acetone and filtered off to yield a white solid (0.925g, 63%).

¹H-NMR (300MHz, ppm, D₂O): 1.87 (m, 4H), 2.24 (m, 8H), 2.87 (m, 2H), 3.39 (m, 8H), 3.79 (s, 3H), 4.05 (m, 2H), 4.39 + 4.42 (2s, 2H), 7.07 (s, 1H), 7.08 (s, 1H)

4-(2,5-Bis-chloromethyl-4-methoxy-phenoxy)-butane-1-sulfonic acid sodium salt 46



4-(2,5-Bis-chloromethyl-4-methoxy-phenoxy)-butane-1-sulfonyl chloride (0.5 g, 1.32 mmol) is dissolved in 10 ml acetone and stirred at room temperature. Sodium hydroxide solution (5% in water) is added dropwise until all sulfonyl chloride has disappeared on TLC. Precipitation in acetone and drying under vacuum yields the desired sodium sulfonate salt (0.45g, 89%).

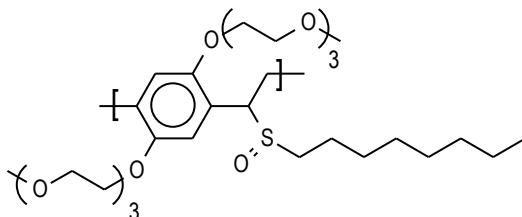
¹H-NMR (300MHz, ppm, D₂O): 1.73 (m, 4H), 2.80 (m, 2H), 3.65 (s, 3H), 3.87 (m, 2H), 4.42 + 4.48 (2s, 2H), 6.84 (s, 1H), 6.86 (s, 1H)

Polymerisation of the monomers

All precursor polymers were synthesised according to a general procedure. Solutions of the monomers and base (Na-*t*-BuO, 1.3 equivalents) were prepared and degassed for one hour by a continuous flow of nitrogen at 30 °C. The base solution was added in one portion to the stirred monomer solution. During the reaction the temperature was maintained at 30 °C and the passing of nitrogen was continued. After one hour the reaction mixture was poured into well stirred water whereupon some precursor polymer precipitated. The water layer was extracted with chloroform or dichloromethane to ensure that all polymer and residual fraction was collected, and the combined organic fractions were concentrated *in vacuo*. The polymer

was precipitated in a non-solvent, depending on the polymer composition, collected by filtration and dried *in vacuo*. The residual fraction was concentrated *in vacuo*.

Precursor polymer 15



The polymerisation of monomer **8** (624 mg, 1 mmol) in *s*-butanol (6 mL) is performed in a thermostatic flask. Sodium *t*-butoxide (96 mg, 1.3 equivalents), dissolved in the same solvent (4 ml), is added in one portion via a thermostatic funnel after both solutions are made oxygen-free by passing through a continuous stream of N₂. Polymerisation is allowed to proceed for one hour at 30°C. The reaction is terminated by pouring the reaction mixture in a well stirred amount of ice-cold water whereupon the precursor polymer precipitates. After extraction with CH₂Cl₂, the combined organic layers are concentrated in vacuum.

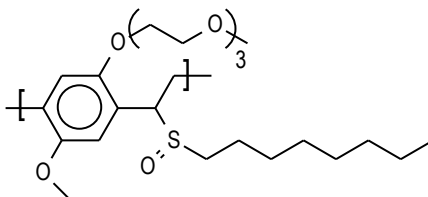
FT-IR (NaCl, cm⁻¹): 2925, 2871, 1509, 1456, 1420, 1215, 1109, 1042, 953

Molecular weight determination by Size Exclusion Chromatography (SEC) in THF against polystyrene standards gave a M_w = 230000 Dalton and a polydispersity of 4.

¹H-NMR (300MHz, ppm, CDCl₃): 7-6.4, 4.6-4.4, 4.1, 3.6, 3.4, 3.25, 2.8, 2.2, 1.6, 1.2, 0.8.

The spectra of unpurified samples were recorded and hence they were contaminated with low weight impurities such as monomer, solvent substituted product etc.

Precursor polymer 16



The polymerisation of monomer **14** (492 mg, 1 mmol) in *s*-butanol (6 mL) is performed in a thermostatic flask. Sodium *t*-butoxide (127 mg, 1.3 equivalents), dissolved in the same solvent (4 ml), is added in one portion via a thermostatic funnel after both solutions are

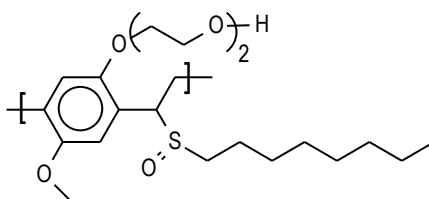
made oxygen-free by passing through a continuous stream of N₂. Polymerisation is allowed to proceed for one hour at 30°C. The reaction is terminated by pouring the reaction mixture in a well stirred amount of ice-cold water whereupon the precursor polymer precipitates. After extraction with CH₂Cl₂, the combined organic layers are concentrated in vacuum.

FT-IR(NaCl, cm⁻¹): 2926, 2857, 1510, 1464, 1407, 1217, 1110, 1044, 931

Molecular weight determination by Size Exclusion Chromatography (SEC) in THF against polystyrene standards gave a M_w = 214000 Dalton and a polydispersity of 3.7.

¹H-NMR (300MHz, ppm, CDCl₃): 7-6.2, 4.6-4.4, 4.1, 3.75, 3.6, 3.4, 3.25, 2.6, 2.2, 1.6, 1.2, 0.8. The spectra of unpurified samples were recorded and hence they were contaminated with low weight impurities such as monomer, solvent substituted product etc.

Precursor polymer 23



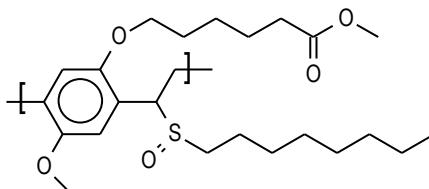
The polymerisation of monomer 22 (200 mg, 1 mmol) in *s*-butanol (3 mL) is performed in a thermostatic flask. Sodium *t*-butoxide (58 mg, 1.3 equivalents), dissolved in the same solvent (2 ml), is added in one portion via a thermostatic funnel after both solutions are made oxygen-free by passing through a continuous stream of N₂. Polymerisation is allowed to proceed for one hour at 30°C. The reaction is terminated by pouring the reaction mixture in a well stirred amount of ice-cold water whereupon the precursor polymer precipitates. After extraction with CH₂Cl₂, the combined organic layers are concentrated in vacuum.

FT-IR(NaCl, cm⁻¹): 2926, 2857, 1510, 1464, 1407, 1217, 1110, 1044, 931

Molecular weight determination by Size Exclusion Chromatography (SEC) in THF against polystyrene standards gave a M_w = 72000 Dalton and a polydispersity of 1.6.

¹H-NMR (300MHz, ppm, CDCl₃): 7-6.2, 4.6-4.4, 4.1, 3.75, 3.6, 3.4, 3.25, 2.6, 2.2, 1.6, 1.2, 0.8. The spectra of unpurified samples were recorded and hence they were contaminated with low weight impurities such as monomer, solvent substituted product etc.

Precursor polymer 35



The polymerisation of monomer (2.0 g, 4.21 mmol) in *s*-butanol (30 mL) is performed in a thermostatic flask. Sodium *t*-butoxide (0.53 g, 5.47 mmol), dissolved in the same solvent, is added in one portion via a thermostatic funnel after both solutions are made oxygen-free by passing through a continuous stream of N₂. Polymerisation is allowed to proceed for one hour at 30°C. The reaction is terminated by pouring the reaction mixture in a well stirred amount of ice-cold water whereupon the precursor polymer precipitates. After extraction with CH₂Cl₂, the combined organic layers are concentrated in vacuum. 1.18 g of precursor polymer (64%) was obtained.

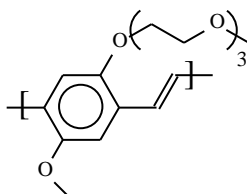
FT-IR(NaCl, cm⁻¹): 2929, 2856, 1728($\nu_{C=O}$), 1506, 1463, 1409, 1212, 1032

Molecular weight determination by Size Exclusion Chromatography (SEC) in THF against polystyrene standards gave a $M_w = 251000$ Dalton and a polydispersity of 2.1.

Conversion of the precursor polymer to the conjugated structure

A solution of the precursor polymer (0.5g) in toluene (50 ml) was degassed for 1 hour passing through a continuous stream of nitrogen. The solution was heated to 110°C and stirred for 3 hours. After cooling, the toluene is evaporated and the resulting red polymer is dissolved in a few ml chloroform and again precipitated in a non-solvent for the polymer (hexanes). The conjugated polymer is filtered off, washed with the non-solvent and dried at roomtemperature under reduced pressure. In all cases, a red fibrous polymer is obtained.

Polymer 2



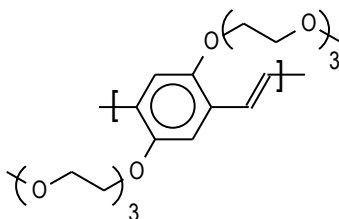
$^1\text{H-NMR}$ (300MHz, ppm, CDCl_3): 7.45 (2H), 7.18 (2H), 4.23 (2H), 3.93 (2H), 3.77 (2H), 3.66 (2H), 3.62 (2H), 3.50 (3H), 3.32 (3H)

$^{13}\text{C-NMR}$ (75MHz, ppm, CDCl_3): 151.7, 150.6, 127.6, 126.9, 123.4, 123.2, 111.4, 111.2, 108.9, 108.6, 71.7, 70.7, 70.5, 70.4, 69.8, 69.2, 58.8, 56.2

UV-Vis spectra were taken in CHCl_3 at room temperature ($\lambda_{\text{max}} = 490 \text{ nm}$)

Photoluminescence spectra were taken in CHCl_3 at room temperature with excitation wavelength $\lambda_{\text{ex}} = 490 \text{ nm}$ ($\lambda_{\text{max}} = 546 \text{ nm}$)

Polymer 1



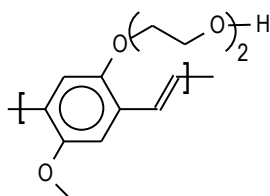
$^1\text{H-NMR}$ (300MHz, ppm, CDCl_3): 7.43 (2H), 7.17 (2H), 4.22 (4H), 3.92 (4H), 3.75 (4H), 3.66 (4H), 3.60 (4H), 3.32 (6H)

$^{13}\text{C-NMR}$ (75MHz, ppm, CDCl_3): 151.1, 127.8, 123.6, 111.2, 71.9, 70.9, 70.6, 70.5, 69.9, 69.2, 58.9

UV-Vis spectra were taken in CHCl_3 at room temperature ($\lambda_{\text{max}} = 488 \text{ nm}$)

Photoluminescence spectra were taken in CHCl_3 at room temperature with excitation wavelength $\lambda_{\text{ex}} = 488 \text{ nm}$ ($\lambda_{\text{max}} = 533 \text{ nm}$)

Polymer 23

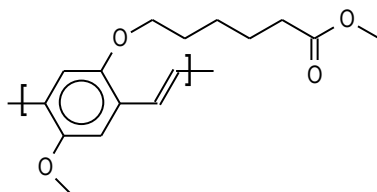


The precursor polymer was treated according to the general route. The precursor was dissolved in toluene and stirred for 3 hours at 110°C . A red precipitate was formed which

Chapter 3

was only very little soluble in hot DMF. The reaction mixture was poured into hexanes and the red polymer was collected by filtration.

Polymer 36



$^1\text{H-NMR}$ (300MHz, ppm, CDCl_3): 7.4, 7.1-6.4, 4.8, 4.1, 3.8, 3.7, 3.6, 2.6, 2.2, 2.0-1.0, 0.8

$^{13}\text{C-NMR}$ (75MHz, ppm, CDCl_3): 173, 151, 127, 124, 114, 108, 72, 69, 56, 34, 33, 32, 29, 22+23

UV-Vis spectra were taken in CHCl_3 at room temperature ($\lambda_{\text{max}} = 510 \text{ nm}$)

Photoluminescence spectra were taken in CHCl_3 at room temperature with excitation wavelength $\lambda_{\text{ex}} = 510 \text{ nm}$ ($\lambda_{\text{max}} = 569 \text{ nm}$)

Molecular weight determination by Size Exclusion Chromatography (SEC) in THF against polystyrene standards gave a $M_w = 290000$ Dalton and a polydispersity of 1.98.

Copolymer 27

$^1\text{H-NMR}$ (300MHz, ppm, CDCl_3): 7.4, 7.1, 4.2, 3.9, 3.7, 3.6, 3.5, 3.4, 3.2

$^{13}\text{C-NMR}$ (75MHz, ppm, CDCl_3): 151, 150, 127, 123, 116-112, 72, 70, 69, 68, 61, 58, 56, 50

UV-Vis spectra were taken in CHCl_3 at room temperature ($\lambda_{\text{max}} = 485 \text{ nm}$)

Photoluminescence spectra were taken in CHCl_3 at room temperature with excitation wavelength $\lambda_{\text{ex}} = 485 \text{ nm}$ ($\lambda_{\text{max}} = 540 \text{ nm}$)

Molecular weight determination by Size Exclusion Chromatography (SEC) in DMF against polystyrene standards gave a $M_w = 357000$ Dalton and a polydispersity of 6.33.

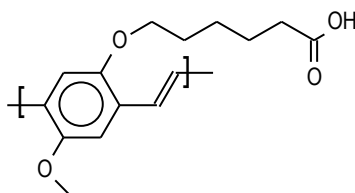
Copolymer 28

UV-Vis spectra were taken in CHCl_3 at room temperature ($\lambda_{\text{max}} = 487 \text{ nm}$)

Photoluminescence spectra were taken in CHCl_3 at room temperature with excitation wavelength $\lambda_{\text{ex}} = 487 \text{ nm}$ ($\lambda_{\text{max}} = 531 \text{ nm}$)

Molecular weight determination by Size Exclusion Chromatography (SEC) in DMF against polystyrene standards gave a $M_w = 151000$ Dalton and a polydispersity of 3.21.

Poly(1,4-(2-(5-carboxypentyloxy)-5-methoxyphenylene)vinylene 37



In a three-necked round-bottom flask equipped for stirring were added conjugated ester-substituted polymer (200 mg, 0.72 mmol) and dioxane (40 mL). The mixture was heated to reflux and a solution of KtBuO (0.87 g, 7.6 mmol) in water (1 mL) was added. After 4 h stirring at reflux temperature the reaction mixture was poured dropwise in a well stirred amount of ice water (400 mL), neutralised with aqueous HCl and the resulting precipitate was filtered off and washed with water. The red, fibrous polymer was dried at room temperature under reduced pressure to yield the poly(1,4-(2-(5-carboxypentyloxy)-5-methoxyphenylene)vinylene (0.57 mmol, 79%).

FT-IR (NaCl, cm^{-1}): 2952, 2869, 1707($\nu_{\text{C=O}}$), 1503, 1464, 1412, 1207, 1036, 972

UV-Vis spectra were taken in CHCl_3 at room temperature ($\lambda_{\text{max}} = 446 \text{ nm}$)

Photoluminescence spectra were taken in CHCl_3 at room temperature with excitation wavelength $\lambda_{\text{ex}} = 446 \text{ nm}$ ($\lambda_{\text{max}} = 540 \text{ nm}$)

7. References

¹ Pinto, M.R.; Schanze, K.S., *Synthesis*, 9, **2002**, 1293.
² Carvalho, L.M.; Santos, L.F.; Guimaraes, F.; Goncalves, D.; Gomes, A.; Faria, R.M., *Synth. Met.*, 119, **2001**, 361. Garay, R.O.; Mayer, B.; Karasz, F.E.; Lenz, R.W.; *J. Polym. Sc. Part A*, 33, **1995**, 525.
³ Huang, C.; Huang, W.; Guo, J.; Yang, C.Z.; Kang, E.T. *Polymer*, 42, **2001**, 3929. Li, F.; Coa, Y.; Gao, J.; Wang, D.; Yu, G.; Heeger, J.A. *Synth. Met.*, 99, **1999**, 243. He, G.; Yang, C.; Wang, R.; Li, Y. *Displays*, 21, **2000**, 69. Garay, R.O.; Mayer, B.; Karasz, F.E., Lenz, R.W. *Journal of the polymer Science*, 33, **1995**, 525. Morgado, J.; Cacialli, F.; Friend, R.H.; Chuah, B.S.; Rost, H.; Holmes, A.B. *Macromolecules*, 34, **2001**, 3094. Yang, C.; He, G.; Sun, Q.; Li, Y. *Synth. Met.*, 124, **2001**, 449.

Chapter 3

Tasch, S.; Holzer, L.; Wenzl, F.P.; Gao, J.; Winkler, B.; Dai, L.; Mau, A.W.H.; Sotgiu, R.; Sampietro, M.; Scherf, U.; Müllun, K.; Heeger, A.J.; Leising, G. *Synth. Met.*, 102, **1999**, 1046. Morgado, J.; Friend, R.H.; Cacialli, F.; Chuah, B.S.; Rost, H.; Moratti, S.C.; Holmes, A.B. *Synth. Met.*, 122, **2001**, 111. Sun, Q.J.; Wang, H.Q.; Yang, X.G.; Wang, C.H.; Liu, D.S.; Li, Y.F. *Thin Solid Films*, 417, **2002**, 14. Huang, C.; Huang, G.; Guo, J.; Huang, W.; Kang, E.T.; Yang, C.Z. *Polymer preprints*, 43, **2002**, 574.

⁴ Holzer, L.; Winkler, B.; Wenzl, F.P.; Tasch, S.; Dai, L.; Mau, A.W.H.; Leising, G. *Synth. Met.*, 100, **1999**, 71.

⁵ Fujii, A.; Sonoda, T.; Fujisawa, T.; Ootake, R.; Yoshino, K., *Synth. Met.*, 119, **2001**, 181.

⁶ Becker, H. et al., *Macromol.*, 32, **1999**, 4925.

⁷ *Spectroscopic Methods in Organic Chemistry*, Williams, D.H.; Fleming, I.; 5th edition, The McGraw-Hill Companies, London, **1995**.

⁹ Els Kesters, *PhD Dissertation*, Limburgs Unoversitair Centrum, Diepenbeek, **2002**.

¹⁰ Onoda, M.; Kazuya, T.; *Thin Solid Films*, 438, **2003**, 187.

¹¹ Ajayagosh, A.; George, S.J. *J. Am. Chem. Soc.*, 123, **2001**, 5148.

¹² Benjamin, I.; Hong, H.; Avny, Y.; Davidov, D.; Neumann, R. *J. Mater. Chem.*, 8, **1998**, 919.

¹³ Peng, Z; Xu, B.; Zhang, J.; Pan, Y.; *Chem. Comm.*, **1999**, 1855.

¹⁴ Fujii, A.; Sonoda, T.; Yoshino, K., *Jpn. J. Appl. Phys.*, 39, **2000**, 249.

¹⁵ Benjamin, I.; Hong, H.; Avny, Y.; Davidov, D.; Neumann, R. *J. Mater. Chem.*, 8, **1998**, 919.

¹⁶ Van Severen, Ineke, *Internal Communication*, Diepenbeek, **2003**.

¹⁷ Van Severen, I.; Motmans, F.; Lutsen L.; Vanderzande, D., *publication submitted for Macromolecules*.

¹⁸ Shi, S.; Wudl, F. *Macromolecules*, 23, **1990**, 2119. Wang, J.; Wang, D.; Miller, E.K.; Moses, D.; Bazan, G.C.; Heeger, A.J. *Macromolecules*, 33, **2000**, 5153. Fan, C.; Plaxco, K.W.; Heeger, A.J. *J. Am. Chem. Soc.*, 124, **2002**, 5642. Gaylord, B.S.; Wang, S.; Heeger, A.J.; Bazan, G.C. *J. Am. Chem. Soc.*, **2001**, 18. Hong, J.W.; Gaylord, B.S.; Bazan, G.C. *J. Am. Chem. Soc.*, 124, **2002**, 11868. Wallace, G.G.; Kane-Maguire, L.A.P. *Adv. Mater.*, 14, **2002**, 13.

¹⁹ Nobuaki, H.; Naoki, H.; Shigehiro, M. *Synth. Met.*, 80, **1996**, 67.

Chapter 4

Mechanistic study on the *p*-quinodimethane formation through the sulfinyl precursor route

1. Introduction

Chemical kinetics deals with the rates of chemical reactions and with how the rates depend on factors such as concentration and temperature. Such studies are important in providing essential evidence for elucidation of the mechanisms of chemical processes. A deeper insight into the mechanism may enable the researcher to control the outcome of a chemical reaction.

In this chapter we will study the *p*-quinodimethane formation through the sulfinyl precursor route. First we will briefly discuss the different kinetic equations that are possible in a chemical reaction such as a first order reaction, a second order reaction, a pseudo-first order reaction and the equations and features of two first-order consecutive reactions. Further on a short overview on different kinetic pathways for 1,2- and 1,6-elimination reactions is given. In a next part of this chapter the *p*-quinodimethane formation of some sulfinyl and sulfonyl monomers is studied and the data resulting from these experiments will be discussed and some conclusions concerning the mechanism of this reaction will be given. As a last part of this chapter a possible application of the study performed in the previous part will be presented. Here some copolymerisation reactions are performed in order to study the eventual outcome and monomer distribution in the copolymer.

1.2. A kinetic refreshment

1.2.1. Kinetics of a first and second order reaction

We will give a short overview on the kinetics of a first and second order reaction. The main features of both reaction types are overviewed in table 1. Plots of the concentration versus the reaction time are depicted in figures 1 and 2.

	First order reaction kinetics	Second order reaction kinetics
Reaction	$A \rightarrow B$	$A + B \rightarrow C (+ D)$
Rate equation	$v = k_1 [A]$	$v = k_2 [A][B]$ or $v = k_2[A]^2$ when $[A] = [B]$
Rate constant	$k_1 \text{ (s}^{-1}\text{)}$	$k_2 \text{ (s}^{-1} \text{ mol}^{-1}\text{)}$
Integration	$\ln [A] = \ln[A]_0 - k_1 t$	$1/[A] - 1/[A]_0 = k_2 t$
Linear plot	$\ln [A]$ versus time	$(1/[A] - 1/[A]_0)$ versus time
Slope of plot	$-k_1$	k_2

Table 1. General kinetic features of a first and second order reaction

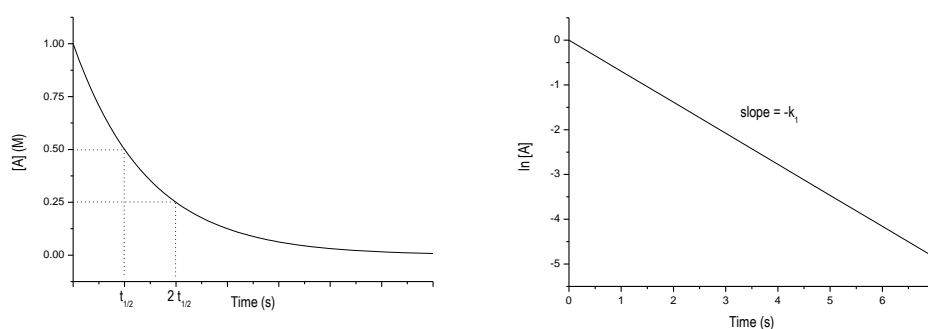


Figure 1. First order reaction: plot of $[A]$ versus time of a (left) and plot of $\ln [A]$ versus time (right)

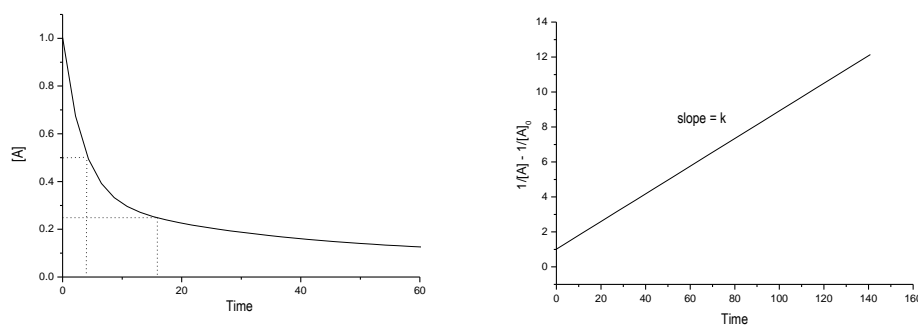
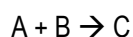


Figure 2. Second order reaction Plot of $[A]$ versus time (left) and plot of $(1/[A]-1/[A]^0)$ versus time, slope = k_2 (right)

1.2.2. Pseudo first order reaction kinetics

When one of the reagents in a second order reaction is present in large excess compared to the other reagent, the change in its concentration is only a fraction of the total concentration and hence this concentration may be considered to be constant throughout the reaction¹. One frequently arranges conditions deliberately so that the reaction under study will follow first-order kinetics, because first-order data are easier to treat than data from higher-order systems. The higher-order rate constants are found by performing subsequent experiments at different constant concentrations of the reagent in excess.



$$\frac{-d[A]}{dt} = k_2 [A][B]$$

When $[B] \gg [A]$, the reaction and the equation becomes

$$\frac{-d[A]}{dt} = k_{\text{obs}} [A]$$

$$\text{where } k_{\text{obs}} = k_2 [B]$$

Chapter 4

Integration yields : $\ln [A] = -k_{obs} t + c^{te}$

and plotting $\ln [A]$ versus time yields a straight line with slope $-k_{obs}$.

Plotting of k_{obs} at different concentrations of B gives a straight line with slope k_2 , the second order rate constant (figure 3).

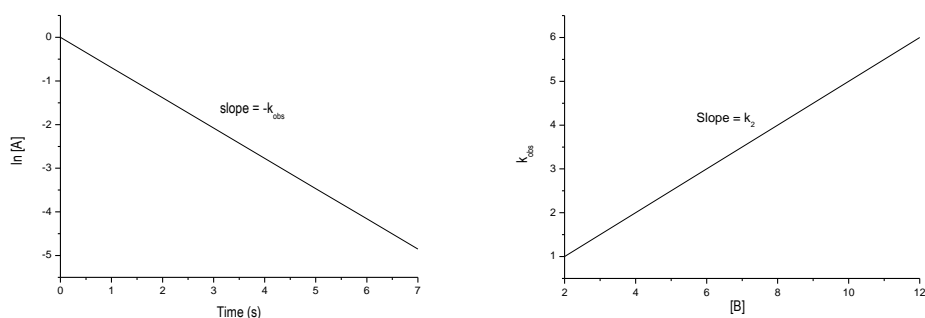
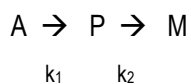


Figure 3. Pseudo-first order reaction: plot of $\ln [A]$ versus time, slope = $-k_{obs}$ (left), plot of k_{obs} versus $[B]$, the reagent in excess (right)

1.2.3. Consecutive first order reaction kinetics

When a reagent A reacts to a product P and this product P is subsequently consumed to yield a third product M, the reaction is said to proceed in a consecutive way. Consecutive reactions are frequently reported in literature often when a highly reactive or unstable species acts as the intermediate in a chemical reaction. A general reaction scheme is given by:



A typical plot of the three products present in such a reaction is given in figure 4. The decrease of compound A can be written with the following equation:

$$\frac{d[A]}{dt} = -k_1[A]$$

The formation and subsequent decrease of the intermediate compound P is given in equation 1

$$\frac{d[P]}{dt} = k_1[A] - k_2[P]$$

Integration of both equations yields²:

$$[A] = [A]^0 e^{-k_1 t}$$

$$[P] = A e^{-k_2 t} + \frac{k_1 [A]^0}{k_2 - k_1} e^{-k_1 t}$$

$$[P] = \frac{k_1}{k_2 - k_1} [e^{-k_1 t} - e^{-k_2 t}] \quad (\text{Equation 1})$$

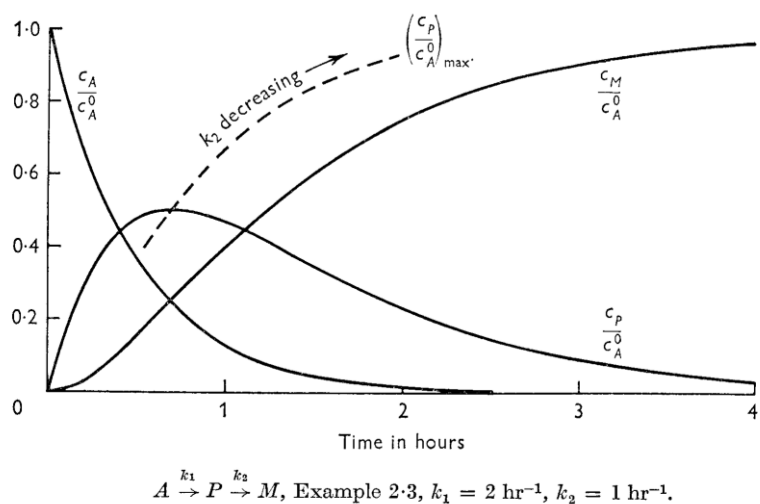
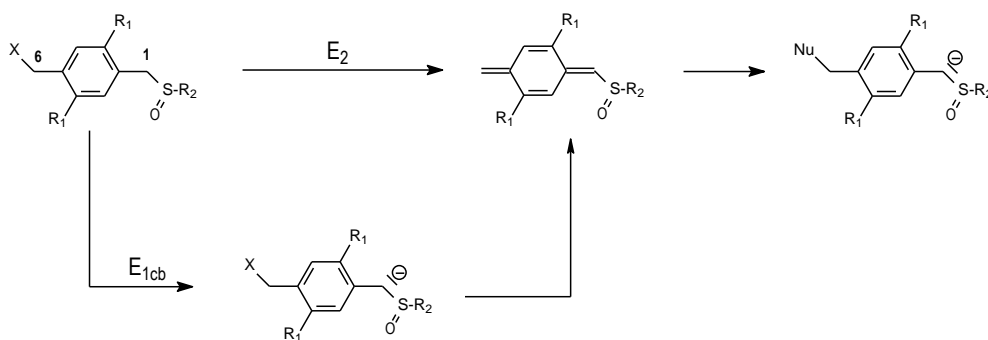


Figure 4. Typical plot of a consecutive first-order reaction

2. Different types of elimination reaction

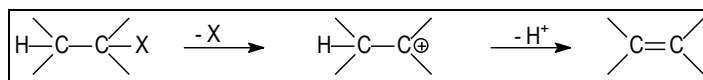
Since the formation of a *p*-quinodimethane system from a sulfinyl monomer is indeed an elimination reaction, we will discuss the possible reaction pathways for this kind of reactions. Generally four different types of 1,2-elimination reactions are known (scheme 1). They differ one from another in the order of the reaction and the kind of intermediate or transition state i.e. whether the reaction proceeds in a concerted way or not. Note that the terminology used in literature for 1,6-elimination reactions is the same as for 1,2-elimination reactions. Hence we will also use this same terminology.



Scheme 1. General reaction scheme for *p*-quinodimethane formation through the sulfinyl precursor route

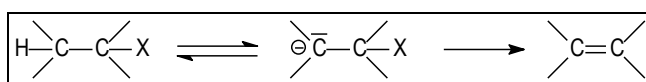
E₁ reaction

This is a first order elimination reaction. First a well-stabilised carbenium ion is formed by expulsion of the leaving group. In the second step a proton is abstracted to yield the double bond. The rate determining step in this kind of reaction is the formation of the carbenium ion. Since this reaction includes formation of a cation, the reaction is very unlikely to occur under the basic conditions present in the precursor route. Such mechanism would also imply the possibility of a spontaneous formation of the quinoid system, which has never been observed.

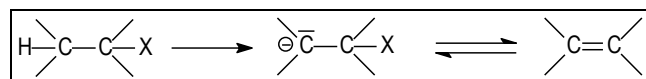


(E_{1cb})_{rev} reaction

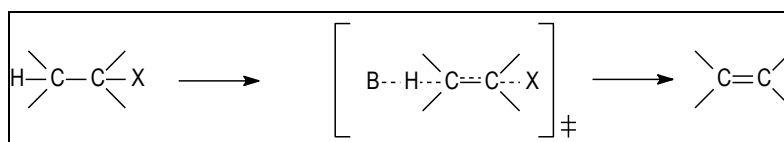
This kind of elimination reaction involves the formation of a carbanion. If the anion is formed from the starting product in a rapid equilibrium and the leaving group departs in a subsequent slow step the mechanism is called (E_{1cb})_{rev} (reversible first order elimination reaction of the conjugated base). The energy diagram is depicted in figure 5. Here the rate-determining step is the expulsion of the leaving group to yield the double bond.

(E_{1cb})_{irr} reaction

If the leaving group expulsion from the carbanion formed starting from the begin product is so fast that proton abstraction becomes rate determining the elimination mechanism is called (E_{1cb})_{irr} (irreversible first order elimination reaction of the conjugated base). The reaction rate is dependent of the base concentration in a proportional way.

E₂ reaction

This is an elimination reaction in which neither a cationic nor an anionic intermediate is formed. Expulsion of the leaving group and proton abstraction occurs at the same moment in a concerted way. Here a rate increase of the reaction will occur when an atom or group with better nucleofugal properties replaces the leaving group.



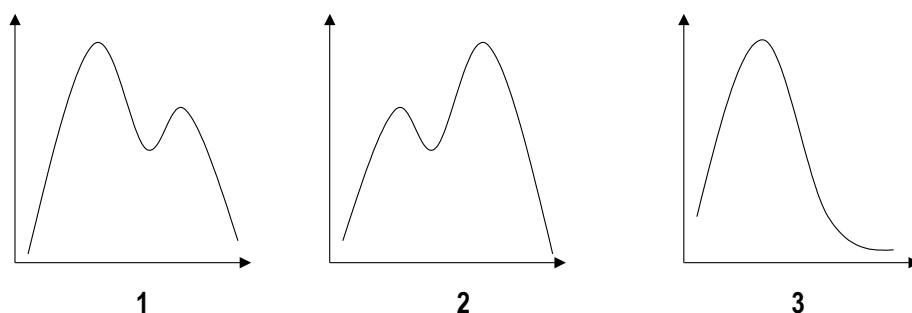
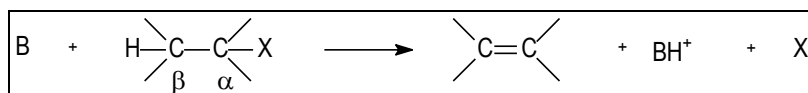


Figure 5. Energy diagrams of 1: $(E_{1cb})_{irr}$, 2: $(E_{1cb})_{rev}$, 3: E_2 elimination reactions

In table 2 an overview is given about the mechanistic features of the last three elimination mechanisms³.



Mechanism	β -proton exchange faster than elimination	Electron withdrawal at C_β	Leaving group effect
$(E_{1cb})_{rev}$	Yes	small rate increase	substantial
$(E_{1cb})_{irr}$	No	rate increase	small to negligible
E_2	No	rate increase	substantial

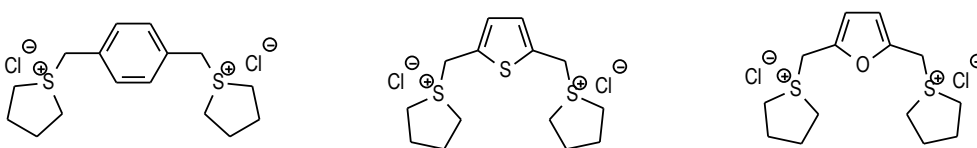
Table 2. Overview of the mechanisms of base induced elimination reactions

3. Previous work and literature data on p-quinodimethane formation

3.1. Wessling route

In literature up till now only few papers have been published on the mechanistic features of p-quinodimethane formation through a precursor route towards PPV. However Cho and co-

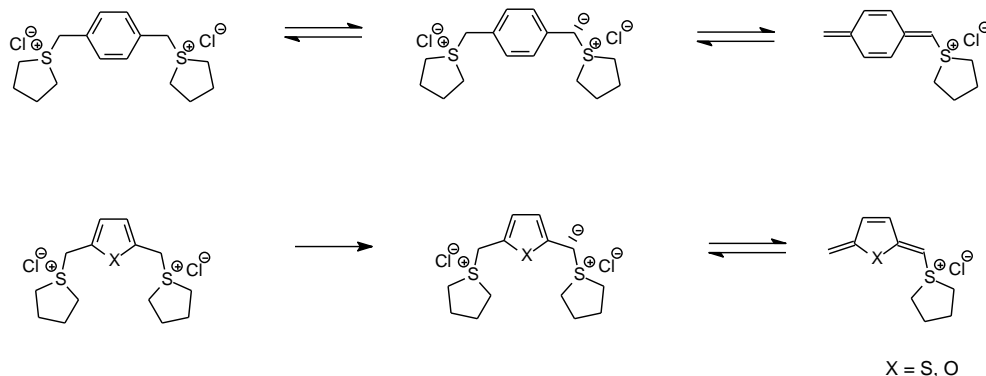
workers have performed a lot of research on the formation of the *p*-quinodimethane systems⁴ and the polymerisation properties of α,α' -bis(tetrahydrothiophenio)-*p*-xylene dichloride, α,α' -bis(tetrahydrothiopheniomethyl)-thiophene dichloride and α,α' -bis(tetrahydrothio-pheniomethyl)furan dichloride through the Wessling precursor route (scheme 2).



Scheme 2. Overview of the premonomers studied by Cho

They studied the influence of different parameters such as substituent effects on the aromatic ring, the THT concentration, addition of OH⁻ anions and several nucleophiles, radical initiators and inhibitors on the polymerisation rate and the rate of *p*-quinodimethane formation. Also some proton-deuterium (H-D) exchange NMR-experiments were performed on the different monomers. At low temperatures the normal PPV monomer underwent a benzylic H-D exchange reaction, which may indicate a reversible deprotonation step. Hence for the corresponding PPV-monomers a (E_{1cb})_{rev} mechanism was proposed. For hetero-aromatic PPV-analogues such as PTV and the furan derivative a (E_{1cb})_{irr} mechanism was proposed because the lack of this H-D exchange reaction in the first step. The change in the elimination mechanism with variation of the substrate is attributed to the smaller resonance energy of the five membered heterocyclic aromatic compounds compared to benzene (scheme 3).

Chapter 4



Scheme 3. Mechanistic features of the elimination reaction of normal PPV monomer (upper) and the 5-membered heterocyclic analogues (below)

3.2. The Gilch precursor route (dehydrohalogenation)

For the Gilch route, no papers have been published on the mechanism of p-quinodimethane formation. Probably also here, the quinoid intermediate is formed through a basic treatment of a α, α' -dihalo-*p*-xylene derivative (scheme 4). Since this kind of polymerisation demands very dry and pure reaction conditions under an inert atmosphere, it may be rather difficult to obtain reliable measurements about the p-quinodimethane formation.

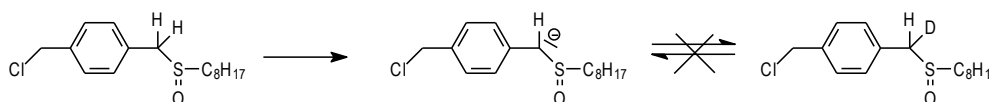


Scheme 4. General scheme of the Gilch precursor route

For the polymerisation mechanism through the Gilch route two different mechanisms were proposed⁵. Hsieh and others proposed an anionic polymerisation mechanism while other groups found evidence for a radical chain polymerisation yielding high molecular weight products. However it cannot be excluded that even in such case low molecular weight products are formed due to the occurrence of a competing anionic mechanism.

3.3. The Sulfinyl precursor route

A few years ago, dr. Anna Issaris from our research group studied the polymerisation mechanism of the sulfinyl precursor route in MMF⁶. Different attempts were made to elucidate the exact mechanism of *p*-quinodimethane formation. Similar to the work of Cho *et al.*, a proton-deuterium (H-D) exchange experiment was performed at very low temperatures (scheme 5). At these temperatures (-40°C), almost no polymerisation occurs. The benzylic proton signal next to the sulfinyl group was not affected by the experimental conditions indicating that a base promoted proton abstraction should be the rate determining step in the quinoid formation.



Scheme 5. H-D exchange experiment according to the sulfinyl precursor route in MMF

This experiment ruled out all mechanisms but E₂ and a (E_{1cb})_{irr} mechanism. To determine which one of these mechanisms proved to be the correct one in MMF, the influence of the leaving group and the polariser on the yield and molecular weight of the polymerisation was analyzed. There seemed to be no difference in yield and molecular weight upon changing the leaving group from chlorine over bromine to iodine. However when the sulfinyl polariser was replaced with a sulfonyl group the molecular weight increased significantly while the yields were not affected. (Table 3) Therefore an irreversible E_{1cb} mechanism was proposed.

	Polariser	
	<u>sulfinyl</u>	<u>sulfonyl</u>
Leaving group	M _w (yield %)	M _w (yield %)
Cl	170000 (24)	633000 (22)
Br	130000 (30)	586000 (16)

Table 3. Overview of the influence of the polariser and leaving group on the molecular weight and yield (between brackets) of the polymerisation in MMF

4. Study of the p-quinodimethane formation in 2-butanol

For this chapter, both a quantitative and a qualitative study on the p-quinodimethane formation through the sulfinyl precursor route were performed in 2-butanol using UV-Vis spectroscopy. 2-Butanol was used as the solvent because it already has proven to be a suitable solvent for obtaining the precursor polymers in a high yield and a high molecular weight⁷. First some qualitative experiments were performed. In a second stage more detailed data were pursued by performing quantitative measurements. In the quantitative part the influence of the polariser and the leaving group were studied and from the kinetic data some mechanistic conclusions could be drawn. The available data on the p-quinodimethane formation can be of major interest because they can give us an indication about the outcome of a copolymerisation reaction involving two different p-quinodimethane systems because in an extreme case, when the theoretical assumption is made that the polymerisation rate of a p-quinodimethane system is not or only little affected by the specific substitution pattern of the system the outcome of such copolymerisation reaction will be totally determined by the formation rate of the two p-quinodimethane systems.

4.1. Experimental set-up

To allow very fast and accurate measurements, the UV-Vis spectrophotometer is equipped with a so-called stop flow accessory. The working principle is depicted in figure 6. Two syringes **1** and **2**, containing a base solution and a monomer solution respectively, are

driven forward in such a way that equal amounts of the two solutions meet in the mixing chamber where a static mixer **3** makes a homogeneous solution. This solution is then transferred in the sample cell **4**. When driving forward syringe **1** and **2**, syringe **5** is driven out and it will hit an electric switch **6** which will start the recording of the measurement. With this equipment UV-Vis detection will be started within a few milliseconds.

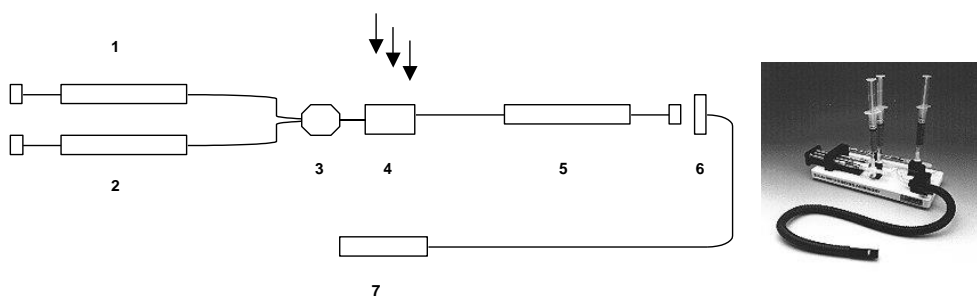


Figure 6. Set-up of the UV-Vis principle stop flow accessory

4.2. Experimental procedure

When mixing a 1×10^{-4} molar solution of a sulfinyl monomer with an excess of base, a typical plot is observed using UV-Vis spectroscopy (Figure 7). Three different signals can be distinguished. The signal at 228 nm corresponds to the premonomer. The signal at 313 nm is assigned to the p-quinodimethane system and a third signal at 260 nm stems from a solvent substituted premonomer. The signal of the premonomer is decreasing constantly in time. The signal of the p-quinodimethane system first increases rapidly and decreases subsequently. The signal of the solvent substituted product only increases as the reaction progresses.

Chapter 4

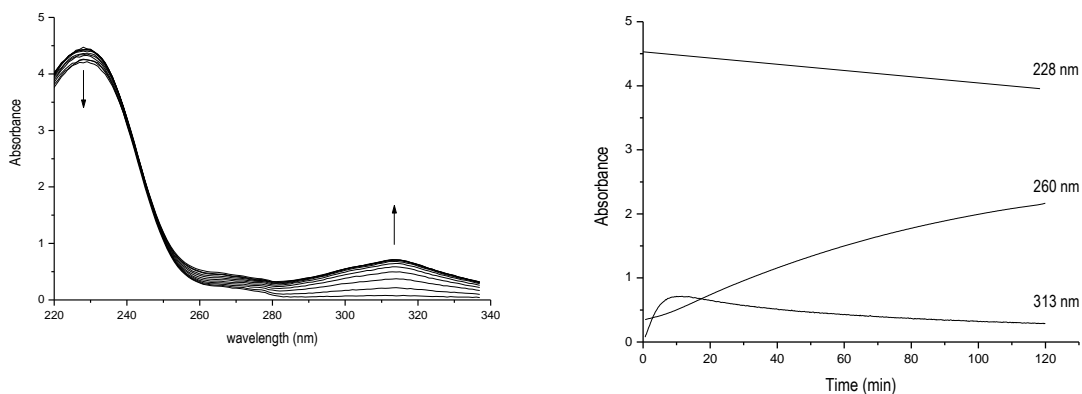
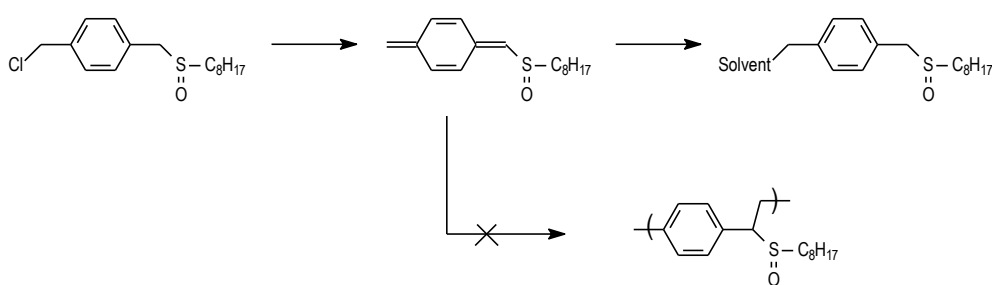


Figure 7. UV-Vis spectrum of *p*-quinodimethane formation (left). Plot of the absorptions at 224, 260 and 313 nm versus time (right)

This solvent substitution reaction was also performed at larger scale (scheme 6). When the monomer was dissolved in 2-butanol, an excess of base was added and the reaction was allowed to proceed for one hour under polymerisation conditions. After work up of the reaction the organic fraction was analysed through mass spectroscopy, indicating the formation of the solvent substituted product. Also reaction of benzyl bromide with an excess of sodium tertiary butoxide in 2-butanol yields a compound with the same absorption signal. No indications for polymer formation were found probably due to the concentration that is too low to initiate the polymerisation.



Scheme 6. Reaction scheme of the *p*-quinodimethane formation and solvent substitution according to the sulfinyl precursor route

4.3. Qualitative study on *p*-quinodimethane formation

Since it is generally known that *p*-quinodimethane systems show a typical absorption band around 320 nm in the UV-Vis spectrum, UV-Vis spectroscopy is an excellent tool in providing kinetic data through constant monitoring of this specific signal. When mixing a monomer solution and a base solution in a cuvette and monitoring the signal around 320 nm versus time a graph is obtained as depicted in figure 8.

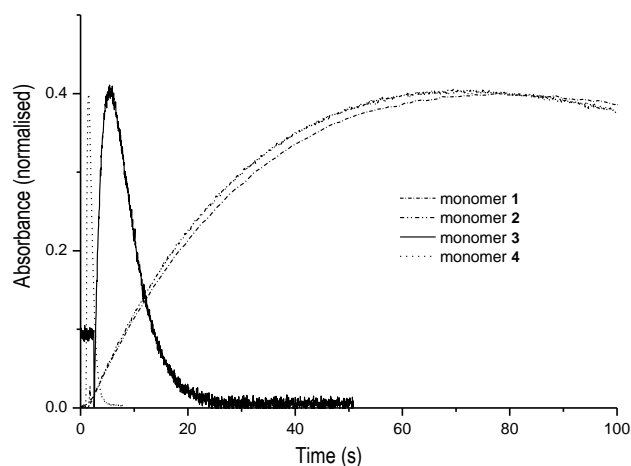


Figure 8. Plot of *p*-quinodimethane signal versus time for monomer 1-4

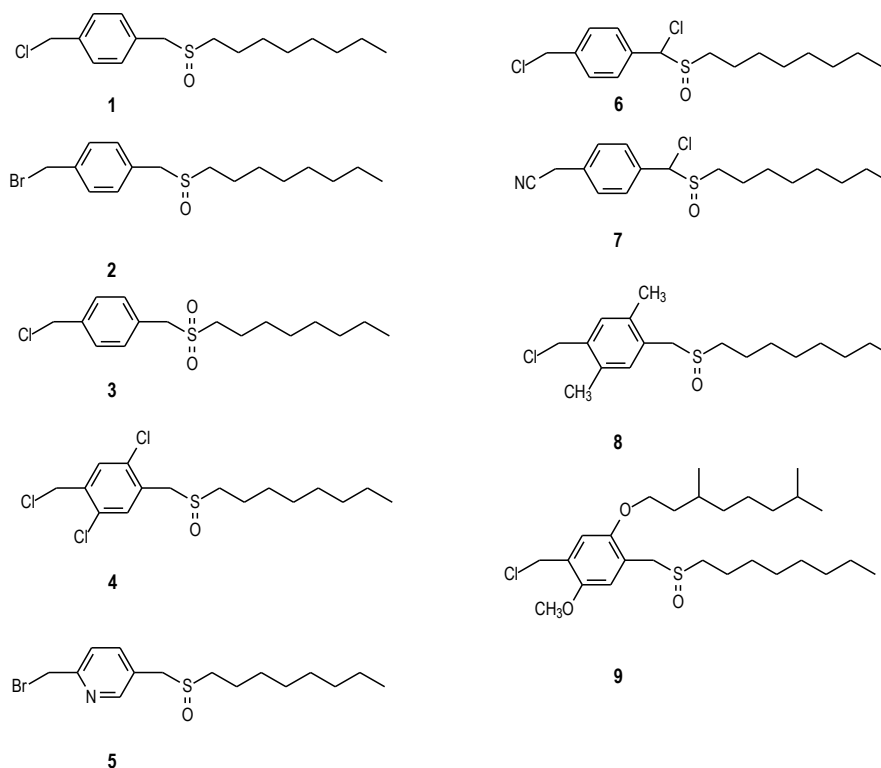
Some preliminary measurements were performed on nine different sulfinyl monomers (scheme 7) differing in polariser, leaving group, aromatic moiety and substituents on the aromatic core. The time at maximum absorbance (T_{\max}) was chosen as a reference for the qualitative rate of *p*-quinodimethane formation. Some general trends become clear when comparing the different values for T_{\max} . There is no significant difference in the *p*-quinodimethane formation rate of the monomers 1 and 2 indicating that there is no significant influence of the leaving group. When the polariser is changed from sulfinyl monomer 1 to the sulfonyl monomer 3 there is a strong decrease of the T_{\max} value. This means that the pK_a of the benzylic protons has a major influence on the *p*-quinodimethane formation. The lower this value (the higher the acidity) the faster the reaction seems to occur. The value of the dichloro analogue 4 is even smaller than the sulfonyl monomer 3.

The chlorine atoms on the phenyl ring can lower the pK_a value of the benzylic protons drastically due to their electron withdrawing properties. The implant of a chlorine atom next to the sulfinyl group in monomer **6** also lowers the pK_a value of the benzylic position, which is reflected in a low T_{max} value. Changing the aromatic moiety to the pyridine analogue **5** yields a lower value compared to monomer **2**. For this phenomenon two reasons can be given. Due to the electron poor character of the pyridine ring compared to the phenyl core the pK_a of the benzylic position is changed. Another reason is the lower resonance energy of the pyridine ring, which facilitates the formation of a non-aromatic species that is the p-quinodimethane system. The implant of a cyano group, a very electron withdrawing group, as the polariser in monomer **7** instead of the sulfinyl group gives the lowest value of T_{max} . On the other hand, electron donating substituents on the phenyl core like in monomer **8** and **9** give higher T_{max} values compared to monomer **1**. These substituents decrease the acidity of the benzylic protons hence resulting in a lower p-quinodimethane formation rate. All these data lead to the conclusion that proton abstraction is the rate-determining step in the p-quinodimethane formation.

Monomer	T_{max} (s)	Monomer	T_{max} (s)
1 (313)	77	6 (330)	1.4
2 (313)	69	7 (350)	0.6
3 (313)	5.5	8 (318)	211
4 (313)	1.5	9 (317)	252
5 (318)	8		

Table 4. Overview of T_{max} value of monomers **1-9** (λ_{max} between brackets)

Kinetic study on p-quinodimethane formation



Scheme 7. Overview of the monomer used for the qualitative study

Notice however that good or fast quinoid formation does not guarantee high polymerization yields. In the polymerization process other parameters like steric hindrance or electronic effects may have their influence on the polymerization rate. These processes will not be discussed here.

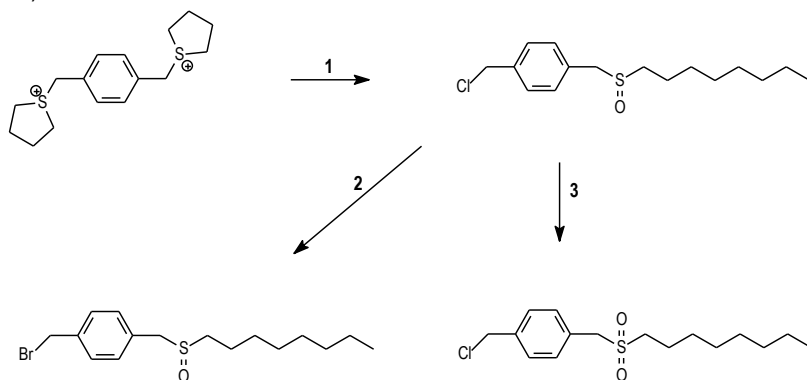
4.4. Quantitative study on p-quinodimethane formation

The qualitative data obtained and discussed in the previous part already give an indication of the elimination mechanism of the p-quinodimethane formation. The rate was severely affected when the acidity of the benzylic protons next to the polarising group is increased. The leaving group seemed to have little influence on this rate. For the quantitative measurements the influence of both leaving group and polariser were analyzed.

4.4.1. Synthesis of the required monomers

The monomer in the sulfinyl precursor route shows a chemical differentiation between the leaving group and the polariser and hence the influence of both groups on p-quinodimethane formation can be studied separately. Also both groups can be easily replaced which enables us to study the influence of the nature of the benzylic groups.

For the quantitative kinetic study of the p-quinodimethane formation in 2-butanol through the sulfinyl precursor route we used three different monomers. The normal n-octyl chloro compound **1** was synthesised according to the general route developed by Van Breemen *et al.* starting from the bisulfonium salt. Treatment of this salt with a thiolate anion in methanol yields a thioether that can be oxidised to the corresponding sulfoxide using mild oxidation conditions. The sulfinyl compound **1** can be further oxidised to the sulfonyl analogue **3** using m-chloroperbenzoic acid in dichloromethane giving the desired compound as white needles in excellent yield. The n-octyl bromo compound **2** is synthesised through a halogen exchange reaction using a tenfold excess of lithium bromide in 3-pentanone at reflux (scheme 8).



Scheme 8. Synthesis of the monomers used for the quantitative measurements. Reaction conditions:

1: Na-*t*BuO, *n*-octane thiol, MeOH/ *n*-octane/ H₂O₂/TeO₂, MeOH, 2: LiBr (10 eq.), 3-pentanone, reflux, 3: *m*-CPBA, CH₂Cl₂

4.4.2. Treatment of experimental data

The data obtained from the UV-Vis measurements were used to obtain the rate constant of the p-quinodimethane formation reaction. Two methods were used for this purpose: The Guggenheim method and a non-linear least-squares computational fitting program.

The Guggenheim method¹¹

The reaction rate constant of a first-order (figure 9) or a pseudo-first-order reaction can be calculated by measuring the decrease or increase of a physical parameter as a function of time. In general the so-called infinity value of this physical parameter will be necessary. The infinity value usually means the value of the physical parameter after eight to ten half-lives. Sometimes consecutive reactions make it impossible to measure a reliable infinity value. In such case the rate constant can be obtained by the Guggenheim method if during a period of 3 or 4 half-lives reliable measurements are possible.

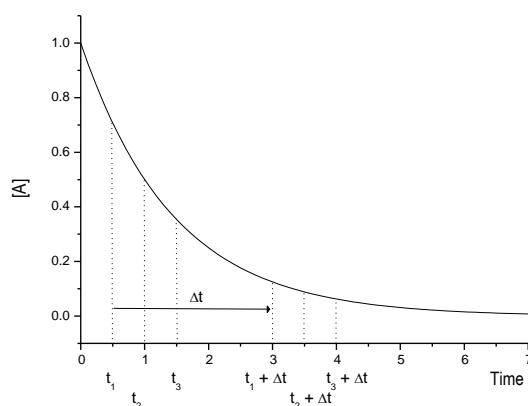


Figure 9. Plot of $[A]$ versus time in a first-order reaction

Earlier we discussed the kinetic features of a first-order reaction. Equation below stems for the linear correlation between the concentration versus reaction time.

$$\ln (A_t - A_{t=\infty}) = \text{constant} - kt$$

$$A_t - A_{t=\infty} = \text{constant}' \exp (-kt)$$

Chapter 4

where A_t represents the observed value at time t . Observations are made at regular time intervals so that the series of measurements are separable into two groups corresponding to times:

$$t_1, t_2, t_3, \dots$$

$$\text{and } t_1 + \Delta t, t_2 + \Delta t, t_3 + \Delta t, \dots$$

$$A_{t_i} - A_{t=\infty} = \text{constant}' \exp(-kt_i)$$

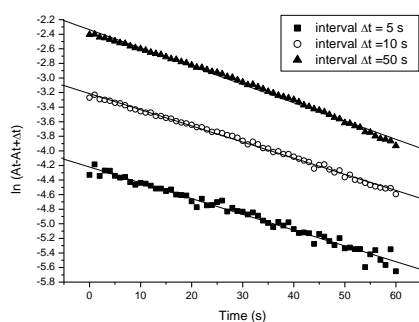
$$A_{t_i + \Delta t} - A_{t=\infty} = \text{constant}' [\exp(-k(t_i + \Delta t))]$$

$$A_{t_i} - A_{t_i + \Delta t} = \text{constant}' [1 - \exp(-k \Delta t)] \exp(-kt_i)$$

Since the term $[1 - \exp(-k \Delta t)]$ is constant during a run, a plot of $\ln(A_{t_i} - A_{t_i + \Delta t})$ versus time gives a straight line with slope $-k$. Clearly, the rate constant from this exercise has no reference to either the initial or infinity values of parameters that are measured.

In literature several attempts have been made to estimate the rate constant of a chemical reaction through the Guggenheim method¹².

In our case however treatment of the experimental data through the Guggenheim method appeared to be not reliable since treatment with different time intervals yields values that differ much from another. Consequently the data from different measurements will not be comparable and no or wrong conclusions could be drawn from the experiments (table 5).



Entry	Time interval Δt (s)	Slope k	Error %
Line ■	5	0.02163	4.2505
Line ▲	15	0.02214	1.8516
Line ○	50	0.02506	2.4738

Table 5. Slope of straight line according to the Guggenheim method with different time intervals.

Non-linear least-squares method¹³

Since the Guggenheim method failed to afford reliable rate constants the obtained data were fitted using a least-squares computational program. From equation 1 it can be derived that

$$\text{Abs}_{313} = k_3 \cdot \left(e^{-k_{1\text{obs}}t} - e^{-k_{2\text{obs}}t} \right) + k_4 \quad (\text{Equation 2})$$

Here Abs_{313} is the absorption at 313 nm, k_3 and k_4 are constant values to fit the equation and $k_{1\text{obs}}$ and $k_{2\text{obs}}$ are the observed pseudo first-order rate constants for p-quinodimethane formation and solvent substitution respectively.

The absorbance at 313 nm originating from the p-quinodimethane system is proportional to its concentration according to Beer's law ($A = \epsilon \cdot c \cdot d$). Hence it is not necessary that the exact concentration of the products is known. Only the change in a proportional physical constant has to be observed.

For the kinetic measurements pseudo-first order conditions were used throughout the study of the p-quinodimethane formation reactions. A solution of the monomer was prepared (10^{-4} M) and four base solutions were prepared. Both monomer and base solution were brought in a stop flow module and mixed together whereupon the UV-Vis detection at λ_{max} of the p-quinodimethane signal was started. A typical trace is observed for every case: the absorption rapidly rises and the decrease of the signal is somewhat slower (Figure 11). The different traces were analyzed by means of a non-linear least-squares method, where k_1 and k_2 were used as unknown parameters to fit the equation 2.

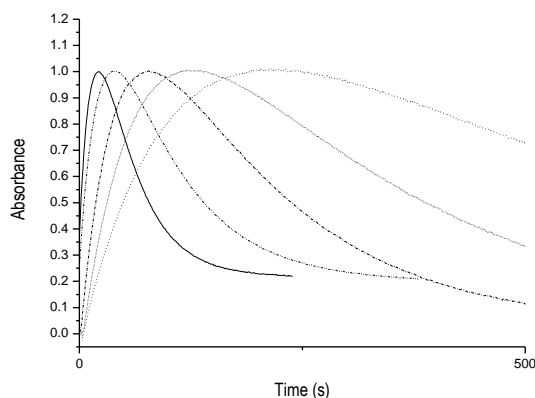


Figure 11. Plots of p-quinodimethane signal of monomer 1 at increasing base concentrations

Excellent correlation factors (> 0.999) were obtained for every run. Measurements were performed at least three times to ensure good reproducibility. In table 6 the observed rate

constants of the different monomers are depicted. To obtain the absolute rate constant for the p-quinodimethane formation the observed k_{obs} values were plotted versus the different base concentrations (figure 12) to yields straight lines with acceptable correlation and the slope of the line was determined as the second order rate constant k_2 . The values of the absolute rate constant are depicted in table 7.

[Base] (10^{-4}M)	$k_{1\text{obs}} (\times 10^{-2} \text{ s}^{-1})$		
	Monomer 1	Monomer 2	Monomer 3
4.03	0.571 ± 0.027	0.961 ± 0.018	11.039 ± 0.706
10.08	1.107 ± 0.041	1.588 ± 0.058	22.162 ± 2.655
20.16	1.815 ± 0.024	2.340 ± 0.124	41.949 ± 3.301
40.33	3.258 ± 0.296	4.343 ± 0.314	75.661 ± 4.669

Table 6. $k_{1\text{obs}}$ values at different base concentrations

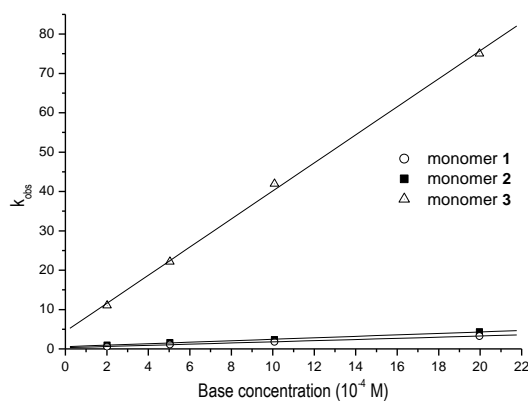
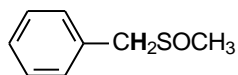


Figure 12. Plot of the observed pseudo first-order rate constant versus different base concentrations

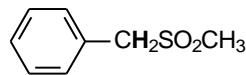
	$k_1 (\text{mol}^{-1} \text{ s}^{-1})$	R
Monomer 1	0.07313 ± 0.00179	0.9994
Monomer 2	0.09221 ± 0.00342	0.9986
Monomer 3	1.78238 ± 0.04683	0.9993

Table 7. First-order rate constants for monomers 1-3

These kinetic data reveal that the nucleofugal properties of the leaving group have not that much influence on the reaction rate. The reaction rate of the bromo analogue is only 1.26 times the value of the chloro analogue. However changing the polariser from a sulfoxide to a sulfon gives rise to a large increase of the reaction rate since the rate constant for monomer **3** is 24 times the rate constant for monomer **1**. Apparently, the change in pK_a value of the benzylic proton next to the polariser has a major effect on the reaction rate. The pK_a value of the two derivatives was not determined but literature data may give us an indication. The pK_a value of a benzylic proton next to a sulfinyl group is 29 in DMSO, whereas the pK_a of a benzylic proton next to a sulfonyl group is 25.4 in the same solvent.



$pK_a = 29$



$pK_a = 25.4$

Hence the deprotonation of the benzylic position is assumed to be the rate-determining step in the reaction process. Combining these two effects (leaving group and polariser) we conclude from the data in table (overview of elimination reactions) that the mechanism through which *p*-quinodimethane formation occurs in 2-butanol is an irreversible E_{1cb} mechanism where stabilizing effects of the anion have a major effect on the reaction rate. Literature data indicate that for an E_2 elimination reaction the ratio of the rate constants for a bromine/chlorine atom as the leaving group is in the order of 25 or more and that there can be a little influence of the leaving group on the reaction rate in an irreversible E_{1cb} mechanism¹⁴. This effect can in some cases be explained by hyper-conjugation. The existence of a reversible E_{1cb} reaction is also excluded since there is no large effect of the leaving group.

So it is concluded that the lower the pK_a i.e. the better the anion is stabilized, the faster the reaction occurs. Electron withdrawing groups on the phenyl core hence should increase the reaction rate whereas electron donating substituents should have the opposite effect. They slow down the reaction. These consequences of the mechanism were already nicely demonstrated through the qualitative measurements.

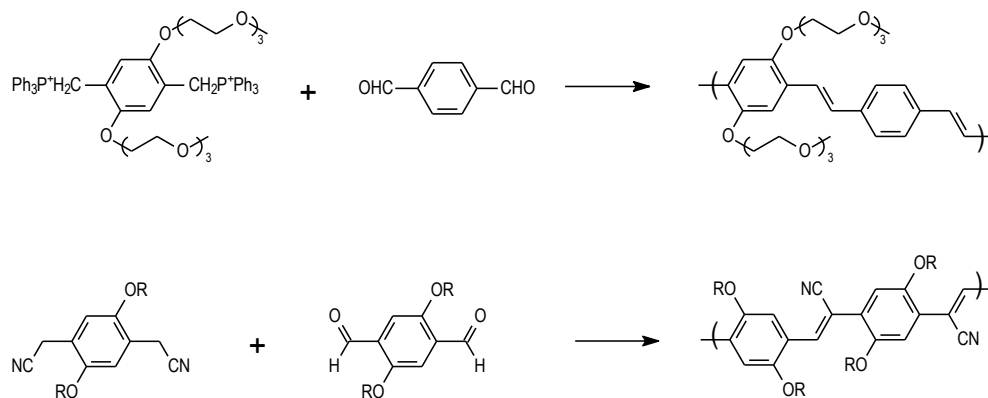
5. Copolymerisations of different p-quinodimethane systems

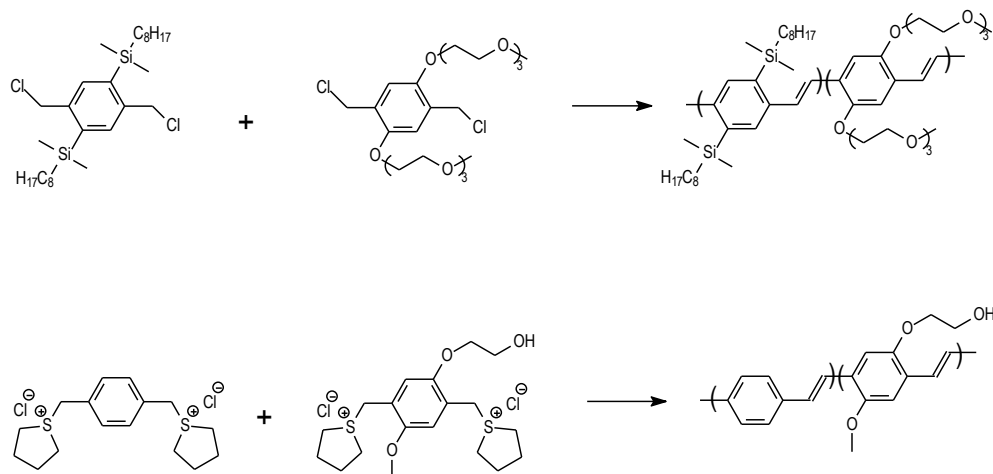
As mentioned earlier in this chapter, the kinetic data obtained from a mechanistic study on p-quinodimethane formation are of major interest to predict the outcome of copolymerisation reactions involving two or more monomers with different p-quinodimethane formation rates. In an extreme case one might end up with a mixture of two homopolymers, because the quinodimethane system of one monomer will be totally consumed before an appreciable amount of the other p-quinodimethane system has been formed.

At present, PPV copolymers are frequently used for tuning the physical and chemical properties of conjugated polymers. Combining different homopolymers in one copolymer may result in new polymers mostly with properties intermediate to the corresponding homopolymers.

Wittig¹⁵ and Knoevenagel¹⁶ stepwise polycondensation reactions have been used frequently in the synthesis of PPV copolymers. Here however the double bond is generated during the reaction, which may cause low molecular weight polymers because of the limited solubility of the conjugated chain. One way to circumvent this problem is to implant long aliphatic chains on the polymer backbone to keep it soluble or to alternate insoluble conjugated fragments with soluble non-conjugated ones.

A totally different approach to synthesise PPV copolymers is through a precursor route.





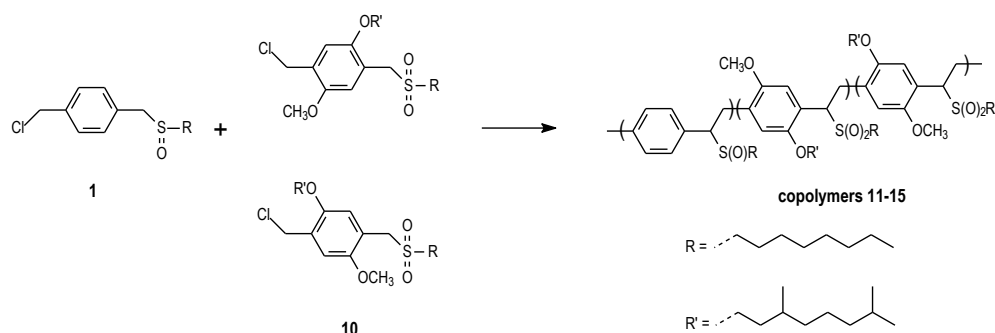
Scheme 9. Different procedures for obtaining PPV derived copolymers

Holmes *et al.* reported on the synthesis of various copolymers via the Gilch precursor route¹⁷. Different monomers were incorporated in the same copolymer to obtain polymers with higher electron affinity, higher photoluminescence efficiency and tuneable optical properties. In all these cases high molecular weight statistical copolymers were obtained and the conjugated structure was generated *in situ* by adding an excess of base to the polymerisation reaction. Long aliphatic side chains were essential to keep the conjugated polymers soluble. Copolymerisation reactions according to the Wessling route were intensively studied by Ayagosh¹⁸ *et al.* The insoluble alcohol and carboxylic acid functionalised homopolymers became soluble upon copolymerisation with the normal PPV monomer.

5.1. Copolymerisation of OC₁C₁₀-sulfon with PPV sulfoxide

Previous work on copolymerisation reactions within our research group was performed by Stijn Gillissen¹⁹. Three different sulfinyl PPV derived monomers were copolymerised in 1,4-dioxane and the exact monomer ratio was determined through ¹H and quantitative ¹³C NMR spectroscopy. For all copolymerisation pairs the same trends were clear. The monomer with the lowest pK_a value of the benzylic sulfinyl position is built in relatively more than the other

monomer. For each pair of comonomers this trend was noticed. The pyridine monomer is built in more than OC₁C₁₀ or normal PPV, which on its turn is built in more than OC₁C₁₀. Here we present some additional information for tuning the monomer composition of the copolymers. Therefore a set of copolymerisations was planned between the OC₁C₁₀ sulfonyl monomer **10** and the unsubstituted sulfinyl PPV monomer **1** (scheme 10).



Scheme 10. Overview of the copolymerisation reactions

Copolymerisation reactions were performed using the standard procedure and copolymerisation results are shown in table 8. GPC measurements were performed in THF versus polystyrene standards. Although there is no clear trend noticeable between the different molecular weights, high molecular weight polymers are obtained in all polymerisations. ¹H-NMR deconvolution analysis revealed the exact copolymer composition. When increasing the amount of PPV monomer in the comonomer feed, the signal at 5 ppm of the OC₁C₁₀ sulfon homopolymer is split up with a second signal at a higher field. The relative amount of this second signal increases as the amount of PPV monomer is increased.

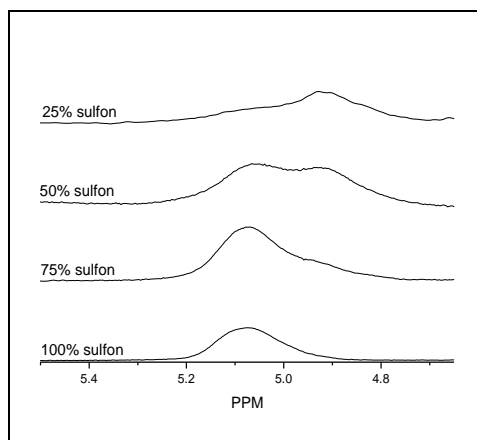


Figure 13. Enlarged ^1H -spectra of polymer **11** and copolymers **12**, **13**, and **14**.

Compared to the copolymerisation reactions performed by Gillissen, the sulfonyl OC_1C_{10} monomer is built in relatively more than the sulfinyl OC_1C_{10} monomer (figure 14). Hence we can conclude that the pK_a of the benzylic positions also for these systems has a major effect on the p-quinodimethane formation and hence on the outcome of the copolymerisation reaction. Chemical modifications on the monomer stage allow the researcher to change the reactivity towards p-quinodimethane formation, which is an excellent tool for altering the copolymers composition.

Entry	Polymerisation				PD	Copolymer			
	OC_1C_{10}	PPV	yield mg	M_w ($\times 10^{-3}$)		OC_1C_{10}	PPV	λ_{max}^a (nm)	λ_{max}^b
11	100	0	271	150	3.80	100	0	447	/
12	75	25	274	170	4.49	78	22	413	352
13	50	50	254	138	3.51	46	54	409	369
14	25	75	372	142	3.49	33	66	404	399
15	0	100	342	162	4.32	0	100	410	410

Table 8: Copolymerisation results of PPV sulfoxide and OC_1C_{10} sulfon. GPC was taken in THF versus polystyrene standards ^a: Maximum wavelength achieved at 291°C, ^b: maximum wavelength achieved at 170°C.

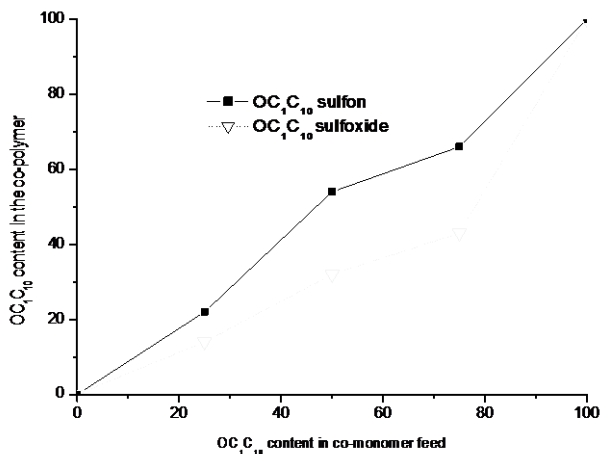


Figure 14. Percentage of the OC₁C₁₀ monomer built into the copolymer versus its percentage in the initial monomer feed for the sulfinyl (dotted) and sulfonyl (solid) monomer.

5.2. Elimination behaviour of the copolymers

The elimination behaviour of the different co- and homopolymers was studied using in situ UV-Vis spectroscopy. UV-Vis spectroscopy measurements were carried out on film, spin-coated on quartz discs. A specially designed oven containing the precursor polymer spincoated on the quartz disk was placed in the beam of the spectrometer. A dynamic heating program of 2 °C/min up to 350°C, under a continuous flow of nitrogen, was used. Before heating, all the precursor polymers show a strong absorption below 250 nm. As the heating program progresses, new absorption bands appear that gradually redshift with increasing temperature. Finally the maximal conjugated polymer with an absorption maximum around 410 nm is obtained. When the absorption at the maximum wavelength of each one of the copolymers is plotted versus temperature, the elimination and stability behaviour of the different polymers becomes clear. (Figure 15).

For the OC₇C₁₀-sulfon homopolymer **11** elimination only starts at around 200°C. At 291°C the maximum absorption is obtained. After this temperature a strong decline is observed in the absorbance due to total degradation of the conjugated polymer. For the three copolymers the elimination is a two-step process. The first elimination is due to the expulsion of the sulfinyl groups and it starts at 69°C. In the interval between 120°C and 200°C a more or less constant absorption value is obtained. This first step in the elimination process is in total accordance with the elimination behaviour of the sulfinyl precursor homopolymers. At 200°C the second elimination process due to expulsion of the sulfonyl groups takes place. For all the copolymers a maximum absorption is obtained at 291°C followed by the same degradation behaviour mentioned for the sulfonyl homo-polymer.

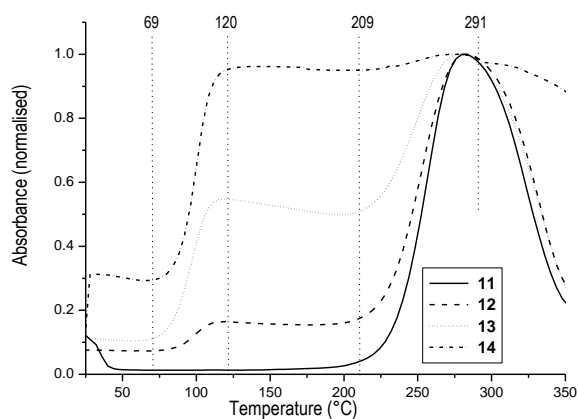


Figure 15. Absorption at λ_{max} nm versus temperature.

From the elimination data it is concluded that indeed a random copolymer was formed in the polymerisation reaction and that there is no occurrence of homopolymerisation in these reactions. In table 8 the maximum wavelength of the three copolymers **12**, **13** and **14** at 170°C is depicted, which is after the sulfinyl expulsion and before the sulfonyl elimination. It is well understood from these observations that there is no formation of the sulfinyl homopolymers since no signal at 410 nm is observed. The value of the maximum absorption at 170°C also decreases as the amount of sulfonyl monomer is increased due to defects interrupting the effective conjugation length.

6. Conclusions

Due to its chemical differentiation the sulfinyl precursor route has proven to be a very versatile route to study p-quinodimethane formation of different monomers. From the quantitative kinetic data some mechanistic conclusions could be drawn and the elimination mechanism towards p-quinodimethane formation was assumed to be an irreversible E_{1cb} mechanism where proton abstraction is the rate determining step in the process. The qualitative data support the evidence for such mechanism.

The fundamental mechanistic conclusions were tested on a set of copolymerisation reactions involving two different monomers with different reactivity towards p-quinodimethane formation. Altering the pK_a of the monomer through a chemical modification increases its amount in the eventual copolymer. Hence the sulfinyl precursor route is a very appropriate tool for adapting the polymer composition and to alter its properties in a well defined manner.

7. Experimental part

All chemicals were purchased from Aldrich or Acros and used without further purification unless otherwise stated. 1,4-Dioxane was distilled over sodium/benzophenone prior to use. NMR spectra were recorded in $CDCl_3$, on a Varian VXR300 spectrometer. Chemical shifts (δ) are given in ppm relative to the residual $CHCl_3$ absorption (7.24 ppm). Molecular weights and molecular weight distributions were determined relative to polystyrene standards (Polymer Labs) by Size Exclusion Chromatography (SEC). Chromatograms were recorded on a Spectra series P100 (Spectra Physics) equipped with two MIXED-B columns (10 μm , 2 x 30 cm, Polymer Labs) and a refractive index (RI) detector (Shodex) at 70 °C. A THF solution is used as the eluent at a flow rate of 1.0 ml/min. Toluene is used as flow rate marker.

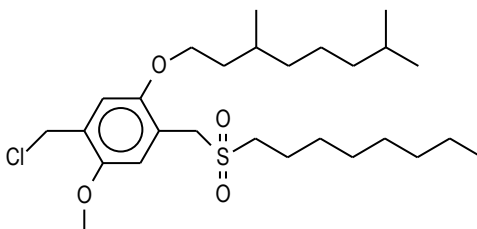
Ultraviolet visible spectroscopy (UV-Vis) was performed on a CARY 500 UV-VIS-NIR spectrophotometer (interval: 1 nm, scan rate: 600 nm/min, continuous run from 200 to 700 nm). The precursor polymer was spin-coated from a chloroform solution (6 mg/ml) onto quartz glass (diameter 25 mm and thickness 3 mm) at 700 rpm. The quartz glass was heated in the same Harrick oven high temperature cell as was used in the FT-IR

measurements. The cell was placed in the beam of the UV-Vis spectrophotometer and spectra were taken continuously. The heating rate was 2°C/minute up to 450°C. All measurements were performed under a continuous flow of nitrogen. Scanning kinetics software was used to investigate the regions of interest.

For the qualitative UV-Vis measurements on the different *p*-quinodimethane systems a CARY 500 UV-VIS-NIR spectrophotometer was used equipped with a stop-flow module allowing very fast measurements. A 10⁻⁴ M solution of the different monomers in 2-butanol and a 10⁻³ M solution of sodium *t*-butoxide in the same solvent were prepared and both solutions were injected simultaneously whereupon the monitoring of the signals of interest was started. For the quantitative kinetic measurements the base solutions were prepared from a stock solution. Both monomer and base solutions were degassed by nitrogen flushing. The obtained data were fitted using a non-linear least-squares method using the program Kaleidagraph 3.0 for Macintosh computer.

Monomers **4-8** were synthesised according to a procedure described elsewhere^{19,20}.

1-Chloromethyl-5-(3,7-dimethyl-octyloxy)-2-methoxy-4-(octane-1-sulfonylmethyl)-benzene and 1-chloromethyl-2-(3,7-dimethyl-octyloxy)-5-methoxy-4-(octane-1-sulfonylmethyl)-benzene



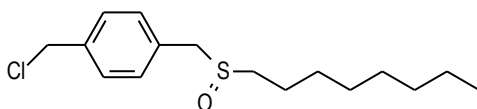
Octane thiol (11.46 g, 78.4 mmol) and sodium tertiary butoxide (7.54 g, 1 equivalent) are dissolved in methanol (150ml) and stirred at room temperature for one hour. This solution is added dropwise to the bisulfonium salt (46.5 g, 1 equivalent) in 250 ml methanol. The resulting solution is stirred for another hour and neutralized if necessary. The solvent is evaporated and *n*-octane is added and evaporated again to remove the THT. This procedure is repeated three times. The residue is dissolved in chloroform and extracted with water. After drying over magnesium sulfate the desired compound is obtained as a yellowish oil (30 g) in a 1/1 ratio of both isomers, yet contaminated with small amount of dichloride

and dithioether. To the crude mixture of the sulfanyl isomers in 300 ml 1,4-dioxane is added TeO_2 (1.5 g, 5 mol%) and H_2O_2 (19 g, 2 equivalents). A few drops of concentrated HCl are added to catalyze the reaction. The progress of the reaction is followed on TLC and when all thioether is disappeared 300 ml of brine is added to stop the reaction. Extraction with chloroform, drying over magnesium sulfate and column purification with hexanes/ethylacetate as the eluent yields the sulfoxide as a yellow oil (60% overall yield starting from the bissulfonium salt).

A 1/1 mixture of 1-chloromethyl-5-(3,7-dimethyl-octyloxy)-2-methoxy-4-(octane-1-sulfinylmethyl)-benzene and 1-chloromethyl-2-(3,7-dimethyl-octyloxy)-5-methoxy-4-(octane-1-sulfinylmethyl)-benzene is dissolved in 200 ml dichloromethane and portionwise is added *m*-chloroperbenzoic acid 70% (6.6 g, 1.5 equivalents). The reaction is stirred at room temperature until all sulfoxide has disappeared. Then the reaction is poured into water and extracted with chloroform and dried over magnesium sulfate. A column purification with chloroform as the eluent yields the pure sulfon regioisomers in a 1/1 ratio as a yellow oil (6.4 g, 95%)

$^1\text{H-NMR}$ (300MHz, ppm, CDCl_3): 6.97-6.99-7.00 (s, 2H), 4.64-4.65 (2s, 2H), 4.29-4.30 (2s, 2H), 4.02 (m, 2H), 3.85-3.86 (2s, 2H), 2.81 (m, 2H), 1.49-1.88 (m, H), 1.27-1.35 (m, H), 0.97 (m, H), 0.88 (m, H)

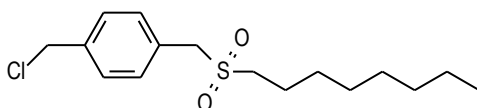
1-Chloromethyl-4-(octane-1-sulfinylmethyl)-benzene 1



A solution of octane thiol (1.46 g, 0.01 mol) and sodium *t*-butoxide (0.96 g, 1 equivalent) in 20 ml methanol is stirred for one hour at room temperature. This solution is added dropwise to a stirred solution of bissulfonium salt (3.8 g, 1 equivalent) in 50 ml methanol and the resulting mixture is stirred for two hours at room temperature. After neutralizing the solution with HCl 1M, the solvent is evaporated and *n*-octane is added and evaporated again to remove the THT. This procedure is repeated three times. The residu is dissolved in chloroform and extracted with water. Drying over magnesium sulfate and evaporation of the solvent yields the crude thioether, which is used furtheron without purification. To 1-

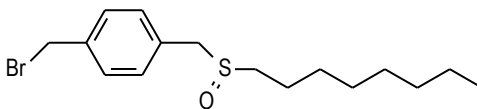
chloromethyl-4-(octane-1-sulfinylmethyl)-benzene (1.6 g, 0.005 mol) in 50 ml methanol is added TeO_2 (40 mg, 5 mol %) and H_2O_2 (0.97 g, 2 equivalents). A few drops of concentrated HCl are added to catalyze the reaction. The progress of the reaction is followed on TLC and when all thioether is disappeared, 50 ml of brine is added to stop the reaction. Extraction three times with chloroform, drying over magnesium sulfate and a column purification with ether/methanol as the eluent yields the sulfoxide as a white solid. Recrystallisation from hexane/dichloromethane yields the product as white crystals. (1.32 g, 79%) $^1\text{H-NMR}$ (300 MHz, δ , ppm, CDCl_3): 7.38+7.28 (dd, 2H), 4.57, (s, 2H), 4.11+3.98 (dd, 2H), 3.92+3.84 (m, 2H), 3.64 (m, 2H), 3.61 (m, 2H), 3.51 (m, 2H), 3.33 (s, 3H), 2.90+2.70 (m, 2H).

1-Chloromethyl-4-(octane-1-sulfonylmethyl)-benzene 3



1-Chloromethyl-4-(octane-1-sulfinylmethyl)-benzene (6.8 g, 0.022 mol) is dissolved in 200 ml dichloromethane and portionwise is added *m*-chloroperbenzoic acid 70% (5.64 g, 1.5 equivalents). The reaction is stirred at room temperature until all sulfoxide has disappeared on TLC. Then the reaction is poured into water and extracted with chloroform and dried over magnesium sulfate. A column purification with chloroform as the eluent yields the pure sulfon as a white solid (6.51 g, 88%). Recrystallisation from dichloromethane/hexanes gives the pure compound as white needles. $^1\text{H-NMR}$ (300 MHz, δ , ppm, CDCl_3): 7.40 + 7.37 (dd, 4H), 4.57 (s, 2H), 4.19 (s, 2H), 2.80 (t, 2H), 1.80 (m, 2H), 1.38-1.23 (m, 10H), 0.85 (t, 3H). Mass (DIP/CI): 317-319 ($\text{M}^+ + 1$), 283, 139

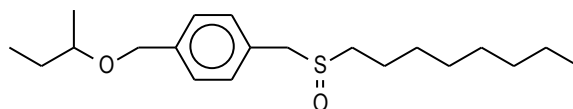
1-Bromomethyl-4-(octane-1-sulfinylmethyl)-benzene 2



1-Chloromethyl-4-(octane-1-sulfinylmethyl)-benzene (0.5 g, 1.6 mmol) is dissolved in 40 ml 3-pentanone. Lithium bromide (10 equivalents) is added and the mixture is stirred for four

hours at reflux. After cooling the solution to room temperature, 100 ml water is added and the aqueous layer is extracted three times with dichloromethane. The organic phase is dried over magnesium sulfate and evaporated to yield the bromide as a white solid (5.2 g, 90%)
¹H-NMR (300 MHz, δ , ppm, CDCl₃): 7.38+7.28 (dd, 2H), 4.46, (s, 2H), 4.11+3.98 (dd, 2H), 3.92+3.84 (m, 2H), 3.64 (m, 2H), 3.61 (m, 2H), 3.51 (m, 2H), 3.33 (s, 3H), 2.90+2.70 (m, 2H).

1-s-Butoxymethyl-4-octylsulfinylmethylbenzene



1-Chloromethyl-4-(octane-1-sulfinylmethyl)-benzene (10 mg, 31 μ mol) is dissolved in 10 ml 2-butanol and the mixture is stirred at room temperature. Then a solution of sodium *t*-butoxide (16 mg, 5 equivalents) in 10 ml 2-butanol is added and the resulting mixture is stirred for one more hour. the mixture is poured into 50 ml water and extracted with dichloromethane. After evaporation the fraction was analyzed with mass spectroscopy (chemical ionisation).

Mass (DIP/CI): 339 (M+1), 265 (M-2-BuO), 177 (M -SO-octyl)

Copolymerisations of sulfonyl OC₁C₁₀ and sulfinyl *n*-octyl PPV

All precursor copolymers **11-15** were synthesised according to a general procedure. The molar monomer feed ratios of the copolymerisations were 100/0, 75/25; 50/50; 25/75 and 0/100. Solutions of the monomers (8 mL, 0.14 M) and base (Na-*t*-BuO, 5.8 mL, 0.34 M) were prepared and degassed for 1 hour by a continuous flow of nitrogen at 30 °C. The base solution was added in one portion to the stirred monomer solution. During the reaction the temperature was maintained at 30 °C and the passing of nitrogen was continued. After 1 hour the reaction mixture was poured into well-stirred ice water whereupon the polymer precipitated. The water layer was extracted with chloroform to ensure that all polymer and residual fraction was collected, and the combined organic fractions were concentrated *in vacuo*. The polymer was precipitated in ether/hexanes or methanol, depending on the copolymer composition, collected by filtration and dried *in vacuo*.

The precursor polymers were precipitated in MeOH and GPC was performed with THF as eluent. The exact copolymer composition was determined using a deconvolution program on the signal around 5 ppm, which is assigned to the benzylic proton next to the sulfonyl group. The comonomer ratios in the copolymer and GPC results are viewed in table 8.

¹H-NMR (300 MHz, δ , ppm, CDCl₃): Copolymer **11**: 7.0, 6.6-6.0, 5.0, 3.8-3.0, 2.4, 1.6, 1.2, 0.8/ Copolymer **12**: 7.0, 6.6-6.0, 5.0-4.9, 3.8-3.0, 2.4, 1.6, 1.2, 0.8/ Copolymer **13**: 7.4, 7.0-6.3, 5.0-4.9, 3.8-3.0, 2.4, 1.6, 1.2, 0.8/ Copolymer **14**: 7.4, 6.9, 4.9, 3.6-2.2, 1.6, 1.2, 0.8

8. References

- ¹ *Fundamentals of Analytical Chemistry*, Skoog, West en Holler, 7th Ed., Saunders College Publishing, 1996.
- ² *Chemical reactor theory: an introduction*. Denbigh, K.G.; Turner, J.C.R.; Cambridge University Press, Great Britain, **1971**, p 30.
- ³ *Mechanisms and theory in organic chemistry*, 3rd ed.; Lowry T.H., Richardson K.T. Eds.; Harper and Row publisher, New York, **1987**; p 592.
- ⁴ a) Cho, B. R.; Kim, Y. K.; Han, M. S. *Macromolecules* 31, **1998**, 2098. b) Cho, B. R.; Kim, T. H.; Kim, Y. K.; Kim, N. S. *Macromolecules* 32, **1999**, 3583. c) Cho, B. R.; Kim, T. H.; Son, K. H.; Kim, Y. K.; Lee, Y. K.; Jeon, S.-J. *Macromolecules* 33, **2000**, 8167. Cho, B. R. *Prog. Polym. Sci.* 27, **2002**, 307.
- ⁵ Hsieh, B.R.; Yu, Y.; Van Laeken, A.C.; *Macromol.*, 30, **1997**, 8094. Yu, Y.; Van Laeken, A.C.; Lee, H.; Hsieh, B.R.; *Polym. Prepr.*, 39, **1998**, 161. Hsieh, B.R.; Yu, Y.; Forsythe, E.W.; Schaaf, G.M.; Feld, W.A.; *J. Am. Chem. Soc.*, 120, **1998**, 231. Neef, C.J.; Ferraris, J.P.; *Macromol.*, 33, **2000**, 2311.
- ⁶ Issaris Anna, *PhD dissertation*, Diepenbeek, **1997**.
- ⁷ Van Breemen Albert, *PhD dissertation*, Diepenbeek, **1998**.
- ⁸ Gillissen Stijn, *PhD dissertation*, Diepenbeek, **2002**.
- ⁹ Paptai, S. *The chemistry of Sulphones and Sulphoxides*, John Wiley & Sons Ltd., Chichester, UK, **1988**.
- ¹⁰ Issaris Anna, *PhD dissertation*, Limburgs Universitair Centrum, Diepenbeek, **1997**.
- ¹¹ Guggenheim, E.A., *Philos. Mag.*, 2, **1926**, 538.
- ¹² Lafis, S.; Konidari, C.N.; Veltsistas, P.G.; Tzerpos, N.; Karayannis, M.I., *International journal of chemical kinetics*, **1997**, 29, 385.
- ¹³ Cai; Liu; Ma; Wu, *The analyst*, 124, **1999**, 751. Reich, L; *Thermochimica acta*, 293, **1997**, 179.

Chapter 4

¹⁴ *The chemistry of the double bonded functional groups*, Patai, S; JW and Sons Ltd, Manchester, **1988**.

¹⁵ Huang, C.; Huang, G. ; Guo, J.; Huang, W.; Kang, E.T.; Yang, C.Z. *Polymer preprints*, 43, **2002**, 574.

¹⁶ Greenham, N.C. ; Moratti, S.C. ; Bradley, D.D.C. ; Friend, R.H. ; Holmes, A.B. , *Nature*, 365, **1993**, 628.

¹⁷ Morgado, J.; Cacialli, F.; Friend, R. H.; Chuah, B. S.; Rost, H.; Holmes, A. B. *Macromolecules* 34, **2001**, 3094.

¹⁸ Ajayaghosh, A.; George, S.J. *J. Am. Chem. Soc.*, 123, **2001**, 5148.

¹⁹ Gillissen, S.; Motmans F. *et al.*, submitted for publication.

²⁰ Gillissen S.; Jonforsen, M.; Kesters, E.; Johansson, T.; Theander, M.; Andersson, M. R.; Inganas, O.; Lutsen, L.; Vanderzande D. *Macromolecules* 34, **2001**, 7294. Henckens Anja, *PhD dissertation*, Diepenbeek, **2003**. Van Der Borght Michael, *PhD dissertation*, Diepenbeek, **1998**.

²¹ Winey, D.A. ; Thornton, E.R. ; *J. Am. Chem. Soc.*, 97, **1975**, 3102. Cho, B.R. ; Choon-Ock, M.Y. ; Song, K.S. ; *Tetrahedron Lett.*, 36, **1995**, 3193.



Summary

In Chapter 1 a general introduction on conjugated polymers and more specifically on poly-(para-phenylene vinylene) or PPV and its derivatives is presented. Different synthetic routes, all with their main properties and advantages, are described. Possible applications for these materials, such as light emitting diodes, photovoltaic cells and (bio)sensors are mentioned as well. The need for functional conjugated polymers is also expressed in the aim of the thesis.

Chapter 2 deals with the synthesis and characterisation of some functional sulfinyl precursor polymers. The four different functional groups are a triethylene glycol derived chain, an alcohol function, an ester and a sulfonate salt. The functional groups are placed on the sulfinyl tail, which means that they will not be present in the conjugated analogues of the precursors. For the synthesis of the monomers some adaptations had to be made to the standard procedure for monomer synthesis because these normal conditions gave only very low yields of the desired thioethers. Diluting ten times versus the standard conditions gave the thioether in a high yield with no occurrence of the unwanted Wessling polymerisation. The polymerisation reactions of the different monomers were performed according to a standard procedure to afford the precursor polymer in high yield. This was true for the oligoethylene oxide monomer. The alcohol monomer gave an insoluble polymer due to strong hydrogen bonding. For the ester monomer, no polymerisation occurred but an E_{1cb} elimination mechanism was found to explain this lack of polymerisation. Also the compatibility of the ester function with a sulfinyl group was demonstrated. Unlike the problems with solubility, the elimination behaviour of all precursor polymers was studied using different in situ techniques that are in good accordance with another. The experiments prove the possibility of synthesis of the functional PPV derivatives if some precautions are taken into account. The knowledge obtained from Chapter 2 will be of major use for the synthesis of the monomers and polymers described in Chapter 3.

In Chapter 3 is dealt with the synthesis of some sulfinyl monomers with a functional group on the phenyl core of the monomer and thus on the polymer backbone. This feature implies, in contrast to the monomers described in Chapter 2, that the functionalities will still be

Summary

present in the conjugated PPV derivatives. The functional groups introduced in this chapter are analogous to the groups in the previous chapter. The oligo-ethylene oxide group is present in two different monomers with one and two of such tails respectively. The second functionality is the alcohol group. Also the ester group was implanted on the phenyl core and some attempts were made to synthesise the sulfinyl monomer with a sulfonate group. Again for the synthesis of these monomers dilution of the standard conditions was necessary to obtain the monomers in high yield. The polymerisation reactions were performed according to the standard procedure to yield the precursor polymers in high yield and with a high molecular weight in every case. The influence of the solvent was tested for one monomer revealing that 2-butanol indeed is the appropriate solvent for the polymerisation reactions. The conversion step of the different precursor polymers was again studied using the same analytical in situ techniques as in Chapter 2. Different experiments demonstrated a very pronounced thermochromic effect for each of the polymers. After conversion of the alcohol precursor polymer, an insoluble conjugated polymer was obtained. This is in accordance to the observations done for the alcohol polymer in Chapter 2. To circumvent this solubility problem some copolymerisation reactions were performed, yielding a soluble conjugated polymer after conversion. The conjugated ester polymer can be hydrolysed to the corresponding carboxylic acid using basic conditions. This function allows the possibility of post-polymerisation functionalisation reactions. Reduction of the ester function towards an alcohol results in an insoluble polymer due to hydrogen bonding. In conclusion the sulfinyl precursor route has proven its versatility throughout this chapter allowing the synthesis of a broad range of PPV derivatives with different functional groups. In a second part (Chapter 4), a kinetic and mechanistic study is performed on the *p*-quinodimethane formation through the sulfinyl precursor route. The kinetics of several monomers, all differing concerning their polariser, their leaving group or their aromatic moiety were studied in both a quantitative and a qualitative approach using UV-Vis spectroscopy, since this technique allows to monitor the formation and decrease of the *p*-quinodimethane system in a very straightforward manner. From the quantitative UV-Vis data some kinetic evidence was found for the mechanistic features of the *p*-quinodimethane formation. It was found that the elimination reaction from the monomer was an irreversible E_{1cb} mechanism where the rate-determining or rate-limiting step is the base induced proton abstraction to yield a carbanion which expels a leaving group towards the *p*-quinodimethane

structure. The results obtained from the qualitative measurements are in very good accordance and they support the presented mechanism. All factors that enhance the acidity of the proton next to the polariser increase the *p*-quinodimethane formation rate significantly. On the contrary the factors that lower this acidity, decrease the formation rate. The kinetic and mechanistic data are of major interest to predict or to adapt the outcome of copolymerisation reactions involving two monomers with different *p*-quinodimethane formation rates. This hypothesis was proven by performing some copolymerisation reactions involving two monomers that differ in acidity of the benzylic proton to a large extent. The results of these reactions is in accordance with the fundamental results obtained from the UV-Vis studies. Compared to earlier results in our research group a larger amount of a certain monomer will be present in the copolymer if the acidity of the benzylic position is enhanced, in our case the sulfinyl group was replaced by a sulfonyl group. The resulting copolymers were analysed through various analytical techniques and the conversion towards the conjugated structure showed some interesting features. The sulfinyl and sulfonyl group are expelled at different temperatures that are well separated from another. In this way a selective conversion can be achieved.

Samenvatting

In hoofdstuk 1 wordt een algemene inleiding geschetst omtrent geconjugeerde polymeren en meer in het bijzonder over poly-(*p*-vinyleen fenyleen) en de afgeleide producten hiervan. Er worden verschillende synthesepaden beschreven, elk met zijn specifieke eigenschappen, voor- en nadelen. Er worden tevens enkele mogelijke toepassingen voor zulke materialen beschreven zoals polymere LEDs, LECs, zonnecellen en (bio)sensoren.

Hoofdstuk 2 handelt over de synthese en karakterisering van een aantal sulfinyl precursorpolymeren. Vier verschillende functionele groepen worden aangehaald: een oligo-ethyleenoxidegroep, een alcoholfunctie, een ester en een sulfonaatzout. Deze functionele groepen bevinden zich op de sulfinylstaart, hetgeen betekent dat ze niet meer aanwezig zullen zijn in de overeenkomstige geconjugeerde materialen. Voor de synthese van de gefunctionaliseerde monomeren werden er enkele aanpassingen aangebracht aan een reeds bestaande standaardprocedure die in onze onderzoeksgroep werd ontwikkeld. Het gebruik van de originele standaardprocedure resulteerde in de vorming van ongewenst Wesslingpolymeer en derhalve zeer lage rendementen voor de reactie tot de benodigde thioëtherverbindingen. Wanneer er echter in een tienvoudige verdunning werd gewerkt, kon het thioëther in hoog rendement afgezonderd worden, terwijl de Wesslingpolymerisatie volledig werd teruggedrongen. De eigenlijke polymerisatie van de monomeren werd volgens een standaardprocedure uitgevoerd waardoor het precursorpolymeer in hoog rendement bekomen werd. Dit bleek inderdaad waar voor de oligo-ethyleenoxideverbinding. De polymerisatiereactie van het alcoholmonomeer leverde echter een onoplosbaar polymeer op door de aanwezigheid van sterke waterstofbruggen. Bij het estermonomeer bleek geen polymerisatie tot precursorpolymeer mogelijk en een E_{1cb} -mechanisme werd voorgesteld om dit gebrek te verklaren. Tevens werd de compatibiliteit van een esterfunctie met een sulfinylgroep aangetoond. Ondanks de oplosbaarheidsproblemen met sommige polymeren werd toch het eliminatiegedrag van de verschillende materialen bestudeerd met enkele in situ technieken waarvan de verschillende resultaten grote gelijkenissen vertonen. Desalniettemin tonen de beschreven experimenten aan dat de synthese van functionele

Samenvatting

PPV derivaten mogelijk is mits in achtname van enkele voorzorgen. De kennis die verworven werd gedurende het werk in hoofdstuk 2 was van groot nut voor de synthese van de monomeren en polymeren die in hoofdstuk 3 zullen beschreven worden.

In hoofdstuk 3 zullen we de synthese bespreken van enkele sulfinylmonomeren die een functionele groep bezitten op de fenyalkern van het monomeer en derhalve ook op deze van de polymeer backbone. Dit houdt in dat, in tegenstelling tot de monomeren en polymeren beschreven in hoofdstuk 2, de functionele groepen nog steeds aanwezig zullen zijn in het uiteindelijk geconjugeerde materiaal. De functionele groepen die in dit hoofdstuk ingevoerd worden, zijn analoog aan deze uit hoofdstuk 2. De oligo-ethyleenoxidegroep is aanwezig in twee verschillende monomeren, hetzij met één respectievelijk twee van zulke staarten. Een tweede functionele groep die hier besproken werd is de alcoholfunctie. Ook werd een estergroep ingeplant op de fenyling en werden er enkele vergeefse pogingen ondernomen om een sulfonaatgroep in te voeren op het monomeer. Voor de synthese van de monomeren in hoofdstuk 3 werd ook gebruik gemaakt van de verdunde reactieomstandigheden vergeleken met de gekende standaardprocedure. Dit was nodig om een hoog rendement te verkrijgen in de thioëthersynthese. De polymerisatiereacties werden uitgevoerd volgens een gekende standaardprocedure hetgeen een hoog rendement aan precursorpolymeer opleverde voor elk van de monomeren. De invloed van het solvent werd tevens nagegaan voor één van de monomeren. Hieruit bleek dat 2-butanol inderdaad het meest geschikte solvent is voor de polymerisatie van de sulfinylmonomeren. Wederom werd de conversiestap tot het geconjugeerde polymeer onderzocht met verschillende in situ technieken. Enkele experimenten geven ook zeer mooi het thermochroom effect weer voor elk van de geconjugeerde polymeren. Voor het alcoholpolymeer werd na conversie een onoplosbaar materiaal verkregen hetgeen goed overeenkomt met het onoplosbare alcoholpolymeer beschreven in hoofdstuk 2. Om dit oplosbaarheidsprobleem te omzeilen werden er enkele copolymerisatiereacties uitgevoerd die na conversie wel een oplosbaar polymeer opleverden. Het geconjugeerde esterpolymeer kon onder basische omstandigheden gehydrolyseerd worden tot het overeenkomstige carbonzuur. Zo een functionele groep laat functionalisatie toe op het polymeer stadium. Echter, reductie van de esterfunctie tot het alcohol resulteert eveneens in een onoplosbaar polymeer te wijten aan waterstofbrugvorming. We kunnen dus besluiten dat de sulfinylprecursorroute opnieuw zijn

veelzijdigheid en toepasbaarheid heeft aangetoond waardoor de synthese van een hele reeks PPV derivaten mogelijk wordt.

Een tweede groot gedeelte van het experimentele werk is gebundeld in hoofdstuk 4. Hierin wordt een kinetische en mechanistische studie uitgevoerd omtrent de *p*-quinodimethaanvorming via de sulfinylprecursorroete. De kinetica van enkele monomeren die van elkaar verschillen wat betreft hun polariserende groep, hun uittredende groep of hun aromatische kern werd bestudeerd op zowel een kwalitatieve als een kwantitatieve manier. Hierbij werd gebruik gemaakt van UV-Vis spectroscopie aangezien deze techniek toelaat om zowel de vorming als het wegreageren van het *p*-quinodimethaansysteem te bestuderen. De gegevens afkomstig uit de kwantitatieve studie verschaffen ons een aantal aanwijzingen voor het optredende eliminatiemechanisme. Er werd gevonden dat de *p*-quinodimethaanvorming uitgaande van het monomeer verloopt via een irreversibel E_{1cb} mechanisme waarbij de protonabstractie de snelheidsbepalende stap is. De gegevens uit de kwalitatieve studie ondersteunen dit mechanisme. Alle factoren die de zuurheid van het benzylicke proton naast de sulfinylgroep verhogen zullen de vorming van het *p*-quinodimethaansysteem versnellen. Factoren die deze zuurheid verlagen, doen de reactiesnelheid dalen. Deze kinetische en mechanistische gegevens zijn van groot nut om de uitkomst van een copolymerisatiereactie tussen twee verschillende monomeren te voorspellen. Deze hypothese werd bewezen door enkele copolymerisatiereacties uit te voeren met twee monomeren die sterk verschillen in de zuurheid van hun benzylicke protonen. De resultaten van deze reacties komen zeer goed overeen met de bevindingen uit de kinetische studies. De verschillende copolymeren werden geanalyseerd met behulp van verschillende technieken en de conversie tot het geconjugeerde polymeer vertoonde enkele interessante eigenschappen. De sulfinyl- en sulfonylgroep worden bij verschillende, goed van elkaar gescheiden temperaturen uitgestoten. Op die manier kan een selectieve conversie bekomen worden.

De resultaten van de kinetische studies en de copolymerisatiereacties hebben duidelijk aangetoond dat kennis omtrent het mechanisme van *p*-quinodimethaanvorming van zeer groot nut kan zijn.